Eye Mechanics And Their Implications For Eye Movement Control

Ansgar R. Koene

Helmholtz Instituut

ISBN 90-393-3185-5

Eye mechanics and their implications for eye movement control

De mechanica van het oog en zijn implicaties voor de besturing van oogbewegingen

(met een samenvatting in het Nederlands)

Proefschrift

ter verkrijging van de graad van doctor aan de Universiteit Utrecht op gezag van de Rector Magnificus, Prof. Dr. W.H. Gispen, Ingevolge het besluit van het College voor Promoties in het openbaar te verdedigen op maandag 18 november 2002 des middags te 12.45 uur

door

Ansgar Roald Koene

geboren op 19 februari 1975, te Braunschweig.

promotor: Prof. Dr. C.J. Erkelens
Faculteit Natuur- en Sterrenkunde
Helmholtz Insituut
Universiteit Utrecht

Contents

1 General Introduction **3**
- 1.1 Anatomy of the eye . . . 4
- 1.2 Types of eye movements . . . 5
- 1.3 Neural circuitry of eye movement control . . . 8
- 1.4 Overview of this thesis . . . 9

2 Cause of kinematic differences during centrifugal and centripetal saccades **13**
- 2.1 Introduction . . . 13
- 2.2 Method . . . 16
- 2.3 Results . . . 19
- 2.4 Discussion . . . 28
- 2.5 Appendix A: The eye plant model . . . 31
- 2.6 Appendix B: Neural activity profiles during saccades . . . 32

3 Quantification of saccadic signal modification as a function of eye orientation **35**
- 3.1 Introduction . . . 35
- 3.2 Method . . . 37
- 3.3 Results . . . 41
- 3.4 Discussion . . . 49
- 3.5 Appendix A: The eye plant model . . . 52

4 Properties of 3D rotations and their relation to eye movement control **55**
- 4.1 Introduction . . . 55
- 4.2 Oculomotor requirements for gaze changes and fixations . . . 56
- 4.3 Axes of action of muscles . . . 59
- 4.4 Effect of eye plant geometry on oculomotor control . . . 61
- 4.5 Discussion . . . 65
- 4.6 Appendix A: Dependence of $\vec{I}$ on eye orientation . . . 68
- 4.7 Appendix B: Analytical derivation of pulley positions . . . 68

5 Errors resulting from the use of eye plant models that treat agonist-antagonist muscle pairs as a single muscle **71**
5.1 Introduction 71
5.2 Implications of the muscle-pairing assumption 72
5.3 Model comparison 79
5.4 Discussion 86
5.5 Appendix A: Dependence of $\vec{I}$ on eye orientation 89

6 Summary and Conclusions **91**
6.1 Chapter 2 91
6.2 Chapter 3 92
6.3 Chapter 4 93
6.4 Chapter 5 94
6.5 General conclusions 96

7 Samenvatting en Conclusies **97**
7.1 Hoofdstuk 2 97
7.2 Hoofdstuk 3 98
7.3 Hoofdstuk 4 99
7.4 Hoofdstuk 5 100
7.5 Algemene conclusies 102

References **105**

Publications **113**

Acknowledgements **115**

Curriculum Vitea **117**

Chapter 1

General Introduction

The topic of this thesis is the investigation of the mechanical properties of the oculomotor system and the implications of these properties for eye movement control. The investigation was conducted by means of computational models and simulations.

The study of motor control in humans and animals is of interest for a variety of reasons. In healthcare it can help us understand the neurological origin of motor control deficits that arise from afflictions such as Parkinson's disease. In engineering it can inspire us to novel ways of solving problems in control engineering and robotics. Above all, however, the study of motor control allows us to make a detailed study of the fundamental processes of the brain because both the inputs (physical stimuli) and the outputs (body movements) are clearly defined and physically measurable.

When thinking of motor control in humans and animals we tend to associate this, primarily, with is the control of arm and leg movements bacause movements of the limbs are more conspicuously visible than movements of other body parts, such as the eyes. The study of the motor control of arm and leg movements, however, is very complex since it involves multiple muscles at multiple joints with variable loads. A much more basic system that offers a clear link between the sensory input and the motor output is the control of eye movements, i.e. the oculomotor system.

The movements of each eye are achieved using three pairs of muscles, involving six muscles in total. Each pair rotates the eye in a different direction. One pair is for horizontal rotations, one is for vertical rotations and one is for torsional (i.e. around the line of sight) rotations. Since the eye-ball is more or less spherical, and does not grasp anything, changes in the mechanical load are negligible. A further simplifying factor is that (even though the velocity of eye movements can vary from 0.05 to 500 deg/s) the kinematics of eye movements (i.e. the velocity profiles) cannot be consciously controlled. The eye movements either follow the sensory input directly (e.g. pursuit) or there is a fixed relation between the velocity profile and the amplitude of the movement (saccades).

Much of the recent research on oculomotor control has concentrated on correlating eye movements with neural activity in the eye muscles (motoneurons) or brain areas

related to motor control (superior colliculus, frontal eye fields, etc.). One of the difficulties with this approach is that it ignores the mechanics of the system executing the movement, which forms an important intermediate stage between the observed eye movements and the measured neural activity. Simple mechanical properties of the oculomotor system, such as coordinate frame transformations related to the direction in which the eye muscles pull at the eye, are thereby overlooked, causing difficulties in the interpretation of the data.

For this thesis we studied the mechanics of the eye movement system (the eye plant) so that we could predict the way in which the muscles have to be controlled in order to achieve a desired eye movement. In order to determine how eye movements are controlled we investigated the control characteristics of the oculomotor system.

The difference between this method of studying eye movement control and the neural correlating method can be clarified with the following analogy. When trying to find out how to drive a car you can either look at the car or at the driver. We chose to look at the car itself: How does it move over the road, how does the steering wheel make the wheels turn etc. The neural correlating approach is like trying to learn how to drive a car by watching someone else driving: observing his arm and foot movements. If you look at the car, you see that the action required to make it stop is to activate the brake. If you look at the driver you see that he needs to press down his foot. In principle both approaches are equally valid and for an overall understanding of the system they are complementary. If you study the car you will easily discover that in order to stop the car you need to activate the brake, not on the accelerator. By observing someone else drive you learn more easily that you should control the brake with your foot and not your hand.

In this thesis we employed a computational modeling approach in order to combine data from anatomy, physiology and psychophysics with basic principles of physics (mechanics) and mathematics (geometry). In the remainder of this introduction we will give a brief overview of the anatomy of the eye, types of eye movements, the neural circuitry driving eye movements, properties of 3D eye rotations and finally we will give an overview of the remainder of the thesis.

1.1 Anatomy of the eye

The anatomy of the eye can be subdivided into two functionally separate categories. On the one hand there are the structures such as the retina and lens that are related to the sensory apparatus, i.e. the front end of the visual system. On the other hand there are the structures such as the eye muscles that are related to the motor apparatus which moves the eye, i.e. the oculomotor system. Since this thesis focuses on the execution of eye movements we will describe the motor apparatus in more detail.

In contrast to electrical motors, which can reverse the direction of force, the biological motors of motion, i.e. muscles, can generate force in only one direction. Eye muscles can only pull the eye, not push it. The eye muscles are therefore arranged in three reciprocally activated agonist-antagonist pairs. When the activity in one

muscle of the pair (the agonist) is increased, causing it to contract, the activity in the other muscle (the antagonist) is reduced, allowing it to relax and be stretched. In order to move the eye back to its original position the roles of the agonist and the antagonist muscles are reversed. The reciprocal innervation is organized centrally by interconnections between the extraocular motor nuclei (Robinson 1975a, Hikosaka et al. 1978, Igusa et al. 1980, Yoshida et al. 1982, Strassman et al. 1986a,b, Scudder et al. 1988, and Cullen and Guitton 1997).

The medial and lateral rectus muscles are responsible for horizontal rotations around the eye's vertical axis. The horizontal recti are attached to the medial and lateral sides of the eye respectively (see figure 1.1). Contraction of the medial rectus rotates the eye towards the midline (i.e. the nose) and the lateral rectus rotates the eye laterally, away from the nose.

The superior rectus and inferior rectus muscles are attached to the eye directly above and below the margin of the cornea. Their major actions when they contract are vertical rotations of the eye around its horizontal axis (see figure 1.1). The superior rectus produces an upward rotation of the eye (elevation) and the inferior rectus produces a downward rotation (depression).

The third pair of muscles, the superior and inferior oblique muscles, is responsible for torsional rotations of the eye (see figure 1.1). Viewed from the front, the superior oblique produces clockwise rotations and the inferior oblique produces counterclockwise rotations.

Any rotation of the eye, be it fast or slow, and any combination of horizontal, vertical and torsional rotation is achieved by means of a precisely controlled increase and decrease of the forces generated in the six eye muscles.

Besides the eye muscles, which are responsible for the active control of eye movements, passive tissue, such as tenons capsule, exerts elastic and viscous forces on the eye (Robinson 1981). These visco-elastic forces affect the dynamics of eye movements and the steady-state muscle activity required to keep the eye at a given orientation. A second effect of these passive tissue structures is that they form sleeves which guide the muscles along the eye ball on their path from their insertion point in the eye to their origin in the eye socket. These sleevelike structures have been called muscle pulleys since they can change the paths of the eye muscles in much the same way as pulleys (Miller et al. 1993, Demer et al. 1995).

In chapters 2 and 3 of this thesis we investigate what effect the contractile, viscous and elastic properties of the eye muscles and passive tissue have on eye movement dynamics and oculomotor control. In chapters 4 and 5 we study the way in which the activity of the six eye muscles has to be coordinated in order to generate 3D eye movements.

1.2 Types of eye movements

As mentioned earlier, one of the simplifying factors about studying oculomotor control is that there are only a limited number of types of eye movements, each with specific

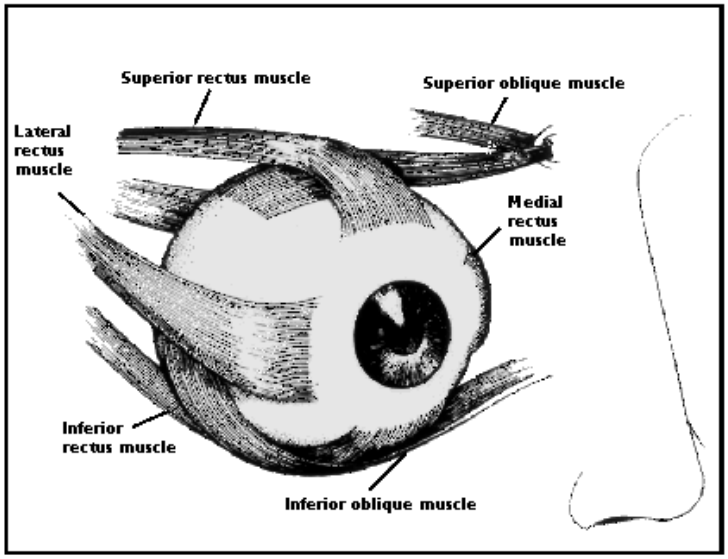

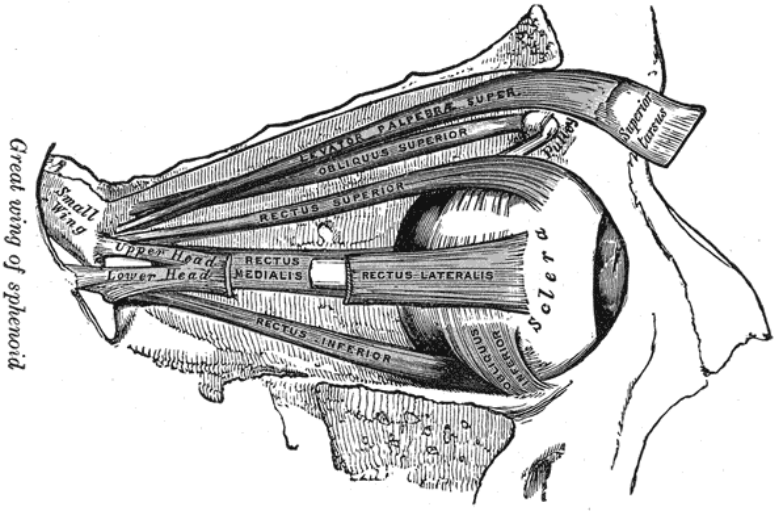

Figure 1.1: Anatomy of the eye.

characteristics. Eye movements can generally be grouped into five types: saccades, smooth pursuit, vergence and the optokinetic and vestibulo-ocular reflexes.

Saccades are the rapid eye movements we make when we look around to examine our environment. Saccadic eye movements can vary considerably in magnitude, from less than 1° to more than 80° as the situation demands (Collewijn et al. 1988). The peak velocity during the movement depends on the size of the saccade. For large saccades it can reach $500°/s$. Because the velocity is so high, the movements are brief. The most frequently occurring saccades, which are smaller than 15°, take less than 50ms from start to finish. Saccades are voluntary eye movements in the sense that we can consciously choose to look, or ignore, things in the visual scene. Once initiated, however, the execution of the movement is automatic. During the eye movement, when the retinal image is sweeping rapidly across the retina, vision is actively suppressed (Burr et al. 1997, Leigh and Zee 1999).

Smooth pursuit movements are visually guided movements in which the eye tracks a small object that is moving relative to a stationary background. The purpose of smooth pursuit movements is to stabilize the retinal image of a moving object in order to allow it to be visually examined. Pursuit movements are voluntary only in so far as we can choose to look at a moving object or ignore it. The kinematics of pursuit movements are completely determined by the motion of the object that is being tracked.

Vergence moves the eyes in opposite directions causing the intersection point of the lines of sight of the two eyes to move closer or further away. The purpose of vergence eye movements is to direct the fovea (area of the retina with the highest resolution) of both eyes at the same object. Under natural conditions vergence movements are accompanied by saccades or pursuit movements.

The optokinetic reflex is a visually guided reflex, the purpose of which is to compensate body and head movements so that retinal image motion is minimized. The optokinetic reflex responds optimally if the stimulus is movement of all, or a large portion of the retinal image. We have no voluntary control over these reflexive eye movements. If the retinal image of the whole field of view moves, our eyes invariably follow this motion. Just as with pursuit movements the kinematics of eye movements resulting from the optokinetic reflex are determined by the motion of the stimulus.

The vestibulo-ocular reflex is similar to the optokinetic reflex in that its function is also to compensate for head motion and stabilize the retinal image. In contrast to the optokinetic reflex however, the vestibulo-ocular reflex is not guided visually, but is generated by receptors in the inner ear (in the semicircular canals and otolith organs) that detect acceleration and changes with respect to gravity. The vestibular-ocular reflex is also beyond our voluntary control. The kinematics of these eye movements are directly linked to the signals that are generated by the vestibular organs in the inner ear.

Regardless of the different degrees of voluntary control that we have over eye movements, and regardless of the different stimulus information that is used to drive them, all eye movements are ultimately generated by the eye muscles. Even though the models in this thesis are discussed primarily in relation to saccadic eye movements,

the models and (most) results are equally valid for the other types of eye movements. The reason we focus on saccades is that they are the most stereotyped eye movements and the ones that are influenced least by the stimulus. Since the movement profiles of saccades are not affected by stimulus properties we can investigate whether they are influenced by the mechanics of the eye, and if so, in what way.

1.3 Neural circuitry of eye movement control

Since this thesis investigates the implications of the mechanics of the eye plant for oculomotor control we need to relate the properties of the eye mechanics not only to the characteristics of eye movements but also to their neural control. We therefore now give a short overview of the neural circuitry that generates the oculomotor control signals.

The six eye muscles are controlled by three brain stem nuclei that innervate the oculomotor muscles and serve as a final common path through which all eye movement must be controlled.

In order to bring about a change in eye orientation the motor neurons generate a burst of force that regulates the velocity of an eye movement and a maintained force that, after the movement has been completed, holds the eye stationary by resisting the elasticity of the muscles which would slowly draw the eye back to a straight-ahead position (Robinson 1964). The longlasting force required to keep the eye at a particular orientation is derived from the burst activity that drives the eye movement by temporal integration of the burst signal. The neural integrator responsible for this appears to be located in the brain stem (for horizontal movements it has been shown to involve the nucleus prepositus hypoglossi). The burst of activity that controls the velocity of the eye movement is specified by different circuits, depending on the type of eye movement, i.e. saccades, smooth pursuit, optokinetic or vestibular-ocular (Leigh and Zee 1999).

Since saccades are eye movements designed to re-orient the eye in a different direction the saccadic system must supply the brain stem circuits with a command that is based on the desired amplitude and direction of a movement. Current evidence indicates that this command can originate in either the superior colliculus of the midbrain or the frontal eye fields of the neocortex. Saccades are too fast to allow feedback control using visual or proprioceptive information. Instead the saccadic system uses an estimate of the neural activity required to generate a saccade (Westheimer 1954, Young and Stark 1963, Leigh and Zee 1999).

In the smooth pursuit system, signals carrying information about target motion are extracted by motion-processing areas in the visual cortex and are then passed to the dorsolateral pontine nucleus of the brain stem. These signals proceed to the cerebellum where neurons have been shown to specifically encode the velocity of pursuit eye movements (Suzuki and Keller 1984). Since smooth pursuit movements are much slower than saccades these eye movements are guided by visual feedback which is used to minimize retinal motion of the pursued target.

The neural control of the optokinetic reflex is very similar to the control of pursuit movements. The main difference between the two types of movement is that the opto-kinetic reflex is linked to the movement of the whole retinal image, whereas smooth pursuit is linked to the movement of a specific target. A further difference is that prolonged optokinetic stimulation, such as the view from the window of a moving train, results in cyclic eye movements, i.e. opto-kinetic nystagmus. When the optokinetic following of the visual field has moved the eye to the periphery of its movement range a saccadic movement brings the eye to the opposite side of its movement range. After this 'quick phase' the eye starts to track the visual field again.

During vestibulo-ocular responses (vestibular ocular reflex) the eye movements are controlled by the signals coming from the vestibular organs (the semi-circular canals and otoliths) in the inner ear. Since the vestibular organs sense the motion of the head they control the resulting vestibular eye movements by simply sending these signals to the appropriate eye muscles. When the head tilts downward with $10°/s$ this movement is detected by the vestibular system and a signal is sent to the superior and inferior rectus muscles causing the eyes to rotate upward by $10°/s$.

In order to investigate the implications of the eye mechanics for the signal processing that needs to be done by these neural circuits we studied how the characteristics of the eye plant affect the relation between muscle innervation and resulting eye movements. For horizontal eye movements we modeled the non-linearities in the contractile, elastic and viscous properties of the muscles and orbital tissue in order to compute the resulting dependence of the (eye velocity) control signal on the initial orientation of the eye (Chapters 2 and 3). For 3D eye rotations we computed the changes in effective muscle pulling direction as a function of eye orientation in order to find out whether the required coordination between the innervations of the six muscles during an eye movement depends on eye orientation and if so, how this is done (Chapters 4 and 5).

1.4 Overview of this thesis

In this thesis we try to determine the consequences of the eye mechanics for the control of eye movements. We try to understand the oculomotor control of observed eye movements by taking the eye plant mechanics into account. Our study of this question consists of two parts. First we concentrate on the mechanical properties of the muscles during horizontal eye movements, modeling the relationship between eye velocity and muscle innervation. Then we analyze the relation between 3D eye orientation and the effective pulling directions of the six eye muscles. Even though we collected some experimental data concerning eye movements in order to obtain input data for the simulations, the main focus of our work is on computational modeling.

In chapter 2 we investigate the degree to which mechanical and neural non-linearities contribute to the kinematic differences between centrifugal and centripetal saccades. On the basis of the velocity profiles of centrifugal and centripetal saccades we calculate the forces and muscle innervations during these eye movements. To

compute the forces in the muscles and the corresponding muscle innervations, we use an inverted model of the eye plant. The results of these simulations show that the non-linear force-velocity relationship (i.e. muscle viscosity) of the muscles is probably the cause of the kinematic differences between centrifugal and centripetal saccades.

In chapter 3 we use the same model that we used in chapter 2 to quantify the required saccadic signal modification as a function of eye orientation. On the basis of the properties of the eye muscles we calculate the adjustment of the saccadic command that is necessary to compensate for the eye plant non-linearities. The results of these calculations show that the agonist and antagonist muscles require different net saccade signal gain changes. In order to gain some insight into the manner in which this gain change is accomplished, i.e. through a change in the duration and/or magnitude of the signal, we measured the velocity profiles of saccades with different starting orientations and use the inverted model of the eye plant to calculate the corresponding muscle innervation profiles. Based on these calculations we conclude that the saccade signal gain changes are accomplished primarily by changes in the magnitude of the saccade signal.

Chapters 4 and 5 deal with changes in the eye muscle pulling directions as a function of 3D eye orientation and the effect of these changes on oculomotor control.

In chapter 4 we examine the geometrical properties that dictate the relationship between the axes of action (i.e. unit moment vectors) of the muscles and 3D eye rotations. First we present the requirements that the oculomotor system must meet for the eye to be able to make the desired gaze changes and fixate at various eye orientations. Then we determine how the axes of action of the muscles are related to eye orientation and the location of the effective muscle origin (i.e the muscle pulleys). Next we show how this relation, between eye orientation and the axes of action of the muscles, constrains muscle pulley locations if the eye movements are controlled by specific rules. This link is illustrated by two examples in which we show how the requirements of oculomotor control strategies limit the possible muscle pulley locations. The two control theories we investigate are: 1. The oculomotor system generates eye movements that obey Listing's law, and the binocular extension of Listing's law, by actively using only the horizontal and vertical muscle pairs. 2. Oculomotor control involves perfect agonist-antagonist muscle pairing. Finally we discuss how the geometrical properties dictating the axes of action of the muscles can be used to test the validity of oculomotor control models.

In chapter 5 we apply the methodology that was developed in chapter 4 to test two assumptions that are commonly made in models of the oculomotor plant. The first is the assumption that the antagonistic muscles can be viewed as a single bi-directional muscle (muscle-pairing). The second is the assumption that the three muscle pairs act in orthogonal directions. On the basis of the geometrical properties governing the muscle paths we show how these assumptions give rise to incorrect predictions for the oculomotor control signals. Using the same muscle activation patterns for eye plant models with and without the muscle-pairing and orthogonality assumptions we calculate the eye orientations that are reached. By comparing the differences in the calculated eye orientations we show the significance of the error in the predictions

made by eye plant models that treat agonist-antagonist muscle pairs as a single muscle. The models we used were variations of the eye plant model used by Raphan (1997) and Quaia and Optican (1998).

Finally in chapter 6 we provide a summary of our results and discuss some general conclusions concerning the consequences of the mechanics of the eye for oculomotor control.

Chapter 2

Cause of kinematic differences during centrifugal and centripetal saccades

Abstract

Measurements of eye movements have shown that centrifugal movements (i.e. away from the primary position) have a lower maximum velocity and a longer duration than centripetal movements (i.e. toward the primary position) of the same size. In 1988 Pelisson proposed that these kinematic differences might be caused by differences in the neural command signals, oculomotor mechanics or a combination of the two.

By using the result of muscle force measurements made in recent years (Miller et al. 1999) we simulated the muscle forces during centrifugal and centripetal saccades. Based on these simulations we show that the cause of the kinematic differences between the centrifugal and centripetal saccades is the non-linear force-velocity relationship (i.e. muscle viscosity) of the muscles.

2.1 Introduction

Studies of saccade velocity profiles by Abel et al. (1979), Collewijn et al. (1988), Pelisson and Prablanc (1988), Rottach et al. (1998) and Eggert et al. (1999) have shown that the kinematics of saccadic eye movements differ for movements towards the primary position (centripetal movements) and movements away from the primary position (centrifugal movements). In his 1988 paper Pelisson proposed that the observed kinematic differences might be caused either by the neural command signals or the oculomotor mechanics, or a combination of the two.

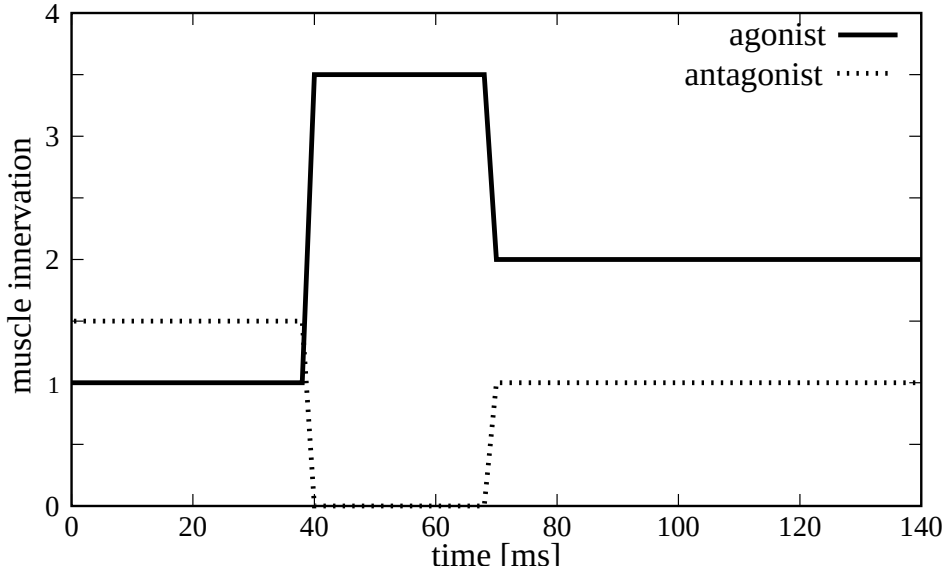

Figure 2.1: Schematic representation of the pulse-step signal sent to the agonist and antagonist muscles.

Regarding the neural command signals it has been known for many years (Robinson, 1964) that for a saccade to occur, a pulse-step signal must be sent from oculomotor nuclei to the extraocular muscles; a high frequency phasic activity (pulse) is required for the eyes to move quickly against high viscous forces and a regular tonic activity (step) to hold the eyes at their new position against elastic restoring forces. The known anatomical connections between the pulse generator for horizontal saccades and the muscles suggest that the antagonistic pair of muscles is organized in a push-pull arrangement (see Fuchs et al., 1985). As a consequence, the phasic command would apparently produce opposite but proportional modulations of firing frequency in the agonist (pulse of activation, figure 2.1) and in the antagonist muscles (pulse of deactivation, figure 2.1). However electrophysiological recordings from motoneurons in monkey have shown that for saccade amplitudes larger then 10° antagonist motoneurons are totally inhibited irrespective of initial eye orientation (Fuchs and Lushei, 1970; Robinson, 1970; Cullen et al., 1997). Therefore the intensity of the deactivation is equal to the tonic activity at the beginning of the saccade (figure 2.1). Since the tonic activity increases with the ocular deviation toward the muscle concerned, the deactivation of the antagonist muscle is proportional to the initial eye deviation in the opposite direction to the saccade (Off direction). Thus the smaller the initial eye position in the Off direction (i.e. the smaller the initial centripetal component) the smaller the deactivation step becomes. Pelisson and Prablanc argued that this loss of signal between premotor burst neurons and motoneurons, related

to the low tonic activity of the latter and proportional to initial eye position, is a reasonable explanation of the observed increase of maximum saccade velocity with initial centripetal component.

Pelisson and Prablanc went on to describe some of the mechanical non-linearities that have been found at the level of the ocular mechanics. In cat (Robinson, 1964) and in man (Collins, 1975; Miller and Robinson, 1984; Miller et al., 1999) extraocular muscles have non-linear length-tension relationships, with increased stiffness of the stretched (antagonist) muscle with ocular deviation. The viscous properties of the mechanical plant also seem non-linear (Cook and Stark, 1968; Collins, 1975). They therefore felt that accurate simulations of the oculomotor plant are required to assess the effect of these mechanical non-linearities and of their complex interplay on the kinematics of saccades initiated from different initial positions.

Pelisson and Prablanc concluded that although the non-linearity of neural commands seems to be a reasonable explanation of the observed velocity changes, peripheral non-linearities cannot yet be ruled out.

In the thirteen years since Pelisson and Prablanc (1988) and Collewijn et al. (1988) published their findings a great deal of work has been done on deriving better models of the oculomotor control system that drives saccades (Quaia et al., 1999; Gancarz and Grossberg, 1998) and new data has allowed the construction of more detailed models of the ocular mechanics (Miller et al., 1999). The degree to which the difference in centrifugal and centripetal saccade kinematics is caused by neural signal saturation or eye plant mechanics, however, has as yet remained unanswered.

Answering this question may help us to gain more insight into the way in which the signal driving the saccades is modulated to account for starting position differences.

In this paper we investigate the degree to which the mechanical and the neural non-linearities contribute to the kinematic differences between centrifugal and centripetal saccades. Based on the velocity profiles of centrifugal and centripetal saccades we calculate the forces and muscle innervations during these eye movements. For the calculation of the forces in the muscles, and the corresponding muscle innervations, we used a model of the eye plant based on the work by Pfann et al. (1995), Robinson (1981), Collins (1975) and Clark and Stark (1974a,b) and the data from implanted force transducer experiments published by Pfann et al. (1995), Miller et al. (1999) and Miller and Robins (1992). In contrast to these earlier studies, however, we did not use the model to synthesize eye movements from muscle innervation profiles. Instead we inverted the model to allow us to calculate the muscle innervations and muscle forces from eye movement profiles. An overview of the step-wise process of calculating the muscle forces and innervation during saccades is shown in figure 2.2. At each step we compared the force (innervation) profiles that were calculated for the centrifugal saccade with the corresponding profiles for the centripetal saccade and correlate this with the kinematic differences.

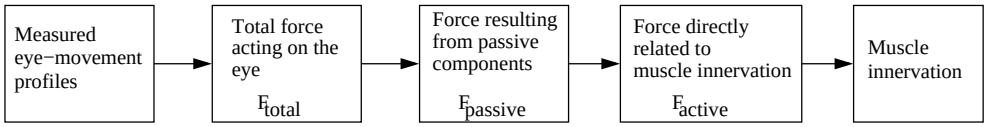

Figure 2.2: Step-wise process of calculating muscle forces and innervation during saccades.

2.2 Method

In order to determine the contributions of the mechanical and neural properties of the saccade system to the kinematic differences between centrifugal and centripetal saccades we measured the eye movements and used a model of the eye plant, based on implanted force transducer data from Miller et al. (1999), to simulate the forces acting on the eye during these saccades.

The total force acting on the eye (F_{total}) was found by taking the second derivative of the measured eye position profiles (resulting in eye acceleration profiles) and applying Newton's third law. The passive forces (F_{passive}), which include the muscle elasticity, orbital viscosity and orbital elasticity and which depends directly on eye orientation and velocity properties, were derived from the measured eye movement profiles using the eye plant model. To find the actively generated forces (F_{active}), which depend directly on the muscle innervation and which includes the contractile and viscous muscle properties, we subtracted F_{passive} from F_{total}. We then used the eye plant model to find the innervation of the muscles that generated F_{active} .

Experimental procedures

The eye movements were recorded using the magnetic search coil technique (Robinson, 1963; Collewijn et al., 1975). The movements of the right eye were sampled at 500 Hz and stored by a computer. The subject sat within the magnetic fields with his head immobilized with a bite bar. The five visual targets were back-projected onto a flat screen at the hight of the subjects eyes. The visual targets were Xs (24.5' of visual angle) and were constantly visible throughout the experiment. The subject was seated 1.5m in front of the screen such that the right eye was aligned with the central target. The targets were positioned at 10° and 20° to the right and to the left of the central target. The subject made self paced saccades between each of these targets. Velocity profiles were computed by taking the first derivative of the measured eye position profiles. The eye movements between points of equal eccentricity were then pooled together to determine the mean eye movement profile (and standard deviation) for saccades between these two respective points. We also averaged over adducting and abducting eye movements in order to remove (average out) movement directional effects caused by inequalities between the lateral and medial rectus muscles. For the remainder of the work only the average movement profiles were used. The acceleration (α) profiles of these averaged eye movements were computed by taking the derivative

of the velocity (ω) profiles ($\alpha = d\omega/dt$).

The total force acting on the eye was determined from the acceleration profiles by applying Newton's third law. The moment of inertia of the eye was assumed to be $4.3 * 10^{-5}$gf s^2/degree which is the average value for humans as reported by Clark and Stark (1974a).

The model of the eye plant that was used to simulate the forces acting on the eye is given in section 2.2.

The eye plant model

The Hill-type mechanistic model of the horizontal saccadic system which is used in our work was based on similar models that were previously developed by Clark and Stark (1974a, b), Collins (1975), Robinson (1981) and Pfann et al. (1995). Most of the parameter values were derived from steady-state measurements of macroscopic muscles properties (Miller et al. 1999, Collins et al. 1975 and Collins et al. 1981) and quick release experiments (Cook and Stark 1967; Collins 1971). The remaining parameter values were taken from the models by Robinson, Pfann and Clark (see Appendix A). The data presented in the above mentioned work was collected from measurements primarily in human strabismus patients (Collins et al. 1981, Robinson et al. 1969), cats (Barmack et al. 1971, Collins, 1971, Robinson, 1964) and monkeys (Fuchs and Luschei, 1971a). Data was collected using non-invasive length-tension forceps (Collins et al. 1981) and chronically implanted muscle-force transducers (Collins et al. 1975, Miller and Robins 1992 and Pfann et al. 1995). A diagram of the model is shown in Figure 2.3.

The neural inputs (i.e. overall motoneuron activities) $\mathrm{MN_{lr}}$ and $\mathrm{MN_{mr}}$ are low pass filtered to generate the active internal muscle forces $F_{a_{\mathrm{lr}}}$ and $F_{a_{\mathrm{mr}}}$. In each muscle, the force generator is in parallel with a non-linear dashpot, B, which represents the force-velocity relation of the active muscle. This unit is in series with an elastic element, K_{se}, which represents the connective tissue in series with contractile elements which has the experimentally measured property that an instantaneous reduction in load results in an instantaneous change in muscle length (i.e. the characteristics of a spring). This group of mechanical elements is in parallel with an elastic element, K_p, which represents the passive elastic properties of the muscle. Both F_a and K_p are non-linear. These muscle models are combined with a dual mass-spring-dashpot ($K_{\mathrm{o1}}, B_{\mathrm{o1}}, K_{\mathrm{o2}}, B_{\mathrm{o2}}, J_o$)(Robinson 1975a) representation of the orbit to model the horizontal saccadic system. Since the contribution of the vertical and oblique muscles to horizontal eye movements is negligible they have been lumped together with the model of the orbit. This simplification is of the same order of magnitude as the simplification that both horizontal muscles were taken to be of equal effective strength.

A more precise description of the model and the parameter values that were used is given in appendix A.

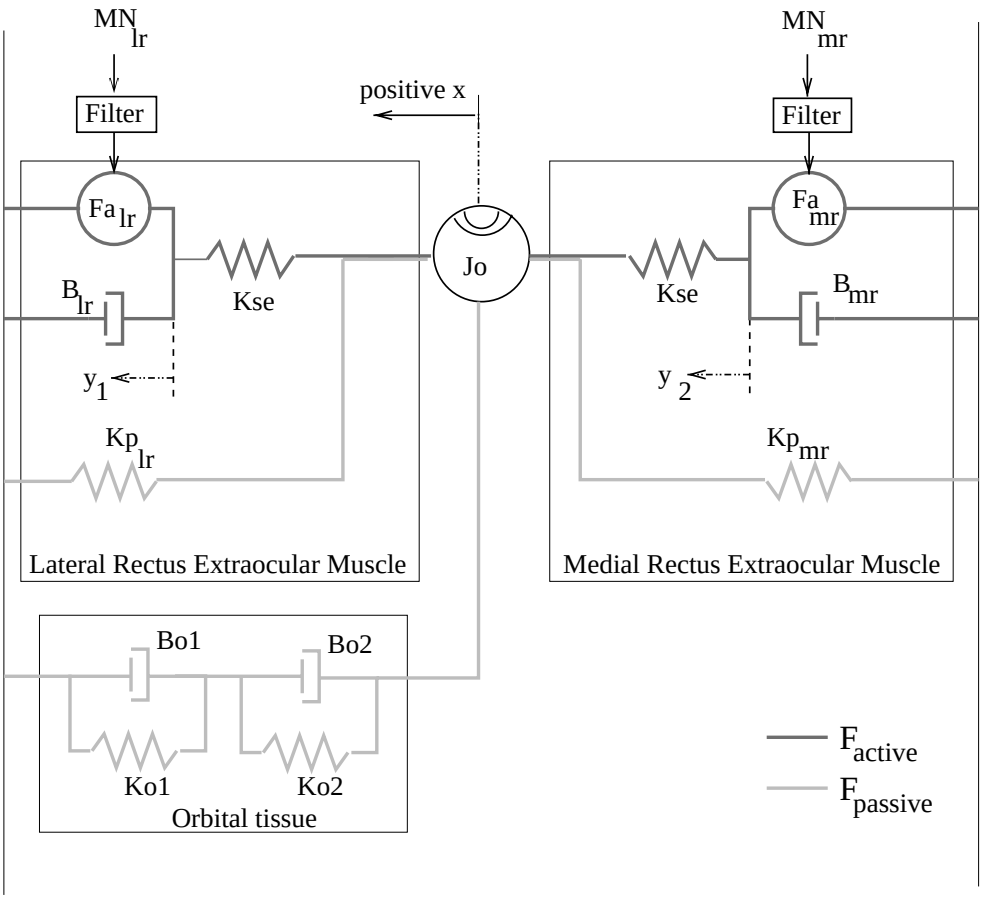

Figure 2.3: Diagram of the model of the horizontal eye plant. The lateral and medial rectus muscle variables are denoted by subscripts lr and mr respectively. The input MN is the neural input converted to its force equivalent. The force generator F_a represents the length-tension-activation relationship of the muscles. The force-velocity relationship is provided by the viscosity B. The series-elastic element is denoted by $K_{\rm se}$. K_p represents the passive muscle elasticity. Orbital mechanics are modeled by a dual spring-dashpot system ($K_{\rm o1}, B_{\rm o1}, K_{\rm o2}, B_{\rm o2}$) together with the mass (J_o).

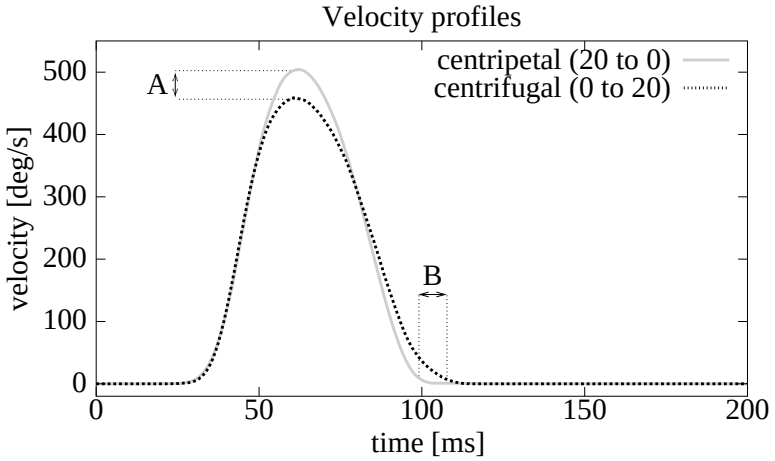

Figure 2.4: Average velocity profiles for the centrifugal and centripetal saccades between the central position and the target at 20° eccentricity. The characteristic difference in maximum saccade velocity (A) and saccade duration (B) are indicated in the top figure.

2.3 Results

The eye movement measurements showed the same pattern of saccade duration, skewness and maximum speed differences between the centrifugal and centripetal saccades as reported by Collewijn et al. (1988) and Pelisson and Prablanc (1988). The average position and velocity profiles for the saccades between primary position (central target) and 20° eccentric are shown in Fig 2.4. The results for the saccades between the primary position and 10° eccentric and between 10° and 20° eccentric showed the same characteristics and will therefore not be shown here.

F_{passive}, the force generated by the muscle elasticity (K_p) and the orbital tissue (B_o, K_o), depends only on eye orientation and velocity. The model of the eye plant therefore allowed us to compute F_{passive} from the measured eye movement data as shown in equation 2.1

$$F_{\text{passive}}(t) = F_{p_{\text{lr}}}(\theta(t)) - F_{p_{\text{mr}}}(\theta(t)) - F_o(\theta(t)), \tag{2.1}$$

where $F_{p_{\text{lr}}}$, $F_{p_{\text{mr}}}$ and F_o are the muscle elasticity and orbital tissue forces as defined in appendix A. Figure 2.5 shows the change in F_{passive} during centripetal and centrifugal saccades. Figure 2.6 shows the change in F_{active} during centripetal and centrifugal saccades which was found by subtracting F_{passive} from F_{total}.

We show the change in force rather than the actual force since this makes it easier to compare the forces during centrifugal and centripetal saccades. No relevant information is lost by doing this since the steady state forces, i.e. the initial offset, of

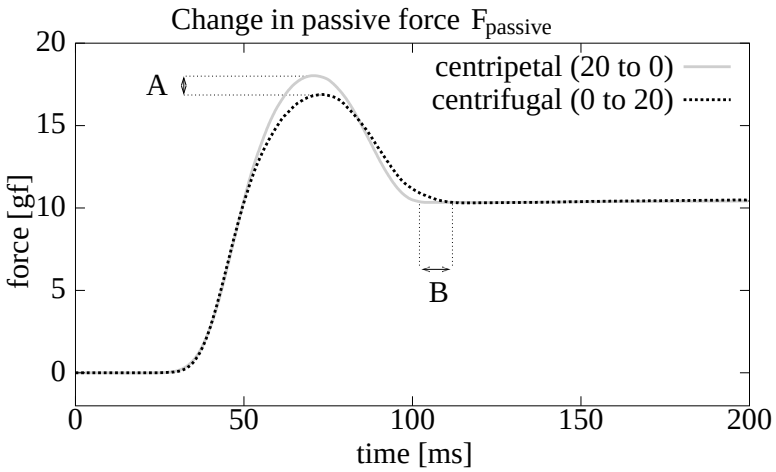

Figure 2.5: Change in total passive force F_{passive} during centripetal and centrifugal saccades between the central position and the target at 20° eccentricity. 'A' indicates the difference in maximum change in F_{passive}. 'B' indicates the difference in duration until steady state is reached.

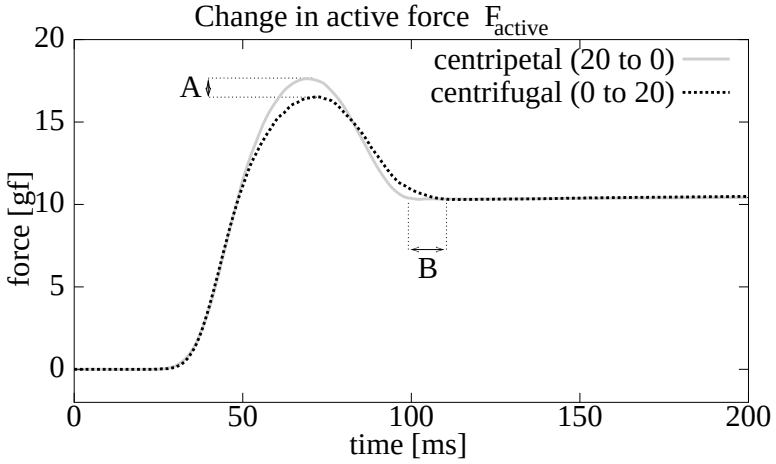

Figure 2.6: Change in total active force F_{active} during centripetal and centrifugal saccades between the central position and the target at 20° eccentricity. 'A' indicates the difference in maximum change in F_{active}. 'B' indicates the difference in duration until steady state is reached.

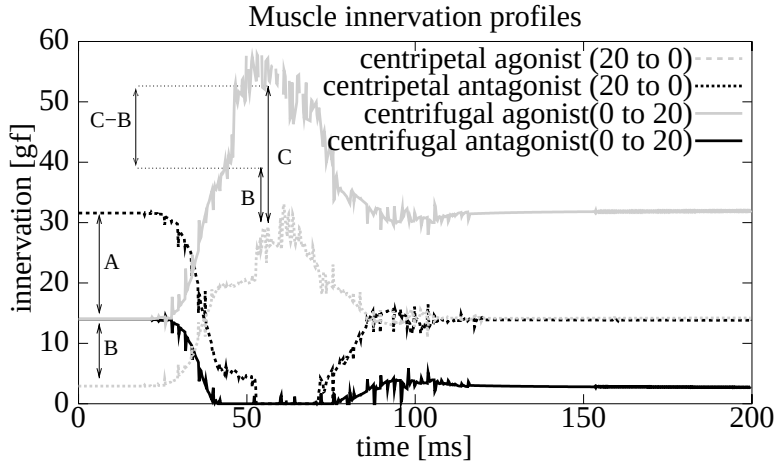

Figure 2.7: Muscle innervation profiles showing the strength of agonist and antagonist activity during the saccade. 'A' indicates the difference in antagonist deactivation pulse amplitude between centripetal and centrifugal saccades. 'B' indicates the difference in initial agonist activity while 'C' indicates the difference in maximum agonist activity. 'C-B' therefore indicates the difference in agonist pulse amplitude between the centripetal and centrifugal saccades.

F_{active} and F_{passive} cancel each other and therefore do not contribute to the generation of eye movements. The profiles of F_{active} and F_{passive} look similar because, as we show in section 2.3, the profile of F_{passive} is a consequence of F_{active}. The muscle innervation that, according to our eye plant model, generates F_{active} is shown in figures 2.7 and 2.8. This muscle innervation was calculated by using a gradient descent search algorithm to find the innervations that would generate F_{active} when used as input to our eye plant model. The search space was reduced to a single dimension by the constraint that the activity change in antagonist is derived from the the activity change in the agonist via inhibitory inter-neurons in the brain stem (Robinson 1975a, Hikosaka et al. 1978, Igusa et al. 1980, Yoshida et al. 1982, Strassman et al. 1986a,b, Scudder et al. 1988, and Cullen and Guitton 1997).

The muscle innervations calculated by us, and shown in figures 2.7 and 2.8, are given in grams of force (gf) rather than spikes per second because the force-length-innervation relationship (Miller et al. 1999, Collins et al. 1981 and Miller and Robinson 1984), which determines $F_{a_{\text{lr}}}$ and $F_{a_{\text{mr}}}$, gives muscle innervation in grams of force. The innervation of the muscles is defined as the isometric developed force (F_a) the muscle would generate if it were set at primary position length. This muscle innervation, although given in grams of force, is always directly related to the neural activity coming to the muscle.

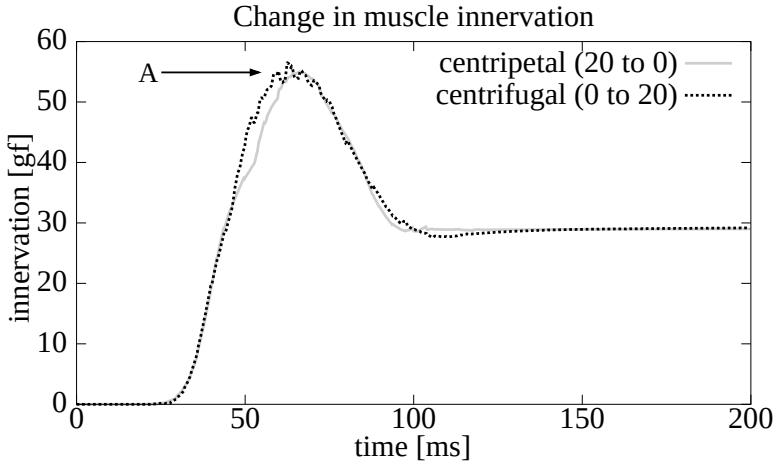

Figure 2.8: Change in total neural muscle activity during centrifugal and centripetal saccades between the central position and the target at 20° eccentricity. 'A' indicates the (lack of) difference in maximum change in muscle activity.

Analysis of the F_{passive} profiles

The force profiles in figure 2.5 reveal that F_{passive} follows the same pattern as the velocity profiles for centrifugal and centripetal saccades. During centripetal saccades the passive-force profiles show a greater maximum change (figure 2.5 'A') and a faster return to a steady state (figure 2.5 'B') than during centrifugal saccades.

As we will now show, however, the direction in which the passive force pulls the eye is such that an increase in passive force corresponds to a reduction in the net-force driving the eye movement. Since the viscous force always acts opposite to the movement direction it is obvious that this component of the passive force should act to reduce movement velocity. The effect of the elastic forces however is less intuitive. The elastic forces pull the eye towards the central position, helping the eye movement during centripetal saccades and hindering the movement during centrifugal saccades. As the eye moves further away from the central position during centrifugal eye movements the passive elastic forces increase and counteract the centrifugal movement more strongly. As the eye moves closer to the central postion during centripetal eye movements the strength of the elastic forces decreases, reducing its positive contribution to the eye movement. The change in passive force therefore acts to reduce the acceleration of the eye during centrifugal saccades as well as during centripetal saccades. Thus the greater maximum change in passive force during centripetal saccades as compared to centrifugal ones (figure 2.5) causes the passive force to slow down the centripetal saccade more than it does the centrifugal saccade.

If the difference in the forces F_{passive} were the primary contribution to the differ-

ence in movement profiles during centripetal and centrifugal saccades, the centrifugal saccade would reach the greater maximum velocity. Since the velocity profiles show the reverse situation, i.e. a greater maximum velocity during centripetal saccades than during centrifugal ones, we must conclude that the cause of the observed difference in velocity profiles must lie somewhere in the active forces F_{active}.

Rather than being the cause of the difference in centrifugal and centripetal velocity profiles the difference in F_{passive} during these eye movements is a consequence of the kinematic differences. The reason why F_{passive} follows the eye movement profiles so linearly is because taken as a muscle pair the non-linearities of the individual passive muscle elasticities cancel each other making F_{passive} quasi-linear (Robinson et al., 1969). Since the orbital tissue forces included in F_{passive}, both the elasticity and viscosity components, are also linear with respect to eye orientation the change in F_{passive} during an eye movement is independent of the starting orientation.

Analysis of the F_{active} profiles

The active force profiles in figure 2.6 illustrate the change in F_{active} during centrifugal and centripetal saccades. During centripetal saccades the active-force profiles show a greater maximum change (figure 2.6 'A') and return to a steady state faster (figure 2.6 'B') than during centrifugal saccades. These characteristics are almost identical to those seen in the passive force profiles of figure 2.5. For the active force, however, the change in force contributes positively to the eye movement. The greater change in F_{active} during centripetal movements, as compared to the change in F_{active} during centrifugal movements, causes a greater acceleration of the eye. This, in combination with the previous results concerning F_{passive}, leads us to conclude that the cause of the velocity difference during centrifugal and centripetal saccades has to do with the properties of F_{active}. We now evaluate the contributions of the muscle innervation, the length-tension-innervation relation and the force-velocity relation of the muscles to the difference in F_{active} during centrifugal and centripetal saccades. By comparing these we will show that even though F_{active} is generated by the neural innervation of the muscles, the difference in F_{active} during centripetal and centrifugal saccades is due to mechanical influences on the generation of F_{active} and not due to differences between the neural signals.

Neural activity

The reduction in antagonist muscle deactivation step that Pelisson and Prablanc (1988) suggested as a possible cause of the kinematic differences between centrifugal and centripetal saccades can clearly be seen in the muscle innervation patterns shown in figure 2.7 ('A'). What the figure also shows however is that the pulse in agonist muscle innervation is greater during centrifugal saccades than during centripetal ones (figure 2.7 'C-B'). The reason for this increase in agonist innervation can be found in the non-linear relation between eye orientation and the required muscle activity to maintain fixation. Figure 2.9 shows the muscle innervation values that were given by

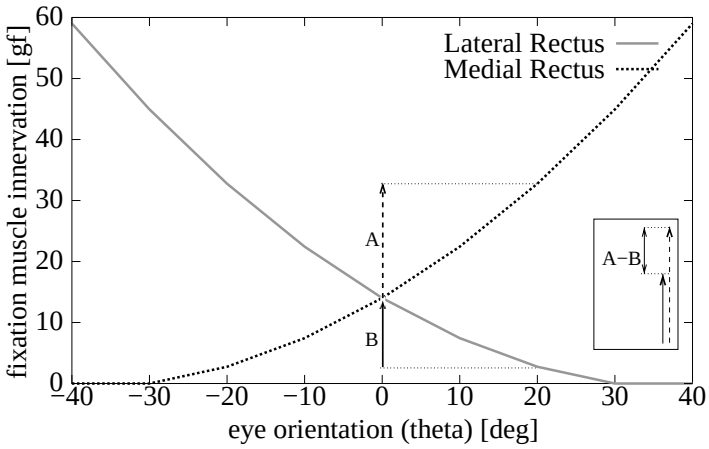

Figure 2.9: Muscle innervation during fixation as a function of eye orientation for the two horizontal muscles, i.e. the medial and lateral rectus muscles. 'A' indicates the step in agonist muscle innervation increase during a centrifugal saccade of 20° away from the central position. 'B' indicates the step in agonist muscle innervation increase during a centripetal saccade of 20° towards the central position. The inset 'A-B' shows the difference between 'A' and 'B'. (Data from Miller 1999)

Miller et al. (1999) for fixation at various eye orientations. Due to this relationship between muscle innervation and eye orientation the agonist muscle must increase its activity more during a centrifugal eye movement (figure 2.9 'A') than during a centripetal one (figure 2.9 'B'), resulting in a greater agonist pulse. The reduction in antagonist deactivation step (figure 2.7 'A') is therefore compensated by the increase in agonist pulse (figure 2.7 'C-B'). The total effect of the reduction of the deactivation pulse in the antagonist and the increase in agonist activity can be seen in figure 2.8 which shows the change in total muscle innervation during centrifugal and centripetal saccades. Since the muscle-innervation-change profiles (figure 2.8) are almost identical for the centrifugal and centripetal saccades, the neural activity patterns cannot explain the observed velocity differences during centrifugal and centripetal saccades.

In order to show that this is not an artifact of our choice of eye plant model, appendix B gives a more detailed analysis of the relation between the required change in steady-state muscle innervation (i.e. activity in the tonic neurons) and the muscle innervation change during a saccade.

Length-tension-innervation relation

The length-tension-innervation relation of the muscles was measured by Robinson (1975b), Miller et al. (1999) and Collins (1975) and is shown in figure 2.10. Depending on the degree of muscle stretch (i.e. the orientation of the eye) the force-innervation

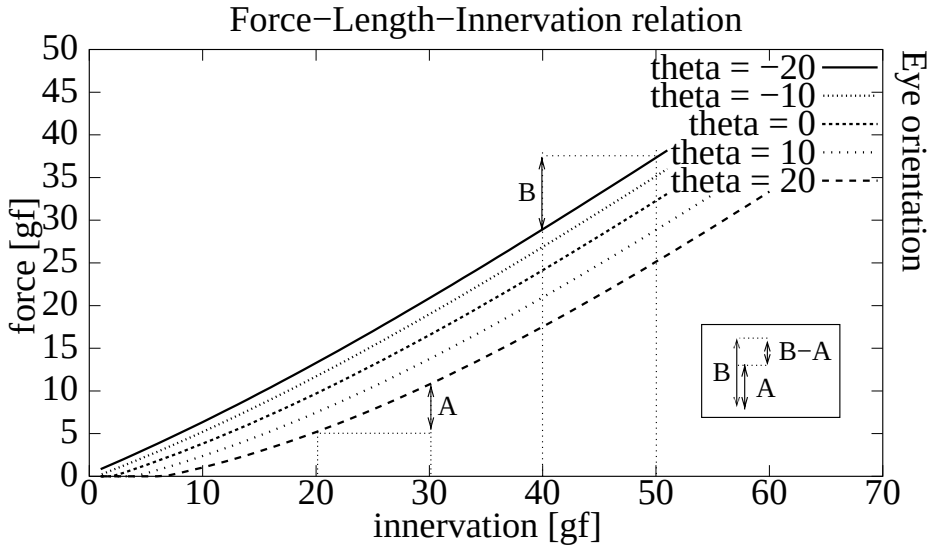

Figure 2.10: Force-Length-Innervation curves showing the relationship between the contractile force generated by an extraocular muscle and its neural innervation for various degrees of muscle stretch (eye orientations). The orientation of the eye ('theta') is given in degrees. The primary position orientation is indicated by 'theta' = 0. Positive values of 'theta' correspond to eye orientations to the right and negative values correspond to orientations to the left of the primary position. 'A' indicates the step in contractile muscle force resulting from a 10gf increase of innervation when the eye is oriented 20° rightward with an initial activity level of 20gf. 'B' indicates the step in contractile muscle force resulting from a 10gf increase in muscle innervation when the eye is oriented 20° leftward with an initial innervation level of 40gf. The inset 'B-A' indicates the difference between 'A' and 'B'. (Data from Miller, 1999)

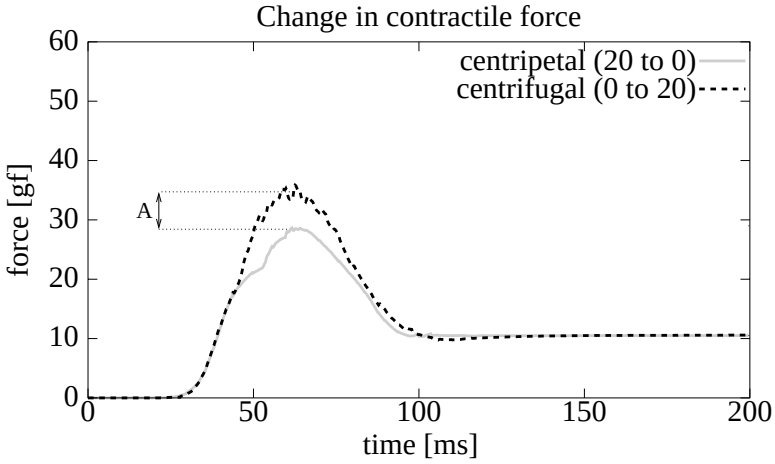

Figure 2.11: Change in total contractile force (& muscle innervation) during centripetal and centrifugal saccades between the central position and the target at 20° eccentricity. 'A' indicates the difference in maximum change in generated contractile force.

relation is altered as indicated by the different curves in figure 2.10. Due to the non-linearity of the force-innervation curves the same step in innervation change will result in different sized steps in force change, depending on the initial eye orientation and muscle innervation (figure 2.10 'B-A').

The effect of this length-tension-innervation relation on centripetal and centrifugal saccades (i.e. the contractile force changes) can be seen in figure 2.11, which shows the simulated change in total force generation (i.e. change in $F_{a_{\mathrm{lr}}} - F_{a_{\mathrm{mr}}}$ in figure 2.3) resulting from the muscle innervation profiles during centrifugal and centripetal saccades (figure 2.7). Even though there was no difference in the maximum change in total innervation (figure2.7 'A') between the centrifugal and centripetal saccades, there is a clearly discernible difference in the resulting maximum change in contractile force (figure 2.11 'A').

The length-tension-innervation relation results in a larger maximum change in contractile force during centrifugal saccades than during centripetal ones (figure 2.11 'A'). This is contrary to the difference in F_{active} where we found that the maximum change in F_{active} is greater for centripetal than for centrifugal saccades (figure 2.6 'A'). The cause of the difference in F_{active} and thus the cause of the kinematic differences during centripetal and centrifugal saccades, therefore, cannot be in the length-tension-innervation relationship of the muscles.

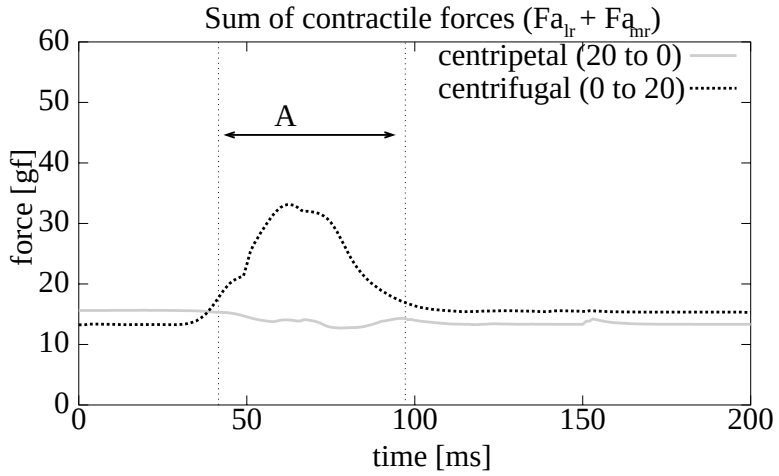

Figure 2.12: Sum of contractile forces $F_{a_{\mathrm{lr}}}$ and $F_{a_{\mathrm{mr}}}$ during centrifugal and centripetal saccades between the central position and the target at 20° eccentricity. 'A' indicates the period during which the muscle contraction rate dy/dt is most significant.

Force-velocity relation

The force-velocity relationship of the muscles (B_{lr} and B_{mr} in figure 2.3) describes the viscous force generated in the muscles as a function of the rate of muscle shortening (lengthening).

The muscle viscosity relationship that was derived by Hill (1938) and which was also used in the models by Pfann (1995) , Cook and Stark (1967) and Clark and Stark (1974a,b) is as follows:

$$F_{\mathrm{viscose}} = B\frac{dy}{dt}, \quad \text{where}$$
$$B = \begin{cases} \frac{3F_a}{H_{v_{\max}}}, & \text{when the muscle expands} \\ \frac{1.25F_a}{H_{v_{\max}}+\frac{dy}{dv}}, & \text{when the muscle contracts} \end{cases} \tag{2.2}$$

where $H_{v_{\max}} = 900\mathrm{deg/s}$ is the Hill constant characterizing the relationship to the maximum rate of muscle shortening, F_a is the contractile force of the muscle and $\frac{dy}{dt}$ is the rate of muscle shortening (lengthening).

The viscous forces in both muscles act against the movement direction. Thus the net viscous force acting on the system is the sum of the viscous forces. This is an important difference between the viscous forces and the elastic and contractile forces, which act in opposite directions in both muscles. The net viscosity coefficient B is therefore a function of $F_{a_{\mathrm{lr}}} + F_{a_{\mathrm{mr}}}$ (figure 2.12). In addition, the viscous force is a function of the contraction rate (dy/dt). The value of the viscosity coefficient B is therefore only of importance during the actual saccade (period 'A' in figure 2.12).

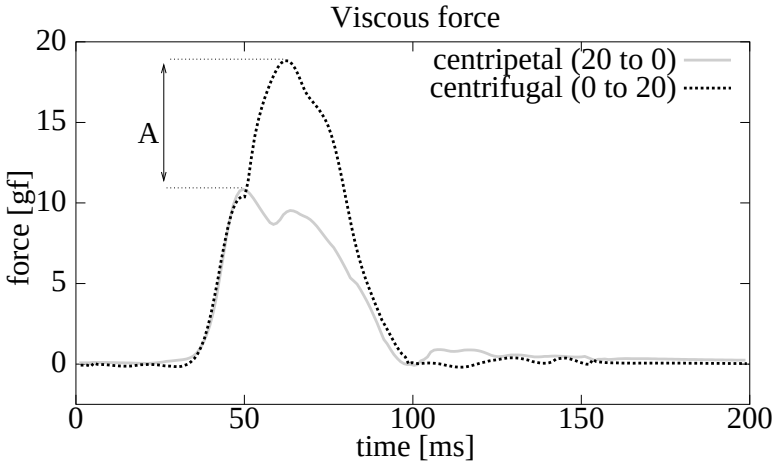

Figure 2.13: Total viscous force during centripetal and centrifugal saccades between the central position and the target at 20° eccentricity. 'A' indicates the difference in maximum viscous force.

When we simulate the viscous forces in the muscles using equation 2.2, we find that the net viscous forces during centrifugal saccades reach a much greater maximum force than during centripetal saccades (figure 2.13 'A'). Subtracting the viscous force, which acts to slow down the eye movement, from the contractile muscle force results in the net muscle force profiles shown in figure 2.14.

During centripetal saccades the resulting force profiles (figure 2.14) show a greater maximum change (figure 2.14 'A') and return to steady state faster (figure 2.14 'B') than during centrifugal saccades. This agrees with the maximum velocity and duration characteristics of centripetal and centrifugal saccades. We therefore conclude that the cause of the kinematic differences between centrifugal and centripetal saccades is in the muscle viscosity.

2.4 Discussion

The intention of the present study was to determine the cause of the kinematic differences between saccades going away from the primary position and saccades going towards the primary position. In other words, what causes centrifugal saccades to have a lower maximum velocity and a longer duration than centripetal saccades?

We measured the eye movements during centrifugal and centripetal saccades and used a model of the eye plant to simulate the muscle and orbital tissue forces acting on the eye during these saccades. Using the resulting force profiles and the data on muscle properties from experiments by Robinson (1975b, 1981), Collins et al. (1975), Miller

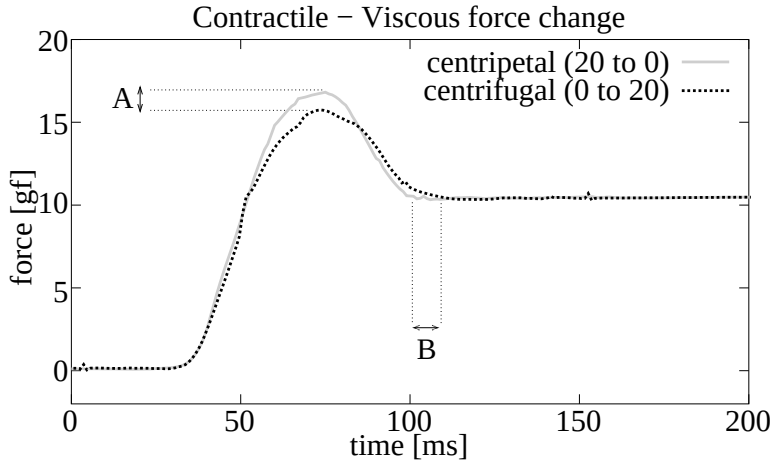

Figure 2.14: The result of subtracting the total viscous muscle force from the total change in contractile muscle force during centripetal and centrifugal saccades between the central position and the target at 20° eccentricity. 'A' indicates the difference in maximum change in the resulting force. 'B' indicates the difference in duration until steady state is reached.

and Robinson (1984) and Miller et al. (1999), we showed that the contribution of the passive forces (i.e. the muscle elasticity and orbital tissue elasticity and viscosity) to the kinematics of centrifugal and centripetal saccades differs only as a result of the difference in movement profiles. In addition, we showed that the contribution of the passive forces to the ocular kinematics favors the centrifugal saccades. From this we concluded that the passive forces cannot be the cause of the kinematic differences.

Next we investigated the active forces, i.e. the muscle contractile force and the muscle viscosity, which both depend directly on the innervation of the muscles. By synthesizing the muscle innervation that would be required to produce the active forces we showed that the total change in muscle innervation during centrifugal and centripetal saccades is nearly identical and therefore cannot be the cause of the kinematic differences. Based on the length-tension-innervation relationship of the eye muscles that was reported by Robinson (1975b) and Miller (1999) we showed that the contractile forces resulting from the innervation change are greater during centrifugal saccades than during centripetal ones. The contractile length-tension-innervation relationship therefore cannot be the cause of the observed kinematic differences either. The muscle viscosity was investigated next. We found that, due to the non-linear characteristics of the muscle viscosity as described by Hill (1938), Cook and Stark (1967), Clark and Stark (1974a,b) and Pfann (1995), the viscous force is much greater during centrifugal movements than during centripetal ones. This means that the muscle

viscosity slows down the eye movement more during centrifugal movements, resulting in a lower maximum velocity.

The muscle viscosity was the only force that showed a difference between centrifugal and centripetal saccades which could explain the observed difference in saccade kinematics. We therefore conclude that the cause of the kinematic differences during centrifugal and centripetal saccades is the non-linear force-velocity relationship of the muscles.

Implications for the saccade generator

It is generally accepted that during saccades the only feedback signal available to the system is some kind of efference copy signal which either encodes eye orientation (Robinson, 1975a) or eye displacement (Jurgens et al., 1981). Any deviations in the eye movements that are not reflected in the muscle innervation, such as mechanical defects, can therefore only be detected if they affect the amplitude and/or duration of the saccade. The result of our current investigation is that the difference between centrifugal and centripetal saccades has its cause in the mechanics of the eye plant, specifically the muscle viscosity. The difference in saccade kinematics is not reflected in the neural feedback signal. Since the amplitude of the saccades is not affected either, the only way that the saccadic system could measure these kinematic differences is if the centrifugal saccade is sufficiently slow so that the difference in duration interferes with the functioning of the visual system. From the data by Collewijn et al. (1988), the difference in saccade duration for saccades of up to 30° is less than 25ms. Considering that the minimal inter-saccadic interval during rapid search is approximately 135ms (Becker and Jurgens, 1979) it is improbable that a difference in saccade duration of (less than) 25ms is noticeable. We therefore conclude that the saccadic system is unable to detect the kinematic differences between centrifugal and centripetal saccades.

Implications for starting position dependent modulation

In section 2.3 and appendix B we showed that regardless of the lower bound cutoff of the antagonist signal the total change in muscle innervation during centrifugal and centripetal saccades is nearly identical. The reason why centrifugal and centripetal saccades have the same pattern in total change in muscle innervation is because the difference in antagonist signal cutoff is compensated by the position dependent increase in agonist signal for centrifugal saccades. According to the more recent models of the saccade generator (Quaia et al., 1999), the superior colliculus generates a saccade drive signal, based on the desired displacement of the eye, and this signal is then modulated by a signal from the cerebellum to compensate for position-dependent differences. The difference in agonist pulse activity (which compensates the cutoff effect) would thus have to be the results of the modulation signal from the cerebellum. Using the same method as we did (see appendix B) to find the difference in agonist

pulse activity during centripetal and centrifugal saccades may therefore provide a useful tool to quantify the modulation signal sent by the cerebellum.

Conclusion

By using the results of force measurements that were made in recent years (Miller et al. 1999) we were able to simulate the muscle forces during centrifugal and centripetal saccades. Using this simulation we found that the cause of the kinematic differences between centrifugal and centripetal saccades is in the muscle viscosity.

2.5 Appendix A: The eye plant model

This appendix describes the implementation of the eye plant model.

As shown in figure 2.3, the model of the eye plant consists of three distinct parts, the passive orbital tissue (including the moment of inertia of the eye ball) and the two horizontal extraocular muscles. For simplicity the models of the lateral and medial rectus muscles are identical. The four percent difference in muscle strength between the lateral and medial rectus muscles which is reported by Miller et al. (1999) was not included in our model.

The moment of inertia of the orbit was taken from (Clark and Stark 1974a) giving a value of $J = 4.3e-5\,\mathrm{gf\,s^2/deg}$. The orbital tissue force parameters were chosen such that the steady-state muscle forces given in Miller et al. (1999) would result in fixation (this determines K_o) while the time constants (τ_1, $\tau_2$and τ_3) were chosen as an average of the values given by other authors (Robinson 1981; Collins et al. 1981; Clark and Stark 1974b). The orbital tissue force is given by the following equation:

$$F_o(\theta(t)) = K_o * (\theta(t) + (\tau_1 + \tau_2)\frac{d\theta(t)}{dt} + \tau_1\tau_2\frac{d^2\theta(t)}{dt^2}) - \tau_3\frac{dF_o(\theta(t))}{dt}$$

where $\tau_1 = \frac{B_{o1}}{K_{o1}} = 50\mathrm{ms}$, $\tau_2 = \frac{B_{o2}}{K_{o2}} = 140\mathrm{ms}$, $\tau_3 = \frac{B_{o1}+B_{o2}}{K_{o1}+K_{o2}} = 80\mathrm{ms}$ and $K_o = \frac{K_{o1}K_{o2}}{K_{o1}+K_{o2}} = 0.27\mathrm{gf/deg}$.

The passive elastic force of the muscles was determined by fitting the data presented in (Miller et al. 1999). For the lateral and medial rectus muscles this works out to:

$$F_{p_{\mathrm{lr}}}(\theta(t)) = 0.002(\max(0, -\theta(t) + 35))^2,\ F_{p_{\mathrm{mr}}}(\theta(t)) = 0.002(\max(0, \theta(t) + 35))^2.$$

For the series elastic stiffness we took the average of the values given in (Robinson 1981; Clark and Stark 1974a; Pfann et al. 1995; Collins 1975) resulting in $K_{\mathrm{se}} = 2\mathrm{gf/deg}$. The muscle activation and deactivation time constants τ_a and τ_d, which determine the low-pass filter characteristic between the motoneuron activity and the muscle contraction, were taken from (Clark and Stark 1974b; Pfann et al. 1995) as 4ms and 8ms respectively. The change in muscle activity (I) as a function of the motoneuron activity is given by:

$$\frac{dI(t)}{dt} = \frac{1}{\tau_{a/d}}(I(t) - \mathrm{MN}(t).$$

The active contractile force generated by the muscles was determined using a polynomial approximation ($F_a(\theta, I) = a\delta\mathrm{l} + bI + cI\delta\mathrm{l}\ldots$, where $\delta\mathrm{l}$ is the percentage change in muscle length in relation to its relaxed length) of the length-tension-innervation data provided by Miller et al. (1999) (figure 2.10). For the lateral rectus muscle $\delta\mathrm{l}_{\mathrm{lr}}(\theta) = -\frac{53.5}{80}\theta + 13.25$, for the medial rectus muscle $\delta\mathrm{l}_{\mathrm{mr}}(\theta) = \frac{53.5}{80}\theta + 13.25$.

The muscle viscosities (B_{lr} and B_{mr}) determining the force-velocity relationship were based on the model presented in (Pfann et al. 1995) and look as follows:

$$B_{\mathrm{lr}} = \begin{cases} \frac{3F_{a_{\mathrm{lr}}}}{H_{v_{\max}}}, & \text{if } \frac{dy_1}{dt} < 0 \\ \frac{1.25F_{a_{\mathrm{lr}}}}{H_{v_{\max}} + \frac{dy_1}{dt}}, & \text{otherwise} \end{cases}$$

$$B_{\mathrm{mr}} = \begin{cases} \frac{3F_{a_{\mathrm{mr}}}}{H_{v_{\max}}}, & \text{if } \frac{dy_2}{dt} > 0 \\ \frac{1.25F_{a_{\mathrm{mr}}}}{H_{v_{\max}} - \frac{dy_2}{dt}}, & \text{otherwise} \end{cases}$$

where $H_{v_{\max}} = 900\mathrm{deg/s}$ is the Hill constant characterizing the relationship to the maximum rate of muscle shortening.

Using these model parameters the relationship of eye movement to muscle innervation is given by the following differential equations:

$$\frac{d\omega}{dt} = \frac{1}{J}(-F_o(\theta(t)) + F_{p_{\mathrm{lr}}}(\theta(t)) + K_{\mathrm{se}} * (y_1(t) - \theta(t)) - F_{p_{\mathrm{mr}}}(\theta(t)) - K_{se} * (\theta(t) - y_2(t))$$

$$\frac{dy_1}{dt} = \frac{F_{a_{\mathrm{lr}}} + K_{\mathrm{se}}(\theta(t) - y_1(t))}{B_{\mathrm{lr}}},\ \frac{dy_2}{dt} = \frac{-F_{a_{\mathrm{mr}}} + K_{\mathrm{se}}(\theta(t) - y_2(t))}{B_{\mathrm{mr}}}$$

2.6 Appendix B: Neural activity profiles during saccades

The motoneuron activity (MN), i.e. muscle innervation, is generally assumed to be the sum of the tonic neuron activity (TN) and the burst neuron activity (excitatory EBN for agonist, inhibitory IBN for antagonist) (Robinson 1975a, Scudder 1988, Gancarz and Grossberg 1998):

$$\mathrm{MN}_{\mathrm{agonist}} = \mathrm{TN}_{\mathrm{agonist}} + \mathrm{EBN}_{\mathrm{agonist}},\ \text{and}$$

$$\mathrm{MN}_{\mathrm{antagonist}} = \max(0, \mathrm{TN}_{\mathrm{antagonist}} - \mathrm{IBN}_{\mathrm{antagonist}}),\ \text{with}$$

$$\mathrm{TN}_{\mathrm{agoniot}}(T) = \mathrm{TN}_{\mathrm{agonist}}(0) + \alpha \int_0^T \mathrm{EBN}_{\mathrm{agonist}}(t)dt,$$

$$\mathrm{TN}_{\mathrm{antagonist}}(T) = \mathrm{TN}_{\mathrm{antagonist}}(0) - \beta \int_0^T \mathrm{IBN}_{\mathrm{antagonist}}(t)dt,$$

where α and β are synaptic gain factors and T is the duration of the saccade.

Tonic neuron activities at the beginning and end of saccades (i.e. the steady-state values) are known from the data by Miller et al. (1999, figure 2.9). Assuming that the shape of the burst neuron activity profile is the same for centrifugal and centripetal saccades, i.e. any difference in motoneuron activity is the result of the lower-bound cutoff effect described by Pelisson and Prablanc (1988) (see section 2.1), the only free parameters that are left are α and β. Different values of α and β result in different MN profile shapes, altering the height of the pulse part in the pulse-step profile. The values that we chose for our main work were chosen to give a pulse-step profile whose shape corresponds to the data reported by Collins (1975), Robinson (1975a) and Cullen et al. (1997). To test the effect of different α and β values we varied α and β from 4 to 32 in steps of 4. Values of α larger than 32 cause the MN profiles to lose the pulse-step shape reported in the literature (Collins, 1975; Robinson, 1975a; Cullen et al., 1997). The values we used in the main text were $\alpha = 16$, and $\beta = 16$.

The maximum change in total activity during the centripetal saccade became larger than the maximum change in activity during centrifugal saccade when $\alpha > 16$ and $\beta < 16$. This difference was greatest when the gain factors $\alpha = 4$, $\beta = 32$ were chosen. When $\alpha < 16$ and $\beta > 16$ the maximum change in activity was larger during the centrifugal saccade than during the centripetal saccade. This difference was greatest when the gain factors $\alpha = 32$, $\beta = 4$ were chosen. Figure 2.15 shows the total change muscle innervation profiles during centripetal and centrifugal saccades for these α, β pairs for saccades between the central target and a target at 20° eccentricity.

In order to see if the greater maximum change in muscle innervation during the centripetal saccade that was achieved when $\alpha = 32$ and $\beta = 4$ could explain the difference in velocity profiles during centripetal and centrifugal saccades we also simulated the contractile muscle forces that would result from these muscle innervation profiles.

As we can see from figure 2.16 the non-linear force-length-activity relation (figure 2.10) of the muscles, which favors the centrifugal eye movement (section 2.3), has resulted in total contractile muscle force changes with the same maximum value for both the centripetal and centrifugal eye movements (figure 2.16 $a = 32$, $b = 4$).

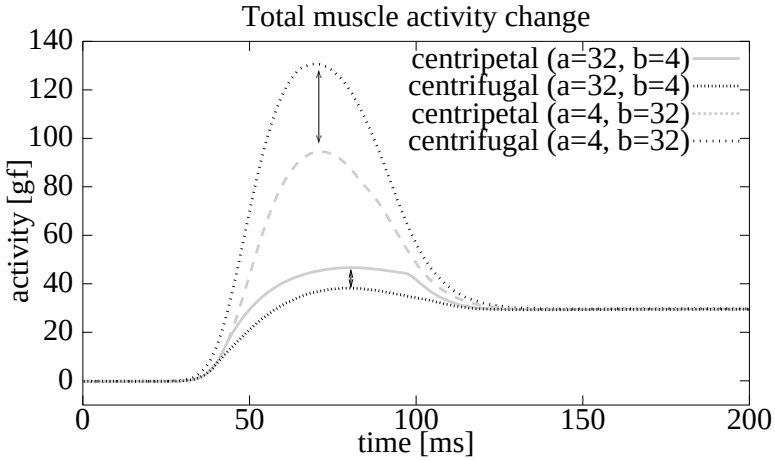

Figure 2.15: Total change in muscle innervation during centripetal and centrifugal saccades between the central target and a target at 20° eccentricity. The arrows indicate the maximum difference in total muscle innervation change for each pair of α(a) and β(b) values.

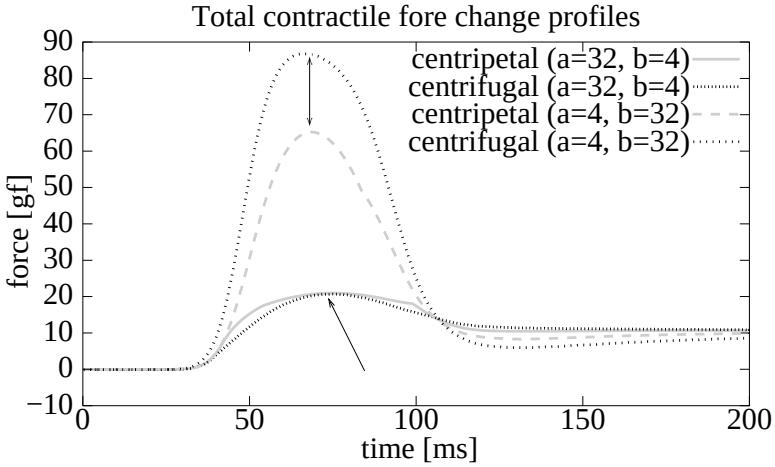

Figure 2.16: Total change in generated contractile force in the muscles during centripetal and centrifugal saccades between targets at the central position and 20° eccentric. The arrows indicate the difference in maximum contractile force change for each pair of α(a) and β(b) values.

Chapter 3

Quantification of saccadic signal modification as a function of eye orientation

Abstract

A number of recent models of saccade generation have proposed that the cerebellum modifies the saccadic signals that are sent to the eye muscles. It has been suggested that the cerebellum adjusts the saccadic command as a function of eye orientation to compensate for eye plant non-linearities. Based on data about the properties of the extraocular muscles we provide a quantification of the saccade signal modification that is needed to compensate for eye plant non-linearities. We show that the agonist and antagonist muscles require different net saccade signal gain changes and use measurements of saccade kinematics together with a model of the eye plant to analyze the dynamics of the saccade signal changes.

3.1 Introduction

More than twentyfive years ago Robinson (1975a) and Zee et al. (1976) published some of the first models of the saccade generator, i.e. the neural system that generates rapid voluntary eye rotations. These early models assumed that the saccade generator used a local feedback loop to compare the desired orientation of the eyes with an internal estimate of their actual orientation. Later work (Jurgens et al., 1981; Moschovakis, 1994; Breznen & Gnadt, 1997; Gancarz & Grossberg, 1998; Scudder, 1988) suggested that the saccadic system did not depend on absolute signals such as eye orientation, but depended on relative signals, i.e. the desired change in eye orientation. Although physiological and anatomical observations showed that several brain

structures cooperate to produce saccades, these models typically focused on the role of the superior colliculus in controlling saccades and on the firing patterns observed in brain stem motor and pre-motor neurons (e.g. Droulez & Berthoz, 1988; Waitzman et al., 1991; Lefevre & Galiana, 1992; Van Opstal & Kappen, 1993; Arai et al., 1994; Optican, 1994). The saccadic system, however, seems to be able to compensate, at least partially, for impairment of its collicular pathway (Schiller et al., 1980; Aizawa & Wurtz, 1998; Quaia et al., 1998). Cerebellar lesions, in contrast, induce permanent deficits which dramatically affect the accuracy and consistency of saccades (Optican & Robinson, 1980; Vilis & Hore, 1981; Optican, 1982; Keller, 1989; Straube et al., 1991; Sato & Noda, 1992). More recent models therefore include the cerebellum. Most studies (Dean et al., 1994; Grossberg & Kuperstein, 1989; Optican, 1986; Optican & Miles, 1985) suggest that the role of the cerebellum is to compensate for alterations of the oculomotor plant due to age or injury, and to adjust the saccadic command as a function of eye orientation (compensating for plant non-linearities). In these models the cerebellum is placed outside the feedback loop, providing a stereotyped signal as a function of initial eye orientation and desired displacement. Other models (Quaia et al., 1999; Lefevre et al., 1998) suggest that the cerebellum is part of the feedback loop and compensates for the variability present in the rest of the saccadic system during the preparation and execution of the movement.

While all of the models mentioned above describe various views of the general architecture of the saccade generator, they all make mainly qualitative predictions concerning the signals that generate saccades. Very few quantitative predictions are made. Here we will focus on the required changes in the saccade signal as a function of eye orientation, i.e. the compensation for plant non-linearities. Measurements of muscle innervation during fixation at various eye orientations (Collins et al., 1981; Collins et al., 1975; Miller & Robins, 1992; Pfann et al., 1995) revealed the non-linear relationship shown in figure 3.1. On the basis of this relationship between eye orientation (θ) and required muscle innervation (MN) we will calculate how the required net muscle innervation change (ΔMN) during a saccade depends on the starting orientation (θ_i). From this we determine the required net saccade signal gain changes in the agonist and antagonist muscles as a function of θ_i. By doing this we quantify the net cerebellar modulation of the saccade signal and show that the agonist and antagonist muscles require different gain changes.

Once we have established the required net saccade signal gain we investigate the manner in which this gain change is accomplished. Is it achieved by a change in the duration of the saccade signal, a change in the magnitude of the signal or a combination of the two? In order to investigate this we measured the velocity profiles of saccades with different starting orientations and used a model of the eye plant to calculate the corresponding muscle innervation profiles. Using these muscle innervation profiles we show that the saccade signal gain changes are accomplished primarily through changes in the magnitude of the saccade signal.

On the basis of on our results we discuss the placement of the cerebellum relative to the local feedback loop and raise the question of how the saccade generator learns the optimal level of co-contraction between the antagonistic muscles for each eye

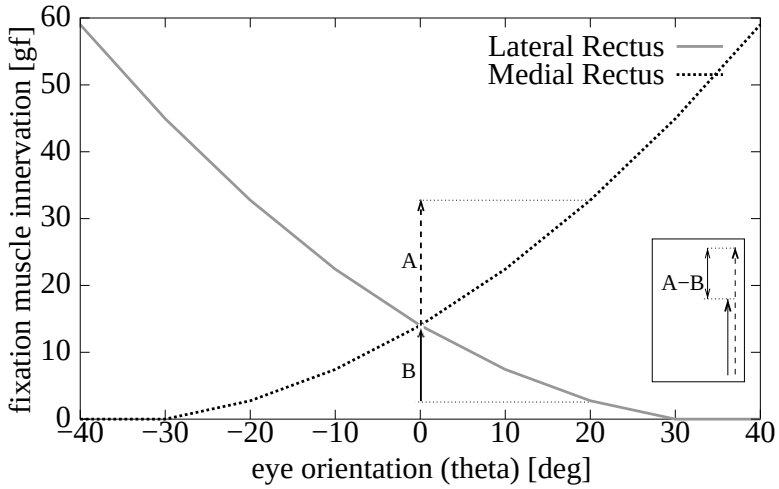

Figure 3.1: Muscle innervation during fixation as a function of eye orientation for the two horizontal muscles, i.e. the medial and lateral rectus muscles. 'A' (0 to 20) and 'B' (-20 to 0) indicate the required innervation changes in the agonist during two rightward saccades of 20° starting from different orientations. The inset 'A-B' shows the difference between 'A' and 'B'. (Data from Miller 1999)

orientation.

In order to simplify matters, and avoid the uncertainties concerning the eye plant mechanics of 3D rotations, this study was restricted to horizontal eye movements at primary position elevation.

3.2 Method

Quantifying net saccade signal changes

The quantification of the required net saccade signal gain changes, as a function of eye orientation, was based on data concerning the mechanical properties of the eye muscles, as published by Miller et al. (1999).

Non-invasive length-tension forceps (Collins et al. 1981) and implanted muscle-force transducers (Collins et al., 1975; Miller & Robins, 1992; Pfann et al., 1995) were used in these studies to measure the forces generated by the eye muscles while subjects fixated at various eye orientations. This allowed Miller et al. (1999) to model the fixation innervation of the muscles as a function of eye orientation. Figure 3.1 shows the innervation of the two horizontal muscles (the lateral rectus LR and medial rectus MR muscles) as a function of horizontal eye orientation.

The required net saccade signal gain change as a function of eye orientation is found by comparing the muscle innervation changes that are required to maintain fixation at different eye orientations. An example of this is shown in figure 3.1 where 'A' and 'B' indicate the required muscle innervation changes in the agonist for two 20° saccades with different starting orientations.

The muscle innervations calculated in this article are given in grams of force (gf) rather than spikes per second because the force-length-innervation relationship (Miller et al., 1999; Collins et al., 1981; Miller & Robinson, 1984) gives muscle innervation in grams of force. The innervation of the muscles is defined as the isometric developed force (F_a) that the muscle would generate if it were set at primary position length. This muscle innervation, although given in grams of force, is therefore always directly related to the neural message coming to the muscle.

Dynamics of saccade signal changes

The dynamics of the saccade signal changes were derived from measurements of eye movement profiles. The muscle innervation driving these saccades was calculated using an inverted model of the eye plant for horizontal movements.

Eye movement profiles

The eye movements were recorded using the magnetic search coil technique (Robinson, 1963; Collewijn et al., 1975). The movements of the right eye were sampled at 500 Hz and stored in a computer. The subject sat within the magnetic fields, his head immobilized by a bite bar. Pairs of visual targets were back-projected onto a flat screen at the height of the subject's eyes. The visual targets were Xs (24.5' of visual angle) and were constantly visible throughout the experiment. The subject was seated 1.5m in front of the screen such that the right eye was aligned with the central target. The targets were positioned at 5° degree intervals from 30° to the right to 30° to the left of the central target. The subject made self-paced saccades between these targets. Velocity profiles were computed by taking the first derivative of the measured eye position profiles. The eye movements between points of equal eccentricity were then pooled to determine the mean eye movement profile (and standard deviation) for saccades between these two respective points. We also averaged over adducting and abducting eye movements in order to remove (average out) directional effects caused by inequalities between the lateral and medial rectus muscles. For the remainder of the work only the average movement profiles were used. The acceleration profiles of these averaged eye movements were computed by taking the first derivative of the velocity profiles.

The eye plant model

The Hill-type mechanistic model of the horizontal saccadic system which is used in our work was based on similar models developed previously by Clark and Stark (1974a, b),

Collins (1975), Robinson (1981) and Pfann et al. (1995). Most of the parameter values were derived from steady-state measurements of macroscopic muscle properties (Miller et al., 1999; Collins et al., 1975; Collins et al., 1981) and quick release experiments (Cook & Stark, 1967; Collins, 1971). The remaining parameter values were taken from the models by developed Robinson, Pfann and Clark (see Appendix A). The data presented in the above-mentioned work were collected from measurements done primarily with human strabismus patients (Collins et al., 1981; Robinson et al., 1969), cats (Barmack et al., 1971; Collins, 1971; Robinson, 1964) and monkeys (Fuchs & Luschei, 1971b). Data was collected using non-invasive length-tension forceps (Collins et al., 1981) and chronically implanted muscle-force transducers (Collins et al., 1975; Miller & Robins, 1992; Pfann et al., 1995). A diagram of the model is shown in Fig 3.2.

The neural inputs (i.e. overall motoneuron activities) $\mathrm{MN_{lr}}$ and $\mathrm{MN_{mr}}$ are low-pass filtered to generate the active internal muscle forces $F_{a_{\mathrm{lr}}}$ and $F_{a_{\mathrm{mr}}}$. In each muscle, the force generator is in parallel with a non-linear dashpot, B, which represents the force-velocity relation of the active muscle. This unit is in series with an elastic element, K_{se}, which represents the connective tissue in series with contractile elements which has the experimentally measured property that an instantaneous reduction in load results in an instantaneous change in muscle length (i.e. the characteristics of a spring). This group of mechanical elements is in parallel with an elastic element, K_p, which represents the passive elastic properties of the muscle. Both F_a and K_p are non-linear. These muscle models are combined with a dual mass-spring-dashpot $(K_{\mathrm{o1}}, B_{\mathrm{o1}}, K_{\mathrm{o2}}, B_{\mathrm{o2}}, J_o)$(Robinson 1975b) representation of the orbit to model the horizontal saccadic system. Since the contributions of the vertical and oblique muscles to horizontal eye movements are negligible they have been lumped together with the model of the orbit. This simplification is of the same order of magnitude as the simplification that both horizontal muscles were assumed to be of equal effective strength.

A more precise description of the model and the parameter values that were used is given in appendix A.

Inverting the eye plant model

In order to calculate the muscle innervation during saccades we apply the eye plant model in reverse. We start with the total force moving the eye and work our way backwards to the innervation of the lateral and medial rectus muscles.

The total force moving the eye (F_{total}) was found by taking the first derivative of the measured eye velocity profiles (resulting in eye acceleration profiles) and applying Newton's third law. The passive forces (F_{passive}), which include the muscle elasticity ($K_{p_{\mathrm{lr}}}, K_{p_{\mathrm{mr}}}$), orbital viscosity ($B_{o1}, B_{o2}$) and orbital elasticity (K_{o1}, K_{o2}) and which depend directly on eye orientation and velocity properties, were derived from the measured eye movement profiles using the eye plant model. The actively generated forces (F_{active}), which depend directly on the muscle innervation and which include the contractile ($F_{a_{\mathrm{lr}}}, F_{a_{\mathrm{mr}}}$) and viscous muscle properties ($B_{\mathrm{lr}}, B_{\mathrm{mr}}$), were found by

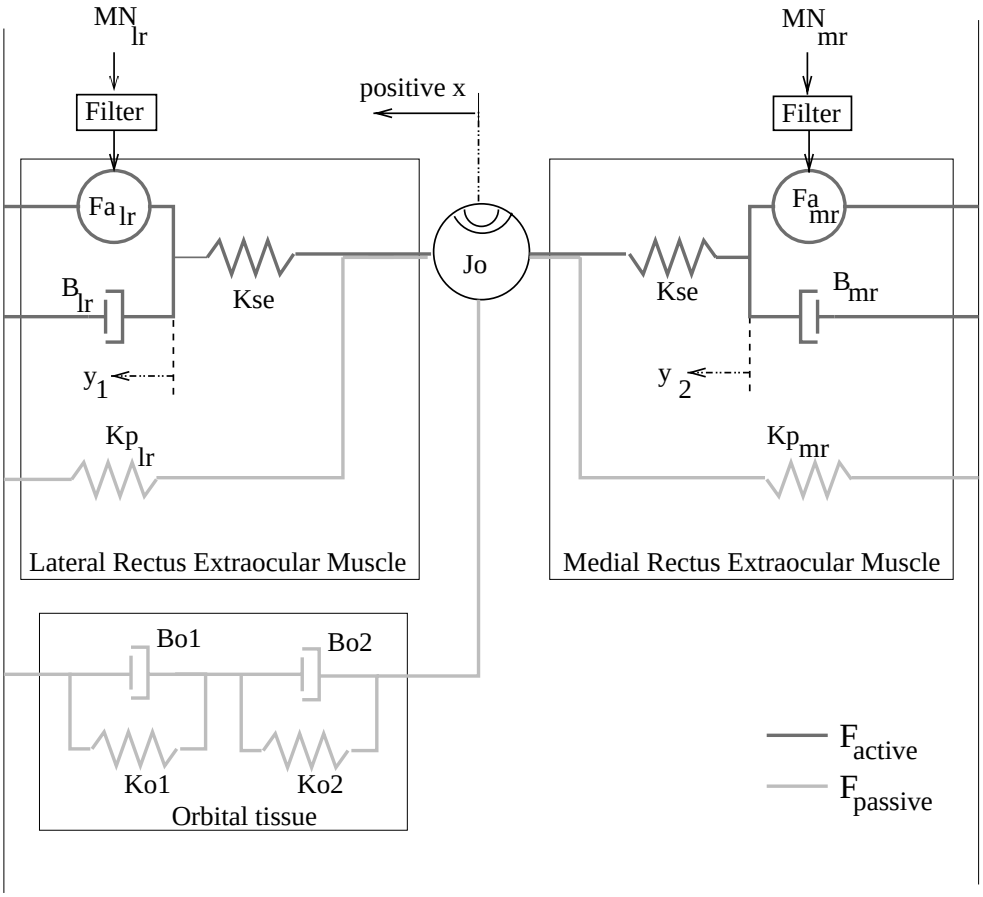

Figure 3.2: Diagram of the model of the horizontal eye plant. The lateral and medial rectus muscle variables are denoted by subscripts lr and mr respectively. The input MN is the neural input converted to its force equivalent. The force generator F_a represents the length-tension-innervation relationship of the muscles. The force-velocity relationship is provided by the viscosities $B_{\rm lr}$ and $B_{\rm mr}$. The series-elastic element is denoted $K_{\rm se}$. K_p represents the passive muscle elasticity. Orbital mechanics are modeled by a dual spring-dashpot system $(K_{\rm o1}, B_{\rm o1}, K_{\rm o2}, B_{\rm o2})$ together with the mass (J_o).

subtracting F_{passive} from F_{total}. We then used a gradient descent search algorithm to find the innervations that would generate F_{active} when used as input to our eye plant model. The search space was reduced to a single dimension by the constraint that the activity change in the antagonist is derived from the the activity change in the agonist via inhibitory inter-neurons in the brain stem (Robinson, 1975b; Hikosaka et al., 1978; Igusa et al., 1980; Yoshida et al., 1982; Strassman et al., 1986a,b; Scudder et al., 1988; Cullen & Guitton, 1997).

3.3 Results

Quantification of net saccade signal gain changes

Following the assumption that the cerebellum modifies the saccadic command as a function of eye orientation (Dean et al., 1994; Grossberg & Kuperstein, 1989; Optican, 1986; Optican & Miles, 1985) we can describe the required signal adjustment as a net gain change in the saccadic signal relative to some default signal. If the default signal generated by the superior colliculus depends only on the magnitude of the desired saccadic gaze shift ($\Delta\theta$) (Scudder, 1988; Tweed & Vilis, 1990a), then the dependence of the net saccadic signal $\Delta\text{MN}(\theta_i, \Delta\theta)$ on the starting orientation (θ_i) can be expressed by equation 3.1.

$$\Delta\text{MN}(\theta_i, \Delta\theta) = \alpha(\theta_i, \Delta\theta)\, \Delta\text{MN}(\theta_d, \Delta\theta) \tag{3.1}$$

where $\alpha(\theta_i, \Delta\theta)$ is the net saccadic signal gain for a saccade of magnitude $\Delta\theta$ and starting orientation θ_i, $\Delta\text{MN}(\theta_d, \Delta\theta)$ is the net saccadic signal for a saccade of size $\Delta\theta$ starting at θ_d and θ_d is the default starting orientation i.e. the orientation for which the signal from the superior colliculus is pre-calibrated.

Based on the steady-state data shown in Fig 3.1, the ΔMN gain α for a saccade going from θ_i to $\theta_i + \Delta\theta$ is given by equation 3.2:

$$\alpha(\theta_i, \Delta\theta) = \frac{\text{MN}(\theta_i + \Delta\theta) - \text{MN}(\theta_i)}{\text{MN}(\theta_d + \Delta\theta) - \text{MN}(\theta_d)} \tag{3.2}$$

A graphical representation of this relationship is shown in Figure 3.3 for the assumption that the default orientation θ_d is the primary position.

As can be seen by comparing the results for the required gain factors α in the agonist and antagonist muscles (left and right columns of figure 3.3), the two muscles require different gain factors for the same saccade.

Since there is good evidence that the innervation change ΔMN in the antagonist is derived from the innervation change in the agonist via inhibitory inter neurons (IBNs) in the brain stem (Robinson, 1975a; Hikosaka et al., 1978; Igusa et al., 1980; Yoshida et al., 1982; Strassman et al., 1986a,b; Scudder et al., 1988; Cullen & Guitton, 1997) we also determine the ratio β between the required ΔMN gains α in the antagonist and the agonist.

$$\beta(\theta_i, \Delta\theta) = \frac{\alpha_{\text{ant}}(\theta_i, \Delta\theta)}{\alpha_{\text{ag}}(\theta_i, \Delta\theta)} \tag{3.3}$$

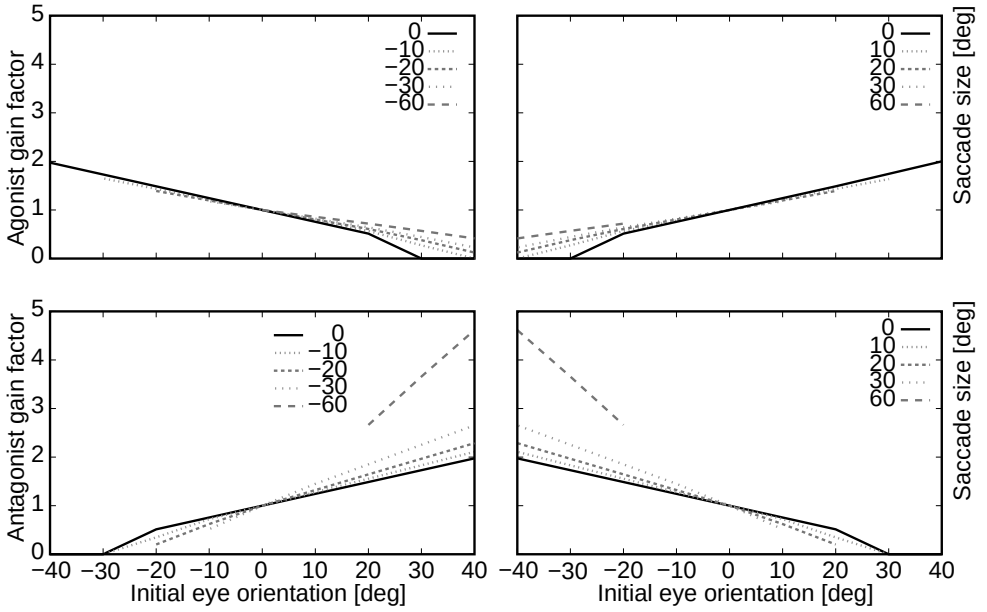

Figure 3.3: ΔMN gain α as function of saccade amplitude and starting orientation. The top plots show the required α for the agonist and the bottom plots show the required α for the antagonist. The left column shows lateral (leftward/negative) saccades and the right column shows the required values for medial (rightward/positive) saccades. The line type indicates the saccade size. Positive values correspond to movements to the right and negative values correspond to movements to the left.

where α_{ant} and α_{ag} are the required ΔMN gains in the antagonist and agonist muscles, θ_i is the initial eye orientation and $\Delta\theta$ is the change in eye orientation. A graphical representation of the ratio β is given in Figure 3.4. As can be seen from figure 3.4 the required gain β increases exponentially when the initial eye orientation of a rightward (leftward) saccade is further to the left (right). For a 10° saccade β changes by about a factor 10 as the initial orientation changes from a 20° leftward to a 20° rightward gaze.

If the saccadic signal adjustment for the agonist muscle, as a function of eye orientation, occurs prior to the signal being sent to the IBNs the antagonist signal needs to be modified by a net gain factor β at, or after, the IBNs.

Dynamics of saccade signal changes

The eye movement measurements showed the same pattern of saccade duration, skewness and maximum speed differences between saccades with different starting orientation as reported by Collewijn et al. (1988) and Pelisson and Prablanc (1988). The average position and velocity profiles for the 20° saccades are shown in figure 3.5. The results for the 10° and 15° saccades had the same characteristics and will therefore not be shown here.

In section 3.3 we quantified how the required net saccade signal gain depends on the starting orientation of the saccade. Now we analyze how this net saccade gain is achieved in terms of saccade signal duration and amplitude (i.e. neural activity). In order to do this we calculate the muscle innervation patterns that, according to our eye plant model, result in the eye movement profiles of figure 3.5. An example of the calculated muscle innervation patterns is shown in figure 3.6. To ensure temporal coordination between the agonist and antagonist muscles any changes in the saccade signal duration as a function of saccadic starting orientation will have to be present in both the muscles. Since the antagonist innervation is derived from the agonist innervation (Robinson, 1975a; Hikosaka et al., 1978; Igusa et al., 1980; Yoshida et al., 1982; Strassman et al., 1986a,b,; Scudder et al., 1988; Cullen & Guitton 1997), multiplied by a gain factor β, we will concentrate on the saccadic signal going to the agonist muscle.

From the work of Robinson (1975a) it is well known that the motoneuron signal (i.e. the muscle innervation) in the agonist muscle is the sum of a phasic pulse from the excitatory burst neurons (EBNs) and a tonic step from the tonic neurons (TNs). Since the tonic neuron activity is the temporal integration of the EBN activity the dynamics of the eye movement are controlled by the shape (amplitude and duration) of the EBN profiles. How the cerebellar contribution alters the magnitude and/or duration of the saccadic signal is therefore reflected by the shape of the EBN burst. By removing the TN signal from the muscle innervation profiles in figure 3.6 we are left with the EBN burst profiles shown in figure 3.7.

To quantify the changes in the EBN burst profile as a function of saccade-starting-orientation we determined the duration and maximum spike rate of the EBN burst profiles. The duration of the EBN burst was defined as the time during which the

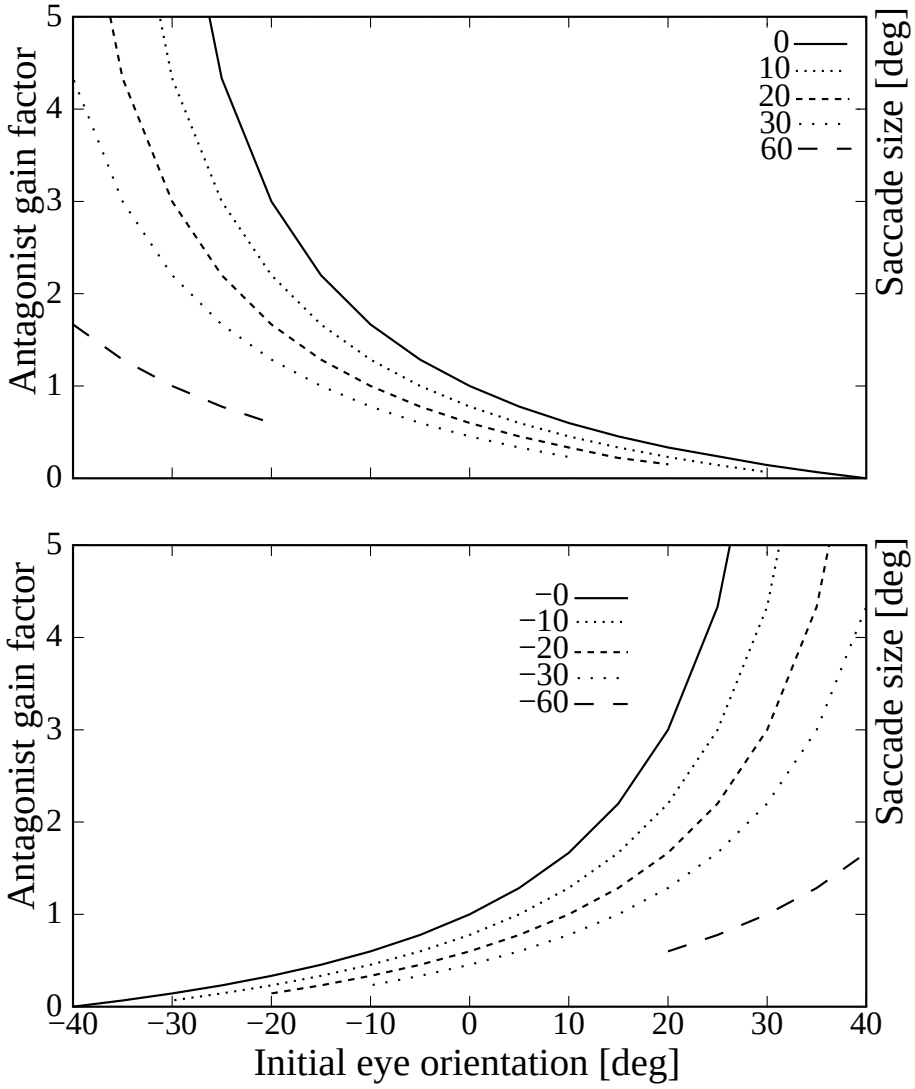

Figure 3.4: Ratio β between required ΔMN gain in antagonist and agonist muscles as a function of saccade amplitude and starting orientation. The top plot shows β for medial (rightward/positive) saccades and the bottom plot shows β for lateral (leftward/negative) saccades. The line type indicates the saccade size. Positive values correspond to movements to the right and negative values correspond to movements to the left. *(for display purposes the gain values higher than 5 are not shown)*

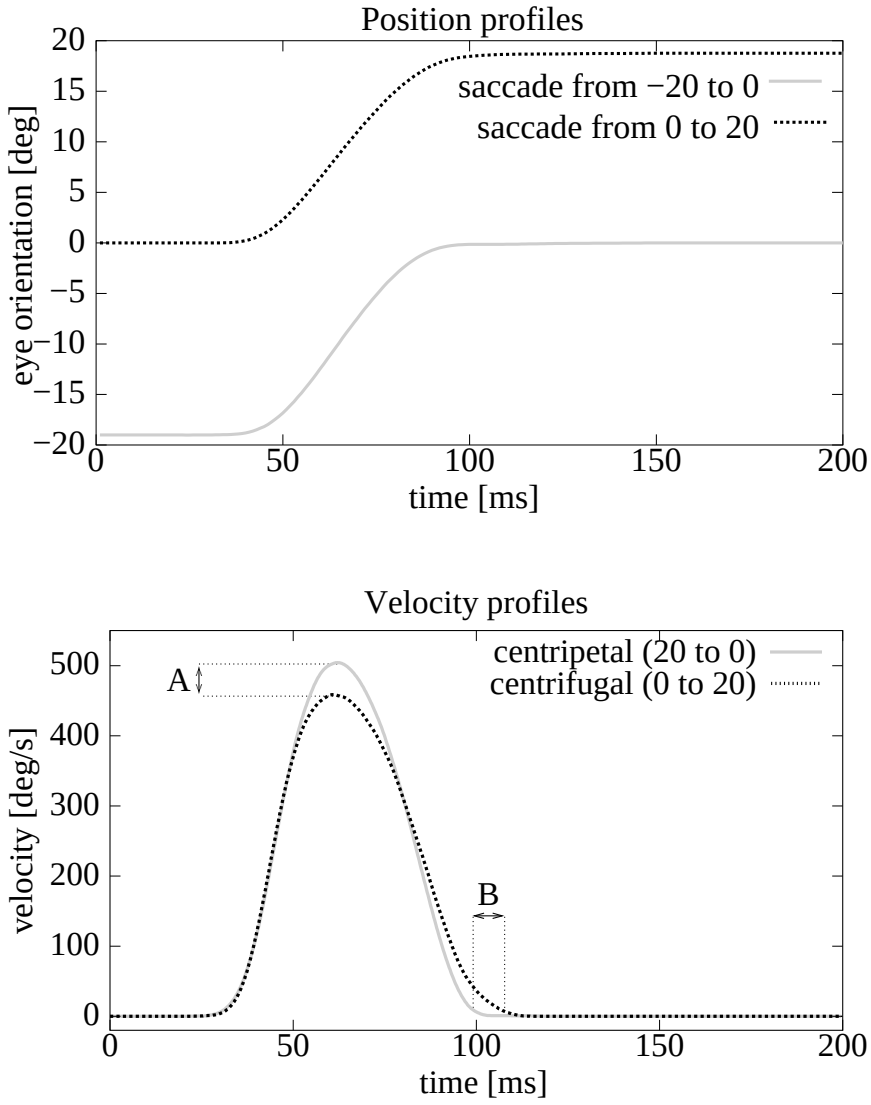

Figure 3.5: Average movement profiles for 20° rightward saccades with starting orientations at −20° and 0° eccentricity. The characteristic differences in maximum saccade velocity (A) and saccade duration (B) are indicated in the lower figure.

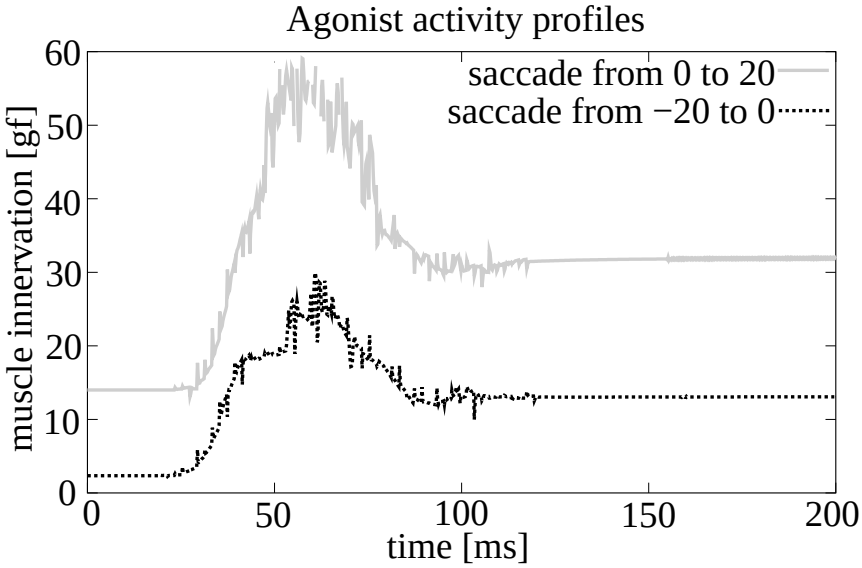

Figure 3.6: Muscle innervation profiles showing the agonist (solid line) and antagonist (dashed line) muscle innervation during 20° saccades. The solid black line shows the innervation pattern for a rightward saccade from 0° to 20° rightward gaze. The dashed gray line shows the innervation pattern for a rightward saccade from −20° to 0° leftward gaze.

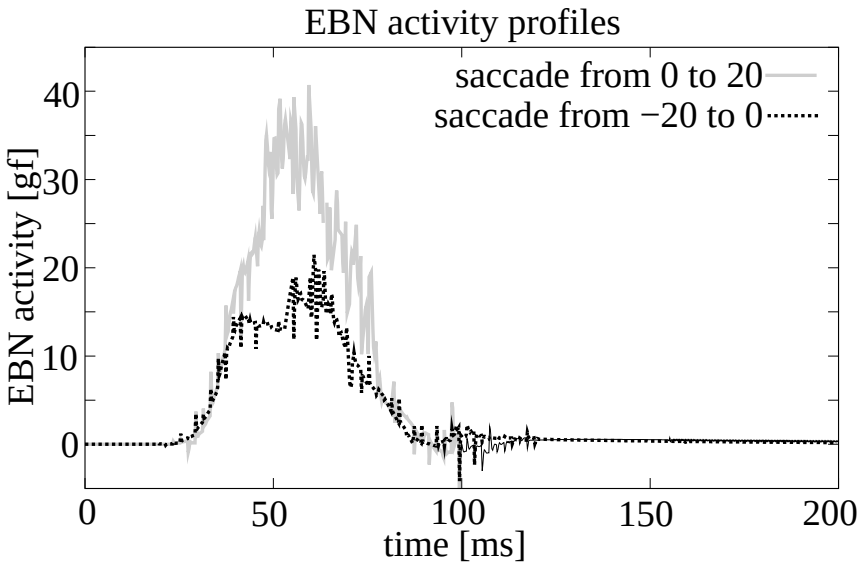

Figure 3.7: EBN burst profiles of 20° saccades with starting orientations at −20° and 0° eccentric.

mean signal over 10ms was greater than 1gf. The max EBN spike rate (amplitude) was defined as the peak mean activity over 10ms. The dashed lines in figure 3.8 show the EBN burst duration (top 2 panels) and max EBN spike rate (bottom 2 panels) of the measured saccades as ratios of the EBN burst duration/spike-rate for a saccade starting at the default orientation (primary position). The solid line in the top panel of figure 3.8 shows the EBN burst durations that would be required to achieve the net saccade signal gain α by only changing the burst duration. The solid line in the bottom panel of figure 3.8 shows the EBN spike rate that would be required to achieve the net signal gain α by only changing the burst amplitude.

By comparing the required EBN signal changes (solid lines) with the EBN signal changes we derived from the eye movement profiles (dashed lines), we show in figure 3.8 that the change in max EBN burst rate as a function of eye orientation generally follows the required EBN signal changes. In contrast, the EBN burst duration shows no clearly consistent dependence on saccade-starting-orientation. A comparison using a t-test showed that the error made by the regression line through the data is not significantly different (at 95% confidence) from the error made by predicting the data using the hypothesis that changes in the max EBN burst rate account for the required changes in the saccade signal. The error in predicting the data, using the hypothesis that changes in the EBN burst duration account for the required changes in the saccade signal, did show a significant difference (at 95% confidence) when compared

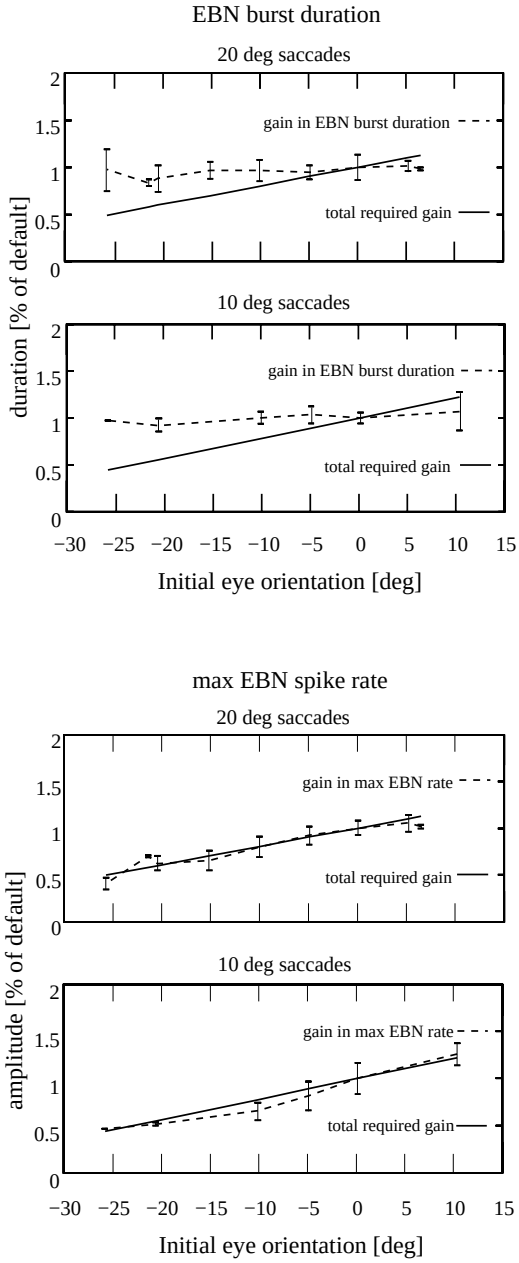

Figure 3.8: EBN burst duration (top) and max EBN spike rate (bottom) relative to the EBN burst duration and spike rate of the signal at the 'default' eye orientation (here chosen as the primary position orientation).

to the regression line.

We conclude that the cerebellar adjustment of the saccade signal, as a function of starting orientation, is achieved primarily by changing the max EBN burst rate.

3.4 Discussion

The purpose of this study was to quantify the cerebellar adjustment of the saccade signal as a function of eye orientation and analyze the dynamics of the signal changes. The required net signal gain changes (α) over the whole saccade were determined from the measured fixation innervations of the muscles published by Collins et al. (1981), Robinson (1975a) and Miller et al. (1999). The dynamics of the saccade signal changes were calculated from saccadic eye movement profiles using a mechanistic model of the horizontal eye plant. Besides the quantification of α shown in figure 3.3 our study revealed two further results. First, different net signal gain changes are required for the agonist (α_{ag}) and antagonist ($\alpha_{\mathrm{ant}} = \alpha_{\mathrm{ag}}\beta$) muscles. Second, the change in saccade signal gain (α_{ag}) is achieved primarily through an increase in the firing rate of the excitatory burst neurons (EBNs) with only a weak contribution from variations in the EBN burst duration.

Based on these results we will now discuss the implications of requiring different signal gains for the agonist (α_{ag}) and antagonist (α_{ant}) muscles and show what our findings concerning the dynamics of the saccade signal adjustment tell us about the placement of the cerebellar signal modification relative to the local feedback loop.

Required net saccadic signal gain changes

As was shown in figure 3.3 the agonist and antagonist muscles need different saccade signal gain changes in order to compensate for the plant non-linearities during the same saccade. The cerebellum must therefore modify the antagonist signal separately. Since there is good evidence that the innervation change ΔMN in the antagonist is derived from the innervation change in the agonist via inhibitory inter neurons (IBNs) in the brain stem (Robinson, 1975a; Hikosaka et al., 1978; Igusa et al., 1980; Yoshida et al., 1982; Strassman et al., 1986a,b; Scudder et al., 1988; Cullen & Guitton, 1997) this signal adjustment must occur in the brain stem at, or after the IBNs. If the duration of the saccadic signal is controlled by a local feedback loop using the signal that goes to the agonist muscles (as proposed by Robinson (1975a), Jurgens et al. (1981), Scudder et al. (1988), Gancarz & Grossberg, (1998)) then the signal to the antagonist will be of the same duration. The best way to ensure that the antagonist receives the required innervation is if the signal sent to the antagonist is the cerebellar modified EBN signal which is re-adjusted by the factor β, as calculated in section 3.4. To maintain signal duration, the adjustment of the antagonist signal by a factor β must take the form of a burst rate (i.e. signal amplitude) modification.

An unanswered question, so far, is how the cerebellum learns these eye-orientation-dependent gain changes. Given that there are two independent gain factors for the

agonist and antagonist muscles, there is in principle an infinite number of possible combinations of gain factors that would result in the desired eye orientation change. During fixation the only difference would be in the level of co-contraction between the two muscles. The problem therefore consists of choosing the desired level of co-contraction. The reason that the oculomotor control system does not simply minimize co-contraction by setting the innervation of the antagonist to zero is to achieve better gaze stability and improve the kinematics of eye movements. The eye can move faster if the movement is generated by a combination of increasing tension in the agonist and decreasing tension in the antagonist. Excessive co-contraction however is a waste of energy. How the cerebellum finds the level of co-contraction which optimizes these factors, and therefore which signal gains should be applied to the agonist and antagonist signals, is not known.

Dynamics of saccade signal change

As was shown in figure 3.8, our results indicate that the saccade gain modification in the agonist path (i.e. the EBN burst adjustment) is achieved primarily by adjusting the EBN burst rate (i.e. amplitude) and that there is no clearly consistent orientation-dependent change in EBN burst duration.

There are in principle three positions relative to the local feedback loop where the cerebellar signal modification can take place: before the feedback loop (figure 3.9 position 'A'), within the feedback loop (figure 3.9 position 'B') or after the feedback loop (figure 3.9 position 'C').

If the signal modification takes place before the feedback loop (figure 3.9 position 'A') the EBN burst profiles of any two saccades that require the same net change in agonist innervation ΔMN_{ag} should be the same. From the data published by Miller et al. (1999) (figure 3.1) we know that a 19° saccade from −5° to 14° requires the same ΔMN_{ag} as a 29.5° saccade from −26° to 3.5°. If we compare the dynamics of the EBN burst profiles belonging to these saccades we find that the duration of the 29.5° saccade is longer ($\overline{\text{EBNdur}} = 0.07$s, $\sigma = 0.006$) than the duration of the 19° saccade ($\overline{\text{EBNdur}} = 0.05$s, $\sigma = 0.005$). Compensating for this we find that the 19° saccade has a larger max burst rate ($\overline{\text{maxEBN}} = 34.1$gf, $\sigma = 2.84$) than the 29.5° saccade ($\overline{\text{maxEBN}} = 21.5$gf, $\sigma = 3.5$). The signal modification, therefore, cannot be limited to an adjustment prior to the feedback loop.

If the signal modification takes place within the feedback loop (figure 3.9 position 'B') then the EBN burst duration and EBN burst rate can both be adjusted. In this case any distribution of the net signal gain over EBN burst duration and firing rate is achievable. This hypothesis is therefore not falsifiable by this study.

If the signal modification occurs after the local feedback loop (figure 3.9 position 'C') then the burst duration is not affected by the signal modification. Hence there should be no eye-orientation-dependent difference in the EBN burst duration. The results shown in figure 3.8 suggest that this might be the case. A comparison using a t-test, however, reveals that the EBN burst duration for saccades with various starting orientations are significantly different (95% confidence) from the EBN burst duration

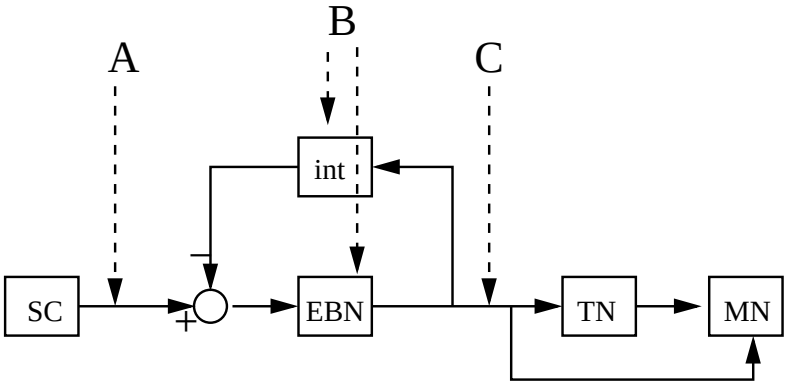

Figure 3.9: Agonist path of the saccade generator as proposed by Jurgens et al. (1981). A signal coding the desired change in eye orientation is sent from the superior colliculus (SC) to the excitatory burst neurons (EBN) and goes from there to the tonic neurons (TN) and the motoneurons (MN). A copy of the EBN signal is integrated in the feedback loop (int) and subtracted from the input signal. 'A', 'B' and 'C' indicate the positions relative to the feedback loop where the cerebellar adjustment of the saccade signal can take place.

of corresponding saccades with the default (primary) starting orientation.

by a process of elimination we find that the saccade signal adjustment by the cerebellum most probably occurs within (figure 3.9 position 'B') the local feedback loop in the saccade generator. While we cannot completely rule out the possibility that the saccade signal adjustment occurs after the feedback loop (figure 3.9 position 'C'), it most certainly does not occur prior to the local feedback loop (figure 3.9 position 'A'). The reason that the EBN burst rate is primarily adjusted, rather than the EBN burst duration, is that this is the most direct way of compensating the eye plant non-linearity. By increasing or decreasing the EBN burst rate in accordance with the length-tension-innervation relationship of the extraocular muscles the force changes generated by these muscles become independent of saccade-starting-orientation and consequently so does the resulting eye movement profile.

While not directly related to the current topic of investigation, it should also be noted that the larger max EBN rate for a 19° saccade (from −5° to 14°) than for a 29.5° saccade (from −26° to 3.5°) implies that the saturation of the maximum saccade velocity for saccades larger than 40° is probably not due to saturation of the max EBN burst rate.

Conclusion

By using the results of force measurements that were made in recent years (Miller et al., 1999) we were able to calculate how the required net muscle innervation change

(ΔMN) during a saccade depends on the starting orientation. This allowed us to quantify the net cerebellar modulation of the saccade signal and revealed that the agonist and antagonist muscles require different gain changes.

Having determined the required net saccade signal gain we analyzed the manner in which this gain change is accomplished. Using a model of the eye plant and velocity profiles of saccades with different starting orientations we calculated muscle innervation profiles. The changes in the muscle innervation profiles as a function of saccade-starting-orientation were found to be primarily in the magnitude of the saccade signal and to a much lesser degree in the signal duration.

Due to the way in which the saccade signal gain, as a function of eye orientation, is distributed over the signal amplitude (EBN burst rate) and duration (EBN burst duration) we conclude that the cerebellar adjustment of the saccade signal must take place within the local feedback loop in the brain stem.

3.5 Appendix A: The eye plant model

This appendix describes the implementation of the eye plant model.

As shown in figure 3.2 the model of the eye plant consists of three distinct parts, the passive orbital tissue (including the moment of inertia of the eye-ball) and the two horizontal extraocular muscles. For simplicity the models of the lateral and medial rectus muscles are identical. The four percent difference in muscle strength between the lateral and medial rectus muscles which is reported by Miller et al. (1999) was not included in our model.

The moment of inertia of the orbit was taken from (Clark & Stark, 1974a), giving a value of $J = 4.3e^{-5}\,\mathrm{gf\,s^2/deg}$. The orbital tissue force parameters were chosen such that the steady-state muscle forces given in Miller et al. (1999) would result in fixation (this determines K_o) while the time constants (τ_1, $\tau_2$and τ_3) were chosen as an average of the values given by other authors (Robinson, 1981; Collins et al., 1981; Clark & Stark, 1974b). The orbital tissue force is given by the following equation:

$$F_o(\theta(t)) = K_o * (\theta(t) + (\tau_1 + \tau_2)\frac{d\theta(t)}{dt} + \tau_1\tau_2\frac{d^2\theta(t)}{dt^2}) - \tau_3\frac{dF_o(\theta(t))}{dt}$$

where $\tau_1 = \frac{B_{o1}}{K_{o1}} = 50\mathrm{ms}$, $\tau_2 = \frac{B_{o2}}{K_{o2}} = 140\mathrm{ms}$, $\tau_3 = \frac{B_{o1}+B_{o2}}{K_{o1}+K_{o2}} = 80\mathrm{ms}$ and $K_o = \frac{K_{o1}K_{o2}}{K_{o1}+K_{o2}} = 0.27\mathrm{gf/deg}$.

The passive elastic force of the muscles was determined by fitting the data presented in (Miller et al., 1999). For the lateral and medial rectus muscles this works out to:

$$F_{p_{\mathrm{lr}}}(\theta(t)) = 0.002(\max(0, -\theta(t) + 35))^2,\ F_{p_{\mathrm{mr}}}(\theta(t)) = 0.002(\max(0, \theta(t) + 35))^2.$$

For the series elastic stiffness we took the average of the values given in (Robinson, 1981; Clark & Stark, 1974a; Pfann et al., 1995; Collins, 1975) resulting in $K_{\mathrm{se}} = 2\mathrm{gf/deg}$. The muscle activation and deactivation time constants τ_a and τ_d, which

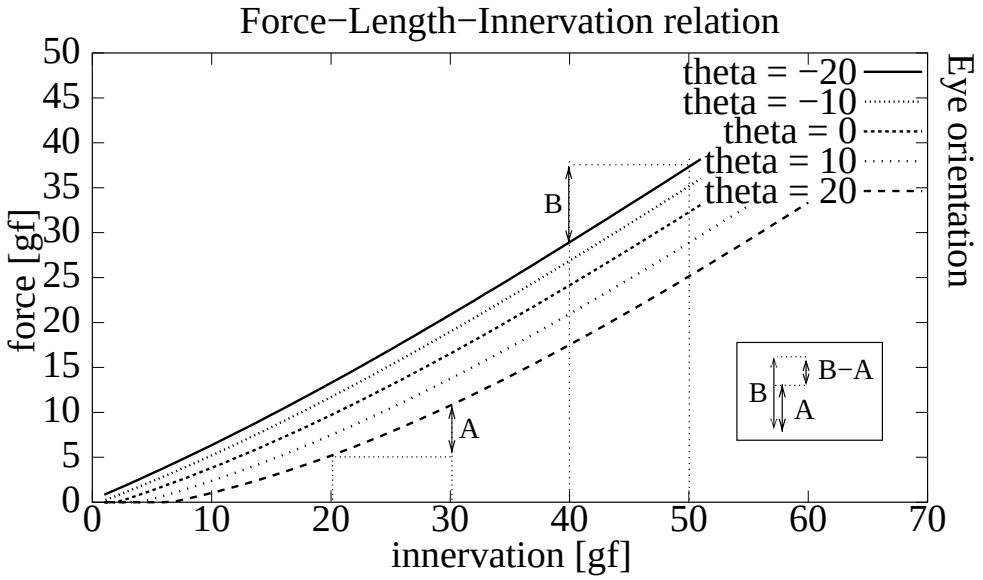

Figure 3.10: Force-Length-Innervation curves showing the relationship between the contractile force generated by an extraocular muscle and its neural innervation for various degrees of muscle stretch (eye orientations). (Data from Miller, 1999)

determine the low-pass filter characteristic between the motoneuron activity and the muscle contraction, were 4ms and 8ms respectively, as given by Clark & Stark (1974b) and Pfann et al. (1995). The change in muscle activity (I) as a function of the motoneuron activity is given by:

$$\frac{dI(t)}{dt} = \frac{1}{\tau_{a/d}}(I(t) - \mathrm{MN}(t)).$$

The active contractile force generated by the muscles was determined using a polynomial approximation ($F_a(\theta, I) = a\delta\mathrm{l} + bI + cI\delta\mathrm{l}\ldots$, where $\delta\mathrm{l}$ is the percentage change in muscle length in relation to its relaxed length) of the length-tension-activation data provided by Miller et al. (1999) (figure 3.10). For the lateral rectus muscle $\delta\mathrm{l}_{\mathrm{lr}}(\theta) = -\frac{53.5}{80}\theta + 13.25$, for the medial rectus muscle $\delta\mathrm{l}_{\mathrm{mr}}(\theta) = \frac{53.5}{80}\theta + 13.25$.

The muscle viscosities (B_{lr} and B_{mr}) determining the force-velocity relationship were based on the model presented in (Pfann et al., 1995) and are as follows:

$$B_{\mathrm{lr}} = \begin{cases} \frac{3F_{a_{\mathrm{lr}}}}{H_{v_{\max}}}, & \text{if } \frac{dy_1}{dt} < 0 \\ \frac{1.25F_{a_{lr}}}{H_{v_{\max}} + \frac{dy_1}{dt}}, & \text{otherwise.} \end{cases}$$

$$B_{\mathrm{mr}} = \begin{cases} \frac{3F_{a_{\mathrm{mr}}}}{H_{v_{\max}}}, & \text{if } \frac{dy_2}{dt} > 0 \\ \frac{1.25F_{a_{\mathrm{mr}}}}{H_{v_{\max}} - \frac{dy_2}{dt}}, & \text{otherwise} \end{cases}$$

where $H_{v_{\max}} = 900\mathrm{deg/s}$ is the Hill constant characterizing the relationship to the maximum rate of muscle shortening.

Using these model parameters the relationship of eye movement to muscle activity is given by the following differential equations:

$$\frac{d\omega}{dt} = \frac{1}{J}(-F_o(\theta) + F_{p_{\mathrm{lr}}}(\theta) + K_{\mathrm{se}} * (y_1(t) - \theta(t)) - F_{p_{\mathrm{mr}}}(\theta) - K_{se} * (\theta(t) - y_2(t))$$

and

$$\frac{dy_1}{dt} = \frac{F_{a_{\mathrm{lr}}} + K_{\mathrm{se}}(\theta(t) - y_1(t))}{B_{\mathrm{lr}}},\ \frac{dy_2}{dt} = \frac{-F_{a_{\mathrm{mr}}} + K_{\mathrm{se}}(\theta(t) - y_2(t))}{B_{\mathrm{mr}}}.$$

Chapter 4

Properties of 3D rotations and their relation to eye movement control

Abstract

Rotations of the eye are caused by the torques that the eye muscles exert on the eye. The relationship between eye orientation and the direction of the torques generated by the extraocular muscles is therefore central to any understanding of the control of three-dimensional eye movements.

Here we investigate the geometrical properties that dictate the relationship between muscle-pulling-direction and 3D eye rotations. Using first principles that describe the requirements for eye rotation and fixation we show how the direction of the torques generated by the eye muscles is related to the way the eye rotates. We show how this relation can be used to determine the muscle pulley locations that would be required by various theories of 3D eye movement control.

4.1 Introduction

The rotations of the eye are generated by the torques that the eye muscles apply to the eye. The relationship between eye orientation and the direction of the torques generated by the extraocular muscles (EOMs) is therefore central to any understanding of the control of three dimensional eye movements.

The need to understand how the direction of the torques, that are induced by the muscles (i.e axes of action of the muscles), are related to eye orientation is illustrated by the continued uncertainty about the way in which the muscle pulleys (connective tissue pulleys that serve as the functional mechanical origin of the EOMs (Miller et

al., 1993; Demer et al., 1995)) influence oculomotor control. After the existence of extraocular muscle pulleys was established (Miller et al., 1993; Demer et al., 1995) various authors (Raphan 1997, Quaia and Optican 1998, Thurtell et al. 2000, Porrill et al. 2000) argued that the muscle pulleys serve as a mechanical substrate for Listing's law, a constraint on ocular kinematics which describes the torsional orientation of the eye as a function of gaze direction (von Helmholtz 1866). The muscle pulleys would therefore allow for an essentially two-dimensional control of saccades. Others (Hepp 1994, Tweed 1997), however, argued against this, pointing out that the frequent violations of Listing's law during VOR and sleep. More recently, Demer et al. (2000) suggested that both Listing's law and its violations during VOR could be explained by actively controlled muscle pulley locations. This suggestion was subsequently brought into question by Misslisch and Tweed (2001) who argued that actively controlled pulleys still could not explain the full kinematic pattern seen in the VOR.

In this paper we examine the geometrical properties that dictate the relationship between the axes of action of the muscles and 3D eye rotations. First we specify the requirements that the oculomotor system must meet in order for the eye to be able to make the desired gaze changes and fixate at various eye orientations. Then we determine how the axes of action of the muscles are related to eye orientation and the location of the effective muscle origin (i.e the muscle pulleys). Next we show how this relation between eye orientation and the axes of action of the muscles constrains muscle pulley locations if the eye movements are controlled by specific rules. This link is illustrated by two examples in which we show how the requirements of oculomotor control strategies limit the possible muscle pulley locations. The two control theories we investigate are: 1. The oculomotor system generates eye movements that obey Listing's law, and the binocular extension of Listing's law, through active use of only the horizontal and vertical muscle pairs. 2. Oculomotor control involves perfect agonist-antagonist muscle pairing.

Finally we discuss how the geometrical properties dictating the axes of action of the muscles can be used to test the validity of oculomotor control models.

4.2 Oculomotor requirements for gaze changes and fixations

There are two basic requirements that have to be met by the oculomotor system. It must be able to generate desired gaze changes (Requirement 1) and it must be able to maintain fixation throughout the oculomotor range (Requirement 2).

The torque, or moment of force, generated by a muscle is given by.

$$\vec{T_i} = \vec{r_i} \times \vec{F_i} = T_i \hat{M_i}, \tag{4.1}$$

where $\vec{F_i}$ is the force exerted by muscle i, $\vec{r_i}$ is its moment arm, T_i is the magnitude of the torque and $\hat{M_i}$ is the axis of action (Quaia and Optican 1998) (i.e. unit moment vector (Miller and Robinson 1984)) of the muscle.

Since muscles can only pull and not push, T_i must always be larger than zero. (The torque exerted by a muscle is never zero since the muscles are stretched during primary position gaze). Using equation 4.1, Requirement 1 states that there must be at least one set of T_i such that,

$$\text{(gaze change :)} \quad \sum_{i=1}^{n} T_i \hat{M}_i(\vec{R}_c) = T_d \hat{M}_d, \tag{4.2}$$

where $T_i > 0$, n is the total number of muscles in the system, T_d and $\hat{M}_d$ are the torque magnitude and rotation axis that induce the desired gaze change and $\vec{R}_c$ is the rotation vector defining the current orientation of the eye.

Using the same notation as above, Requirement 2 states that there must be at least one set of T_i such that

$$\text{(fixation :)} \quad \sum_{i=1}^{n} T_i \hat{M}_i(\vec{R}_d) = 0. \tag{4.3}$$

where $T_i > 0$, n is the total number of muscles in the system and $\vec{R}_d$ is the rotation vector defining the desired fixation orientation of the eye.

In the following sections we will discuss the implications for oculomotor control of these requirements for gaze changes and fixations.

Implications of Requirement 1: Achieving the desired gaze change

In order for the eye to make a desired gaze change, the axis about which the eye rotates must bring the gaze direction of the eye from its initial orientation to the desired new orientation. Based on the geometrical properties of rotations every gaze shift can be achieved by rotating the eye around any axis ($\hat{M}_{\text{median}}$) in the median plane (A_{median}) between the initial and final gaze directions (figure 4.1). Which axis $\hat{M}_d \in A_{\text{median}}$ is chosen for the rotation only affects the torsional orientation of the eye (Fig 4.2). From equation 4.2, however, it follows that the eye is only able to rotate around axes that are part of the vector space (V_{eom}) spanned by the axes of action ($\hat{M}_i$) of the EOMs.

Requirement 1 therefore implies that the rotation axis ($\hat{M}_d$) for a desired gaze change must be part of the intersection of the median plane (A_{median}) and the vector space (V_{eom}) spanned by the axes of action of the eye muscles:

$$\hat{M}_d \in (V_{\text{eom}} \bigcap A_{\text{median}}). \tag{4.4}$$

In section 4.4 we will show how this requirement constrains the orientations of the axes of action of the eye muscles for different oculomotor control strategies.

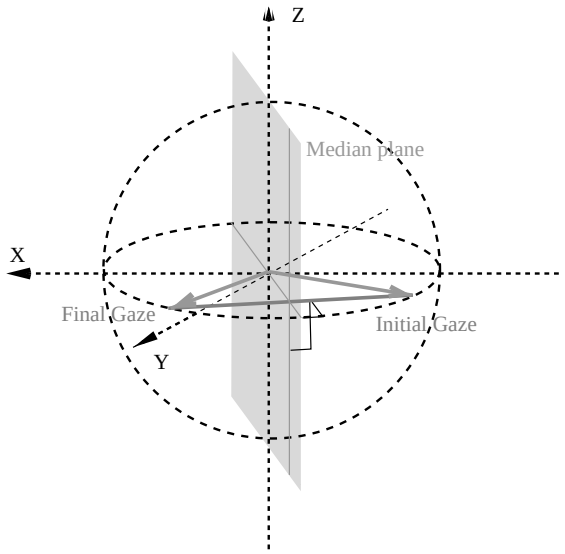

Figure 4.1: Possible rotation axes for bringing eye gaze from the initial to the desired final gaze direction. All possible rotation axes for achieving the desired change in the gaze direction lie in the Median plane between the Initial and Final gaze directions.

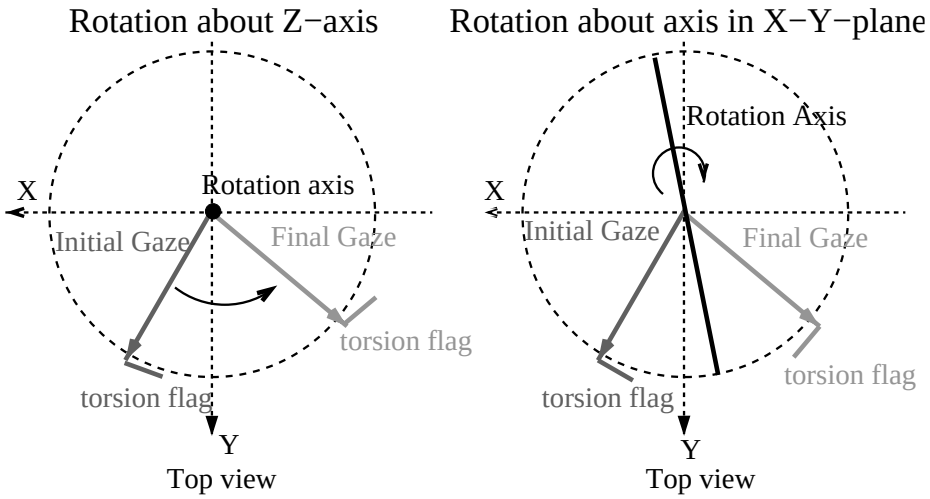

Figure 4.2: The torsional orientation of the eye following the gaze change depends on the axis around which the eye rotated. The torsional orientation of the eye is illustrated by the 'torsion flag' at the end of the gaze direction vectors.

Implications of Requirement 2: Maintaining fixation

For the eye to maintain fixation the sum of the torques ($\vec{T}_i$) generated by the EOMs must be zero (equation 4.3). Since the force exerted by each muscle is always larger than zero, the axes of action ($\hat{M}_i$) of the muscles must form an opposing system so that the torque ($\vec{T}_i$) generated by each muscle can be cancelled by the torques generated by the other muscles. Figure 4.3 shows the resulting arrangement of the axes of action for a system with two, three and four muscles.

Because an opposing system is needed so that the torques ($\vec{T}_i$) generated by the muscles can cancel each other, and allow the eye to fixate, the minimum number of muscles required for gaze changes in N dimensions is $N+1$. Rotations about a fixed axis (1D rotations) require at least two muscles and rotations about any axis in a fixed plane (2D rotations) require at least three muscles (figure 4.3). For an eye to be able rotate about any axis in space (3D rotations) at least four muscles are required, with their axes of action arranged in a tripod configuration (bottom of figure 4.3).

In section 4.4 we will show how this result constrains the orientations of the axes of action of the eye muscles for different oculomotor control strategies.

4.3 Axes of action of muscles

Equations 4.2 and 4.3 showed that the axes of action ($\hat{M}_i$) of the EOMs are central to an understanding the characteristics of the oculomotor system. We will now investigate how the axes of action of the EOMs are related to eye orientation and the location of the effective muscle origin (i.e. the muscle pulleys).

Miller et al. (1993) and Demer et al. (1995) showed that the EOM paths follow the shortest path from their insertion point on the eye to a position in the eye socket. This position is determined by connective tissue pulleys that serve as the functional mechanical origins of the muscles. Anterior to these pulleys, EOM paths shift with gaze, whereas posterior EOM paths are stable in the orbit. The muscle path determining the axis of action of an EOM is therefore given by the shortest path over the globe from the insertion point (I) to the pulley location (P).

In order to simplify the calculations the following two assumptions were made. First, the globe of the eye was modeled as a perfect sphere with the center of rotation at the center of the sphere. Second, the muscle paths were modeled as lines rather than bands (about 10mm wide). Both of these assumptions are also made in (Tweed and Vilis, 1990b; Raphan, 1998; Crawford and Guitton 1997; Quaia and Optican, 1998; Hepp, 1994; van Gisbergen et al., 1985; Demer et al., 2000).

Using a head-fixed coordinate system centered on the eye, the vectors $\vec{I}_i$ and $\vec{P}_i$, determining the insertion point and pulley position of the ith EOM, span the plane of the shortest muscle path between I_i and P_i (figure 4.4). Using a right-handed coordinate system the axis of action ($\hat{M}_i$) of an EOM is determined by

$$\hat{M}_i = \frac{\vec{I}_i \times \vec{P}_i}{\|\vec{I}_i \times \vec{P}_i\|}, \tag{4.5}$$

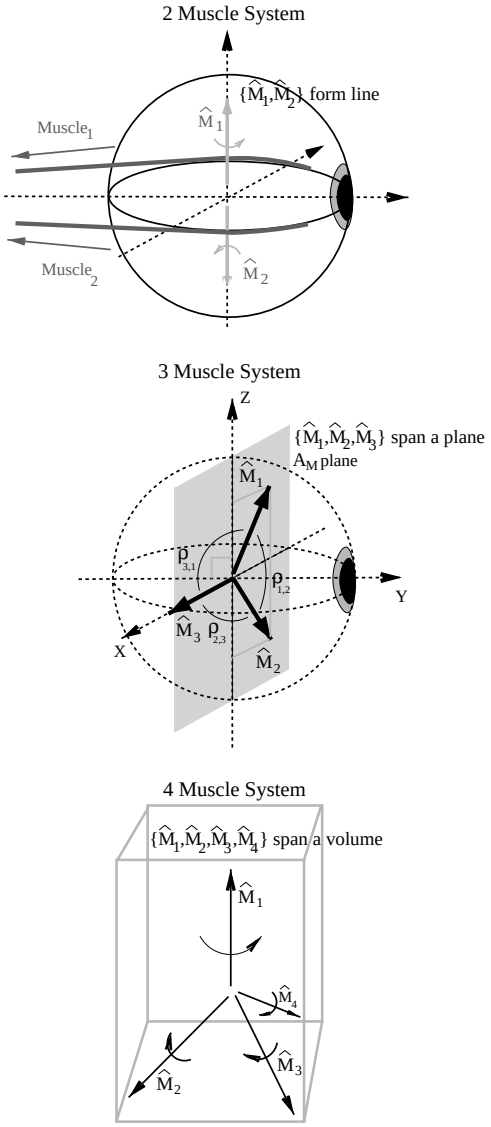

Figure 4.3: General arrangement of axes of action required for fixation. The top figure shows that in a two-muscle system the axes of action ($\hat{M}_1$ and $\hat{M}_2$) must be aligned so that their torques can cancel each other. The middle figure shows that with three muscles the largest vector space that can be spanned by the axes of action of the muscles ($\hat{M}_1, \hat{M}_2$ and $\hat{M}_3$) is a plane (A_M). For the torques to be able to cancel each other the angle (ρ) between the axes of action must be less then 180°. The bottom figure shows that with four muscles a 3D volumetric vector space can be spanned by the axes of action ($\hat{M}_1, \hat{M}_2, \hat{M}_3$ and $\hat{M}_4$).

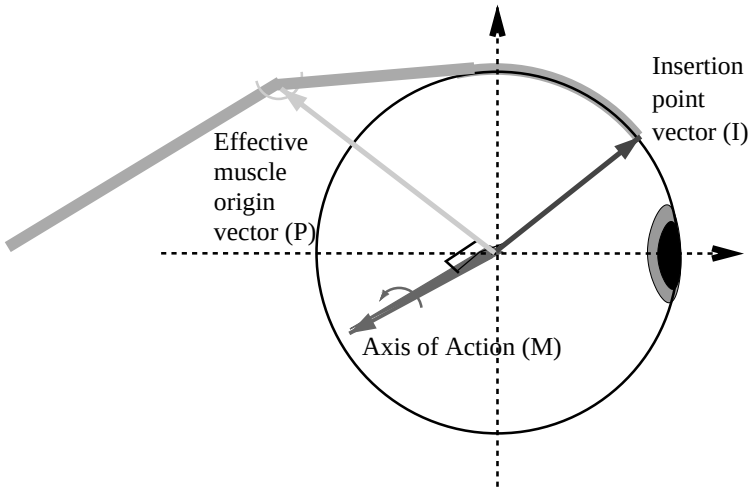

Figure 4.4: Determining the axis of action ($\hat{M}$) of a muscle. The muscle path is constrained at two points, the insertion point I on the eye ball and the effective muscle origin at the muscle pulley P. The muscle pulls I towards P. Thus the eye rotates in the $\vec{I}, \vec{P}$ plane. The axis of action $\hat{M}$ around which the muscle causes the eye to rotate is therefore perpendicular to $\vec{I}$ and $\vec{P}$.

where $\hat{M}_i$ is normalized since the axis of action, i.e. the direction of torque, does not specify anything about the force (magnitude of torque) being exerted.

Since $\vec{I}_i$ is fixed relative to the eye whereas $\vec{P}_i$ is fixed relative to the head, $\hat{M}_i$ will depend on eye orientation. The function determining how $\vec{I}_i$ depends on eye orientation is given in appendix A.

In section 4.4 we will show how this result allows us to predict where the muscle pulleys would have to be located in order for the axes of action of the eye muscles to satisfy the constraints of various oculomotor control strategies.

4.4 Effect of eye plant geometry on oculomotor control

So far we have provided an easy method to calculate the axes of action of the EOMs as a function of eye orientation and muscle pulley location and we have presented the two basic requirements that the oculomotor systems must fulfill in order for the eye to be able to fixate and make desired gaze changes. We have shown that the desired rotation axis must be part of the vector space spanned by the axes of action of the EOMs ($\hat{M}_d \in V_{\text{eom}}$, section 4.2) and that fixation requires the axes of action of the EOMs to form an opposing system (section 4.2).

Now we give three examples to show how these properties of the eye plant help us to predict the oculomotor implications of eye movement control strategies. The two control strategies we investigate are:

1. The oculomotor system generates eye movements that obey Listing's law, and the binocular extension of Listing's law, through active use of only the horizontal and vertical muscle pairs.

2. Oculomotor control involves perfect agonist-antagonist muscle pairing.

In both cases we show how the eye movement control strategy constrains the possible orientations of the axes of action of the muscles. We then demonstrate how the required orientations of the axes of action in turn constrain the space of possible muscle pulley locations that would make the control strategy possible.

Listing's law using only the horizontal and vertical muscles

Listing's law requires that the axis of rotation of a desired gaze change ($\hat{M}_d$) must be part of the plane ($A_{l/2}$) which corresponds to Listing's plane rotated relative to the primary direction over half the angle of eccentricity (half-angle rule).

$$\hat{M}_d \in A_{l/2}. \tag{4.6}$$

From section 4.2 we know that $\hat{M}_d$ must also be part of the intersection of the median plane (A_{median}), the plane between the initial and desired gaze directions, with the vector space (V_{eom}), spanned by the axes of action ($\hat{M}_i$) of the EOMs, (equation 4.4). The vector space (V_{eom}) spanned by the four axes of action of the horizontal and vertical muscles could in principle be a 3D volume (section 4.2) if the axes of action were in a 'tripod' configuration (figure 4.3). Due to the agonist-antagonist coupling of the muscles into horizontal and vertical muscle pairs, however, V_{eom} is a plane A_M. Therefore, the only way in which $\hat{M}_d$ can satisfy both equation 4.4 and equation 4.6 for all desired gaze changes is if $A_{l/2}$ and $V_{\text{eom}} = A_M$ are the same plane.

With the help of equations 4.2 and 4.3 we have so far determined that in order to obey Listing's law, using only the horizontal and vertical muscles, the possible orientations of the axes of action of these muscles ($\hat{M}_i$) are restricted to the $A_{l/2}$ plane. We will now consider the relation between $\hat{M}_i$, the muscle insertion point on the eye-ball (I_i) and the muscle pulley location (P_i) and show how this relation further confines $\hat{M}_i$ to a single possible orientation. Once we have determined $\hat{M}_i$ we will be able to calculate the corresponding muscle pulley locations.

In section 4.3 we showed that $\hat{M}_i$ can be calculated by taking the cross product of $\vec{I}_i$ and $\vec{P}_i$ (equation 4.5). The insertion point vector ($\vec{I}_i$) is known from physiology (Miller and Robinson 1984, Miller et al. 1999) and is fixed to the eye. Whatever the muscle pulley location (P_i) may be, $\hat{M}_i$ will be perpendicular to $\vec{I}_i$. Since we know from the previous paragraph that $\hat{M}_i$ must be part of the plane $A_{l/2}$, $\hat{M}_i$ must be co-linear with the intersection of the plane perpendicular to $\vec{I}_i$ with $A_{l/2}$. The axes of

action $\hat{M}_i$ that satisfy this control strategy are therefore determined by the following equation:

$$\hat{M}_i(\vec{R}) = \frac{\vec{L}_{/2}(\vec{R}) \times \vec{I}_i(\vec{R})}{\|\vec{L}_{/2}(\vec{R}) \times \vec{I}_i(\vec{R})\|}, \tag{4.7}$$

where $\hat{M}_i(\vec{R})$ is the axis of action of muscle i when the eye is at orientation $\vec{R}$, $\vec{L}_{/2}$ is the plane normal vector of $A_{l/2}$ and $\vec{I}_i(\vec{R})$ is the muscle insertion point vector.

Now that we have determined $\hat{M}_i$ we will consider which muscle pulley positions (P_i) would lead to these axes of action. From equation 4.5 we know that $\vec{P}_i$ is perpendicular to $\hat{M}_i$. For any given $\hat{M}_i$ the possible muscle pulley positions are therefore restricted to a plane (A_{P_i}). As indicated in equation 4.7, $\hat{M}_i$, and therefore also the possible muscle pulley locations, depend on the orientation of the eye ($\vec{R}$). The 'half-angle rule' of Listing's law now reveals itself as having a special property. When the rotations of the eye follow the 'half-angle rule' the planes of possible muscle pulley locations ($A_{P_i}(\vec{R})$) all have a common line of intersection. The muscle pulley position vectors $\vec{P}_i$ that fulfill the requirements of this control strategy for all eye orientations therefore have the following orientations,

$$\hat{P}_i = A_{p_i}(0) \cap A_{p_i}(\vec{R}) = \frac{\begin{bmatrix} I_{i,x}(0) \\ -I_{i,y}(0) \\ I_{i,z}(0) \end{bmatrix}}{\|\vec{I}_i(0)\|}, \tag{4.8}$$

where $I_{i,y}(0)$ is the y (anterior) coordinate of the insertion point vector $\vec{I}_i$ of muscle i when the eye is at primary position (analytical proof is given in appendix B). All other possible muscle pulley locations require that the muscle pulleys also move as a function of eye orientation.

The length of the pulley position vector ($\|\vec{P}\|$) does not affect the axis of action ($\hat{M}_i$) of the muscles. $\|\vec{P}\|$ affects the length, or stretching, of the muscle. $\|\vec{P}\|$ therefore only influences the level of muscle innervation that is required for an eye movement, not the direction in which a muscle causes the eye to rotate.

Using the results of sections 4.2, 4.2 and 4.3 we have now shown how the eye movement control strategy constrains the possible orientations of the axes of action of the muscles (equation 4.7) and the muscle pulley locations (equation 4.8).

In section 4.5 we will discuss how these results, and the results of the next subsection, allow us to test the validity of the theory that the oculomotor system generates eye movements that obey Listing's law through active use of only the horizontal and vertical muscle pairs.

Binocular Listing's law using only horizontal and vertical eye muscles

We will now calculate how the muscle pulley locations must change as a function of ocular convergence if only the horizontal and vertical muscle pairs are actively used during eye movements that obey Listing's law. Observations by van Rijn and van den

Berg (1993), Somani et al. (1998) and Stefen et al. (2000) showed that Listing's plane tilts during vergence eye movements. During convergence the Listing's planes for the two eyes rotate temporally, corresponding to the relative excyclotorsion in depression and incyclotorsion in elevation.

In order to find the muscle pulley locations that will allow the oculomotor system to generate eye movements corresponding to this binocular extension of Listing's law while using only the horizontal and vertical eye muscles, we follow the same procedure as in section 4.4 but now with Listing's plane tilted as a function of vergence. The pulley position vectors in section 4.4 are found from the orientation of the insertion point vectors ($\vec{I}_i$) and the orientation of Listing's plane. It is therefore not surprising that the orientations of the pulley position vectors ($\vec{P}_i$) change along with Listing's plane.

If the plane normal vector of Listing's plane ($\vec{L}$) at Φ° vergence is found by rotating the primary position vector by $-\frac{\Phi}{2}^\circ$ around the vertical axis ($\hat{Z}$), the corresponding pulley position vectors ($\vec{P}_i(\Phi)$) are found by rotating the pulley position vectors for zero convergence ($\vec{P}_i(0)$) by $-\Phi^\circ$ around $\hat{Z}$.

As before (section 4.4) we have only determined the orientation of the muscle pulley vectors. The length of the pulley position vectors does not affect the axes of action of the muscles and therefore cannot be calculated on that basis.

Perfect agonist-antagonist muscle pairing

The majority of models that are aimed at modeling the control of eye movements (e.g. Tweed and Vilis 1987; Haustein 1989; Schnablok and Raphan 1994; Raphan 1997; Smith and Crawford 1998; Quaia and Optican 1998; Crane and Demer 1999) assume that the antagonistic muscles work in perfect pairs and can therefore be modeled as a single unit.

Implicitly or explicitly these models assume that co-contraction of the antagonistic muscles in a muscle pair does not produce any net torque acting on the eye. From the results of section 4.2 we know that in order for a system of two muscles to be able to fixate (i.e. generate no net torque) the axes of action of the two muscles must be aligned (i.e. $\angle(\hat{M}_{\text{agonist}}, \hat{M}_{\text{antagonist}}) = 180^\circ \Leftrightarrow \hat{M}_{\text{agonist}} = -\hat{M}_{\text{antagonist}}$).

From equation 4.5 we know that the axis of action of a muscle ($\hat{M}_i$) is perpendicular to the insertion point vector $\vec{I}_i$ of that muscle. Since $\hat{M}_{\text{agonist}}$ and $\hat{M}_{\text{antagonist}}$ are aligned, $\angle(\hat{M}_{\text{antagonist}}, \vec{I}_{\text{agonist}}) = 180^\circ - \angle(\hat{M}_{\text{agonist}}, \vec{I}_{\text{agonist}})$. The axes of action of both muscles in the muscle pair ($\hat{M}_{\text{agonist}}$ and $\hat{M}_{\text{antagonist}}$) must therefore be perpendicular to the insertion point vectors of both muscles ($\vec{I}_{\text{agonist}}$ and $\vec{I}_{\text{antagonist}}$), i.e. the axes of action are perpendicular to the plane spanned by the insertion point vectors. The orientation of the axes of action of the muscles that are required in order for the assumption of perfect agonist-antagonist muscle pairing to be valid are, therefore,

determined by equation 4.9.

$$\hat{M}_{\text{agonist}} = -\hat{M}_{\text{antagonist}} = \frac{\vec{I}_{\text{antagonist}} \times \vec{I}_{\text{agonist}}}{\|\vec{I}_{\text{antagonist}} \times \vec{I}_{\text{agonist}}\|} \tag{4.9}$$

Since the orientation of $\vec{I}_{\text{agonist}}$ and $\vec{I}_{\text{antagonist}}$ is fixed relative to the eye it follows from equation 4.9 that $\hat{M}_{\text{agonist}}$ and $\hat{M}_{\text{antagonist}}$ are also fixed relative to the eye.

Now that we have determined $\hat{M}_i$ we will consider which muscle pulley positions (P_i) would result in these axes of action. From equation 4.5 we know that $\hat{M}_i$ is the cross product of $\vec{I}_i$ and $\vec{P}_i$. Since $\hat{M}_i$ and $\vec{I}_i$ are both fixed relative to the eye one obvious solution would be to have the orientation of the muscle pulley position vector ($\vec{P}_i$) also fixed relative to the eye. This however would require that the muscle pulley positions move along with every rotation of the eye. In order to minimize muscle pulley movement the pulleys would have to be located at positions that are perpendicular to $\hat{M}_i$ for a wide range of eye orientations.

For any given $\hat{M}_i$ the possible muscle pulley positions are restricted to a plane (A_{P_i}). In order to find muscle pulley positions that fulfill the requirements for perfect muscle pairing at various eye orientations we therefore need to determine the intersection of the corresponding A_{p_i} planes ($A_{p_i}(\vec{R}_1) \cap A_{p_i}(\vec{R}_2)$ where $\vec{R}_1$ and $\vec{R}_2$ are two eye orientations). Three cases can now be distinguished:

1. If the eye moves from $\vec{R}_1$ to $\vec{R}_2$ by rotating θ° about an axis $\hat{R}_{1,2}$ that is co-linear with $\hat{M}_i(\vec{R}_1)$ then $A_{p_i}(\vec{R}_1) = A_{p_i}(\vec{R}_2)\,\forall\theta$.

2. If the eye moves from $\vec{R}_1$ to $\vec{R}_2$ by rotating θ° about an axis $\hat{R}_{1,2}$ that is perpendicular to $\hat{M}_i(\vec{R}_1)$ then $A_{p_i}(\vec{R}_1) \cap A_{p_i}(\vec{R}_2) = \hat{R}_{1,2}\,\forall\theta$.

3. If the eye moves from $\vec{R}_1$ to $\vec{R}_2$ by rotating θ° about an axis $\hat{R}_{1,2}$ that is neither co-linear with nor perpendicular to $\hat{M}_i(\vec{R}_1)$ then $A_{p_i}(\vec{R}_1) \cap A_{p_i}(\vec{R}_2)$ changes as a function of θ.

We therefore conclude that there are no pulley positions that significantly reduce the frequency of pulley movement that is required to enable perfect agonist-antagonist muscle pairing.

In section 4.5 we will discuss how this result, together with the results of section 4.4, reveals a conflict between the assumption of perfect muscle pairing and the theory that the oculomotor system generates eye movements that obey Listing's law through active use of only the horizontal and vertical muscle pairs.

4.5 Discussion

The goal of this paper was to examine the geometrical properties that dictate the relationship between the axes of action of the muscles and 3D eye rotations. First we

specified the requirements that the oculomotor system must meet in order for the eye to be able to make the desired gaze changes (section 4.2) and fixate at various eye orientations (section 4.2). Then we determined how the axes of action of the muscles are related to the orientation of the eye and the location of the muscle pulleys (section 4.3). We then showed how this relation between eye orientation and the axes of action of the muscles links muscle pulley locations to oculomotor control strategies (section 4.4). This link was illustrated by two examples. The first example (section 4.4) dealt with the hypothesis that only the horizontal and vertical muscles are actively used during eye movements that obey Listing's law and the binocular extension of Listing's law. The second example (section 4.4) dealt with the assumption of perfect agonist-antagonist muscle pairing.

We will now discuss the assumptions and simplifications that were made by us in this study and then show how the geometrical properties dictating the axes of action of the muscles can be used to test the validity of oculomotor control models.

Assumptions and simplifications

Our most drastic simplification is that we included neither the viscosity in the system nor the torque generated by the combined non-muscular tissues (e.g. Tenon's capsule, optic nerve, suspensory ligaments).

The eye movements we modeled are single axis rotations (the direction of rotation does not change during the eye movement), therefore the torque generated by the viscosity is always opposite to the net-torque of the muscles driving the eye movement. Thus the addition of the viscosity term would not alter the required direction of net-muscle torque for the eye movement, it would only affect the required magnitude of the torque exerted by the muscles.

The torque ($\vec{T}_{\text{pass}}$) generated by the non-muscular tissue serves to return the eye to a mechanical neutral point at the primary position. The direction of $\vec{T}_{\text{pass}}$ when the eye is at orientation $\vec{R}$ is therefore directly opposite to the torque required to rotate the eye from the primary position to $\vec{R}$. Consequently, if, according to our model, the oculomotor system is able to rotate the eye to $\vec{R}$ it is also able to compensate for $\vec{T}_{\text{pass}}$. The inclusion of $\vec{T}_{\text{pass}}$ would not alter the direction in which the muscles can rotate the eye. It would only change the force that each muscle needs to exert to achieve the desired rotation.

Since our study focuses on the axes of action and the direction of rotation, rather than on the forces that the muscles must generate, the inclusion of the non-muscular tissue torque and the system viscosity would not alter our results.

Other simplifications that we made were the assumptions that the eye can be modeled as a perfect sphere which is rotated about its center and that there are no translational movements. In addition we simplified the calculation of the muscle paths by modeling the muscles as lines (or strings) instead of 10mm wide strips. Either explicitly or implicitly these assumptions are also made in (Tweed and Vilis, 1990b; Raphan, 1998; Crawford and Guitton, 1997; Quaia and Optican, 1998; Hepp,

1994; van Gisbergen et al., 1985; Demer et al., 2000).

Relation of eye plant geometry to oculomotor control

In section 4.4 we showed how equations 4.2, 4.3 and 4.5 provide a relation between the eye plant geometry and the oculomotor control strategies. With two examples we demonstrated how these equations enable us to find the axes of action and muscle pulley locations that are required so that the eye can follow a certain eye movement strategy. Now we will discuss how these required axes of action and muscle pulley locations can be used to test the validity of assumed oculomotor control strategies.

Axes of action for Listing's law and perfect muscle pairing

In section 4.4 we calculated the axes of action that are required to rotate the eye in accordance with Listing's law while using only the horizontal and vertical muscles. We found that for this control strategy the axes of action $\hat{M}_i$ must be part of the plane $A_{l/2}$, where $A_{l/2}$ is Listing's plane rotated relative to the primary direction over half the angle of eccentricity (half-angle rule). In section 4.4 we calculated the axes of action that are required in order to achieve perfect muscle pairing so that co-contraction of antagonistic muscles does not produce any net torque acting on the eye. For this assumption we found that the axes of action $\hat{M}_i$ need to be fixed relative to the eye, i.e. rotate with the eye over the full angle of eccentricity. These two oculomotor control schemes are therefore clearly incompatible. In order to fulfill the axis of action requirement for one of these control strategies one needs to violate the requirement for the other control strategy. This finding reveals a problem in the work by Raphan (1998) and by Quaia and Optican (1998). In both studies the eye plant is simplified by lumping the muscles into three bi-directional muscles. The authors thereby implicitly assume perfect agonist-antagonist muscle pairing. In the main part of the articles they then go on to show how the muscle pulleys (abstracted into a pulley factor) can allow their model to produce saccades that obey Listing's law without requiring active use of the oblique (torsion) muscles. The reason why the conflict between these two control strategies did not become apparent in the work by Raphan (1998) and by Quaia and Optican (1998) is that the lumped muscle pair model which they used does not reveal the requirements for keeping the agonist-antagonist axes of action aligned. Instead of ensuring that the axes of action of the antagonistic muscles remained aligned, so that the co-contraction of the muscles does not produce a net torque on the eye, they simply did not take the co-contraction into account.

Muscle pulley movement and binocular Listing's law

In section 4.4 we calculated the muscle pulley locations that will allow eye movements to obey the binocular extension of Listing's law while using only the horizontal and vertical eye muscles. The result of this calculation revealed that the muscle pulleys would have to rotate about the vertical axis ($\hat{Z}$). Recent measurements of muscle

pulley movement during vergence (Demer et al. 2002) however have shown that the primary pulley movement is a rotation of the pulley positions about the anterior-posterior axis ($\hat{Y}$). The experimentally found muscle pulley movements therefore do not support the hypothesis that vergence-related pulley movement is geared towards the control of Listing's law compliant eye movements while using only the horizontal and vertical muscle pairs.

Conclusion

This paper focused entirely on the direction of torque (i.e. axis of action) of the muscles. Using first principles that describe the requirements for eye rotation and fixation we show how the direction of the torques generated by the eye muscles is related to the way the eye rotates. The geometrical properties that dictate the relationship between muscle pulling direction and 3D eye rotations provide further insights into possible oculomotor control strategies and the location and function of the muscle pulleys.

4.6 Appendix A: Dependence of $\vec{I}$ on eye orientation

Using a rotation vector notation, the eye orientation $\vec{R}$ corresponds to the orientation that the eye would have if it were rotated from the primary position around an axis collinear to $\vec{R}$ by an angle θ, where $\theta = 2\arctan(\|\vec{R}\|)$. Using this notation the dependence of $\vec{I}$ on $\vec{R}$ can be written as

$$\vec{I}(\vec{R}) = \overrightarrow{CR} + \overrightarrow{PR}\cos(\theta) + \frac{\vec{R} \times \overrightarrow{PR}}{\|\vec{R}\|}\sin(\theta), \tag{4.10}$$

with

$$\overrightarrow{CR} = \frac{\vec{R} \cdot \vec{I}}{\|\vec{R}\|\|\vec{I}\|}\frac{\vec{R}}{\|\vec{R}\|}\|\vec{I}\| = \frac{\vec{R} \cdot \vec{I}}{\|\vec{R}\|^2}\vec{R},$$

and

$$\overrightarrow{PR} = \vec{I}(0) - \overrightarrow{CR},$$

where $\vec{I}(0)$ is the muscle insertion point vector during primary orientation gaze and $\vec{I}(R)$ is the insertion point vector for an eye orientation described by the rotation vector $\vec{R}$. Figure 4.5 gives a graphical illustration.

4.7 Appendix B: Analytical derivation of pulley positions

In order for the eye rotations to obey Listing's law we must find pulley positions such that the plane (A_M) spanned by the axes of action ($\hat{M}$) of the muscles follows

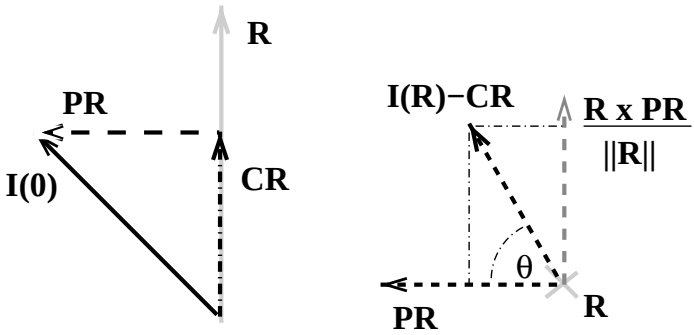

Figure 4.5: Procedure for rotating $I(0)$ around R. The figure on the left shows how $I(0)$ is first decomposed into a component PR perpendicular to R and a component CR co-linear with R. The figure to the right shows how the PR component is rotated around R.

the 'half-angle rule'. If we describe the plane A_M by its normal vector $\vec{N}$, then the 'half-angle rule' requires that at primary position $\vec{N} = [0, 1, 0]$ and that when the orientation of the eye is given by the rotation vector $\vec{R}$, $\vec{N}$ is rotated about $\hat{R}$ by half the angle. If we apply equation 4.10, substituting $\vec{N}$ for $\vec{I}_i$, we find

$$\vec{N}(R) = \cos(\theta/2)[-R_z, 1, R_x],$$

where $\vec{N}(R)$ is the A_M plane normal vector when the eye orientation is given by R and θ is the angle of gaze eccentricity.

From equation 4.5 it follows that the insertion point vector ($\vec{I}_i$) and pulley position vector ($\vec{P}_i$) of muscle i span the plane perpendicular to $\hat{M}_i$. Thus $\vec{N}$ is in the plane spanned by $\vec{I}_i$ and $\vec{P}_i$ and can be parameterized as:

$$\vec{N} = h_i(\vec{I}_i(R) + a_i\vec{P}_i), \tag{4.11}$$

where h and a are scalar values, $i = 1, 2, 3$ indicates the muscle and $\vec{I}_i(R)$ is the insertion point vector for an eye orientation described by the rotation vector $\vec{R}$.

We know that at primary orientation the pulleys are located somewhere along the primary position path of the muscle, i.e. $\vec{P}_i$ is in the $\vec{I}_i(0), \vec{O}$ plane. From this it follows that:

$$\frac{P_{i,x}}{P_{i,z}} = \frac{I_{i,x}(0)}{I_{i,z}(0)},$$

where $P_{i,x}$, $P_{i,z}$ are the x and z coordinates of $\vec{P}_i$ and $I_{i,x}(0)$, $I_{i,z}(0)$ are the x and z coordinates of the muscle insertion point I_i when the eye is in the primary position.

Since $\hat{M}_i$ does not depend on the magnitude of $\vec{P}_i$ (equation 4.5) we are really only interested in the direction of $\vec{P}_i$. Thus we only need to know the ratios $\frac{P_x}{P_y}$, $\frac{P_x}{P_z}$and $\frac{P_y}{P_z}$. We already know $\frac{P_x}{P_z}$. By filling in this result in equation 4.11 we find:

$$\frac{P_{i,y}}{P_{i,x}} = \frac{N_y \left(I_{i,z}(R) - I_{i,x}(R)\frac{I_{i,z}(0)}{I_{i,x}(0)}\right) + I_{i,y}(R)\left(N_x \frac{I_{i,z}(0)}{I_{i,x}(0)} - N_z\right)}{N_x I_{i,z}(R) - N_z I_{i,x}(R)}, \tag{4.12}$$

and

$$\frac{P_{i,y}}{P_{i,z}} = \frac{N_y \left(I_{i,z}(R)\frac{I_{i,x}(0)}{I_{i,z}(0)} - I_{i,x}(R)\right) + I_{i,y}(R)\left(N_x - N_z \frac{I_{i,x}(0)}{I_{i,z}(0)}\right)}{N_x I_{i,z}(R) - N_z I_{i,x}(R)}. \tag{4.13}$$

If we now use equation 4.10 to show how $\vec{I}_i(R)$ depends on $\vec{I}_i(0)$ and $\vec{R}$, and we restrict the eye orientations to Listing's plane (i.e. $\vec{R} = [R_x, 0, R_z]$) and have $\vec{N}$ follow the half-angle rule (i.e. $\vec{N} = \cos(\theta/2)[-R_z, 1, R_x]$) then equations 4.12 and 4.13 can be reduced to:

$$\frac{P_{i,y}}{P_{i,x}} = -\frac{I_{i,y}(0)}{I_{i,x}(0)}$$

and

$$\frac{P_{i,y}}{P_{i,z}} = -\frac{I_{i,y}(0)}{I_{i,z}(0)}.$$

The directions of the pulley position vector $\vec{P}$ and the muscle insertion point vector at primary position $\vec{I}(0)$ are therefore symmetrical with respect to the fronto-parallel (x-z) plane.

Chapter 5

Errors resulting from the use of eye plant models that treat agonist-antagonist muscle pairs as a single muscle

Abstract

We test two assumptions are commonly used in models of the oculomotor plant: the first is that the antagonistic muscles can be viewed as a single bi-directional muscle (muscle-pairing) and the second is that the three muscle pairs act in orthogonal directions. On the basis of the geometrical properties governing the muscle paths we show how these assumptions lead to incorrect predictions concerning the oculomotor signals that control eye movements. Using the same muscle activation patterns for eye plant models with and without the muscle-pairing and orthogonality assumptions we calculate the eye orientations that are reached. By comparing the differences in the simulted gaze shifts we show the significance of the error that is made when eye plant models treat agonist-antagonist muscle pairs as a single muscle and assume that the muscle pairs act in orthogonal directions.

5.1 Introduction

Various models of the oculomotor plant have been made in the past few decades. Depending on their purpose each of the models emphasizes different aspects of the oculomotor system. The more recent work has concentrated on 3D eye rotations containing horizontal, vertical and torsional components.

Some models, such as Squint (Miller and Robinson 1984) and Orbit (Miller et al. 1999), that were developed to help with the diagnosis and treatment of defects of binocular alignment (strabismus), model the forces and pulling directions of each muscle separately, but do so only for static (fixation) situations. The majority of models that are aimed at modeling the control of eye movements (e.g. Tweed and Vilis 1987; Schnablok and Raphan 1994; Raphan 1997; Smith and Crawford 1998; Quaia and Optican 1998; Crane and Demer 1999) are based on the following two simplifying assumptions. First, they treat each agonist-antagonist pair of muscles as a single bi-directional muscle, able to apply either a positive or a negative torque about a single axis. This will be referred to as the 'muscle-pairing' assumption. Second, they suppose that the three pairs of muscles (lateral and medial rectus, superior and inferior rectus and superior and inferior oblique) act in orthogonal planes. This will be referred to as the 'orthogonality' assumption.

The muscle-pairing simplification makes the tension developed by the bi-directional muscles linearly proportional to their innervation (Haustein 1989) and reduces the degrees of freedom (DOFs) for controlling the eye plant from six to three. The orthogonality assumption implies that there is no crosstalk between the torques generated by the horizontal, vertical and torsional muscle pairs.

Even though the muscle-pairing and the orthogonality assumptions are commonly used there is no experimental support for either of them.

In this paper we first show the implications of the muscle-pairing assumption for the modeling of the eye plant mechanics and then determine the errors that are introduced by the muscle-pairing and orthogonality assumptions. The errors that arrise as a result of these assumptions are evaluated by calculating the eye orientations that ensue when the same muscle activation patterns are used for eye plant models with and without these assumptions. The models we used in our examples were variations of the eye plant model developed by Raphan (1997) and Quaia and Optican (1998).

Based on the results of these simulations we discuss the validity of models that treat agonist-antagonist muscle pairs as single ideal muscles.

5.2 Implications of the muscle-pairing assumption

In order to evaluate the consequences of modeling agonist-antagonist muscle pairs as a single muscle we need to know the relationship between the muscle torques and the resulting eye velocity and orientation.

Torque-orientation relationship of the eye

The equation of motion of the eye relative to the head is given by

$$J\frac{d\vec{\omega}}{dt} = -B\vec{\omega} - K\hat{R}\theta + \sum \vec{T_i},$$

where J is the moment of inertia of the eye, $\overrightarrow{\omega}$ is the angular velocity of the eye, B and K are the viscosity and elasticity of the plant, $\hat{R}$ is the orientation of the rotation vector describing eye orientation and θ the amplitude (angle of eccentricity). The last element of the equation, $\sum_i \overrightarrow{T_i}$, is the sum of the muscle torques.

The torque, or moment of force, generated by a muscle is given by.

$$\vec{T_i} = \vec{r_i} \times \vec{F_i} = T_i \hat{M_i}, \tag{5.1}$$

where $\vec{F_i}$ is the force exerted by muscle i, $\vec{r_i}$ is its moment arm, T_i is the magnitude of the torque and $\hat{M_i}$ is the axis of action (Quaia and Optican 1998) (i.e. unit moment vector (Miller and Robinson 1984)) of the muscle.

Modeling agonist and antagonist muscles as a single unit

According to the muscle-pairing assumption the contributions of both the agonist and the antagonist to the total torque acting on the eye are modeled by a single muscle with torque

$$\overrightarrow{T}_{\text{pair}} = \overrightarrow{T}_{\text{agonist}} + \overrightarrow{T}_{\text{antagonist}}.$$

From equation 5.1 it follows that this is equivalent to

$$T_{\text{pair}} \hat{M}_{\text{pair}} = T_{\text{agonist}} \hat{M}_{\text{agonist}} + T_{\text{antagonist}} \hat{M}_{\text{antagonist}}. \tag{5.2}$$

In the models utilizing the muscle-pairing assumption (Tweed and Vilis 1987; Raphan 1997; Quaia and Optican 1998; etc.) equation 5.2 is implicitly simplified to

$$T_{\text{pair}} \hat{M}_{\text{pair}} = (T_{\text{agonist}} - T_{\text{antagonist}}) \hat{M}_{\text{agonist}} \tag{5.3}$$

$$\Rightarrow T_{\text{pair}} = T_{\text{agonist}} - T_{\text{antagonist}}, \text{ and } \hat{M}_{\text{pair}} = \hat{M}_{\text{agonist}}. \tag{5.4}$$

(When talking about the muscle-pairing assumption we will therefore always assume that this simplification is also made.) This simplification, however, is only valid when $\hat{M}_{\text{agonist}}$ and $\hat{M}_{\text{antagonist}}$ are aligned (i.e. $\angle(\hat{M}_{\text{agonist}}, \hat{M}_{\text{antagonist}}) = 180°$) so that $\hat{M}_{\text{agonist}} = -\hat{M}_{\text{antagonist}}$.

The validity of the muscle-pairing assumption, as implemented by the models in the literature, is therefore crucially dependent on the orientation of the axis of action of the muscles.

Axes of action of muscles and muscle pairs

Miller (1989), Miller et al. (1993) and Demer et al. (1995) showed that the extraocular muscles (EOMs) follow the shortest path from their insertion point on the eye to positions in the eye socket that serve as the functional mechanical origins of the muscles. The location of the functional origin of the muscle is determined by a

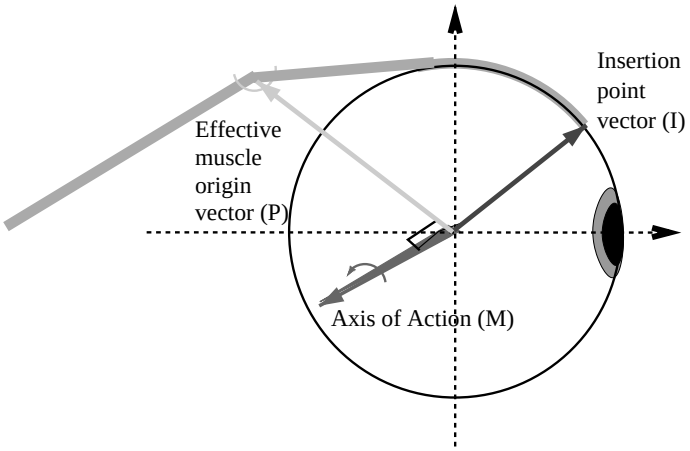

Figure 5.1: Determining the axis of action (M) of a muscle. The muscle path is constrained at two points, the insertion point I on the eye ball and the effective muscle origin at the muscle pulley P. The muscle pulls I towards P. Thus the eye rotates in the $\vec{I}, \vec{P}$ plane. The axis of action $\vec{M}$ around which the muscle causes the eye to rotate is therefore perpendicular to $\vec{I}$ and $\vec{P}$.

structure of connective tissue, referred to as pulleys. Anterior to these pulleys, EOM paths relative to the orbit shift with gaze, whereas posterior EOM paths are stable in the orbit. The axis of action of a muscle is therefore determined by the shortest path between its insertion (I) point and pulley location (P) running along the surface of the globe.

In order to simplify the calculations the following two assumptions were made. First, the globe of the eye was modeled as a perfect sphere with the center of rotation at the center of the sphere. Second, the muscle paths were modeled as lines rather than bands (of about 10mm wide). Both of these assumptions are also made in (van Gisbergen et al. 1985; Tweed and Vilis 1987; Hepp 1994; Crawford and Guitton 1997; Raphan 1998; Quaia and Optican 1998; Demer et al. 2000). The error that arises when the muscles are modeled as lines rather than bands was shown by Miller and Robinson (1984) and Porrill et al. (2000) to be acceptable, as far as normal, non-pathological eye movements are concerned.

Using a head-fixed coordinate system centered on the eye, the vectors $\vec{I}$ and $\vec{P}$, determining the EOM insertion point and pulley position, span the plane of the shortest muscle path between I and P (figure 5.1). Using a right-handed coordinate system the axis of action ($\hat{M}$) of an EOM is determined by

$$\hat{M} = \frac{\vec{I} \times \vec{P}}{\|\vec{I} \times \vec{P}\|}. \tag{5.5}$$

Since $\vec{I}$ is fixed relative to the eye whereas $\vec{P}$ is fixed relative to the head, $\hat{M}$ will depend on eye orientation. An impression of the way in which $\hat{M}$ depends on eye orientation is given in figure 5.2. The function for computing the dependence of $\vec{I}$ (relative to the head) on eye orientation is given in appendix A.

When is the muscle-pairing assumption valid?

From equations 5.2 and 5.3 we know that the muscle pairing assumption, as implemented by the models in the literature, is only valid when $\hat{M}_{\text{agonist}}$ and $\hat{M}_{\text{antagonist}}$ are aligned (i.e. $\angle(\hat{M}_{\text{agonist}}, \hat{M}_{\text{antagonist}}) = 180°$). As shown by the example given in figure 5.2, however, some orientations of the eye will lead to the axes of action of the antagonistic muscles not being aligned.

In order to determine for which orientations of the eye the muscle-pairing assumption is valid and for which it is not we now calculate the angle ρ between the axes of action of the antagonistic muscles as a function of eye orientation. For the calculation of ρ we assume that when the eye is at primary position the antagonistic muscles are aligned and the pairs of muscles (horizontal, vertical, torsional) act in orthogonal planes. This corresponds to the orthogonality assumption. The insertion points I of the muscles on the globe were located 55° out from the center of the pupil (which corresponds roughly to the data given by Miller and Robinson (1984)). The pulley positions P are assumed to be stationary and located 125° out from the center of the pupil when the eye is at primary position (pulley positions which minimize transient torsion and approximate the position suggested by Miller et al. 1999).

The contour plots in figure 5.3 show ρ as a function of gaze direction (in Euler coordinates). The torsional orientations were chosen in accordance with Listing's law (i.e. Listing torsion was set to zero).

The top plot in figure 5.3 reveals that for the horizontal muscles ρ decreases almost linearly from 180° to 155° as a function of the vertical eccentricity of the eye. The middle plot shows that the same linear decrease holds for the ρ of the vertical muscles when the eye moves horizontally. As shown in the bottom plot of figure 5.3 the ρ of the oblique muscles even decreases to 130°. For the oblique muscles this decrease in ρ is also linear but is now a function of both horizontal and vertical eye eccentricity (with a slightly stronger decrease for vertical eccentricities). The exact shape of the contour lines shown in figure 5.3 depends on the position of the muscle pulleys. The curvature of the contour lines decreases as a function of the angle between the pulley positions P and the primary position location of the center of the pupil.

We will now prove that perfect muscle-pairing at all eye orientations cannot be achieved with fixed muscle pulley locations. From equation 5.5 we know that the axis of action of a muscle ($\hat{M}_i$) is perpendicular to the insertion point vector $\vec{I}_i$ of that muscle. For $\hat{M}_{\text{agonist}}$ and $\hat{M}_{\text{antagonist}}$ to be aligned, $\angle(\hat{M}_{\text{antagonist}}, \vec{I}_{\text{agonist}}) = 180° - \angle(\hat{M}_{\text{agonist}}, \vec{I}_{\text{agonist}})$. The axes of action of both muscles in the muscle pair ($\hat{M}_{\text{agonist}}$ and $\hat{M}_{\text{antagonist}}$) must therefore be perpendicular to the insertion point vectors of both muscles ($\vec{I}_{\text{agonist}}$ and $\vec{I}_{\text{antagonist}}$), i.e. the axes of action must be perpendicular to the

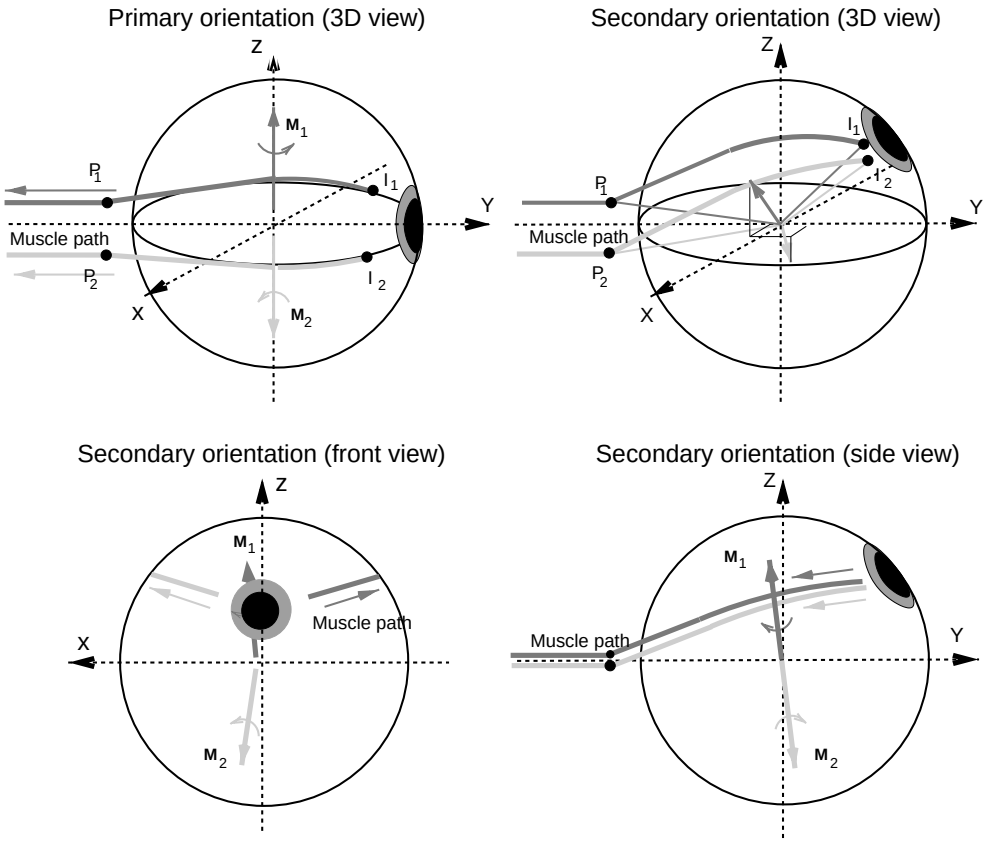

Figure 5.2: Dependence of M on eye orientation. The top left figure shows the muscle paths and axes of action of the two horizontal muscles when the eye is at primary orientation. The top right and bottom figures show how the muscle paths and axes of action shift when the eye is at secondary orientation (looking up). I indicates the location of the insertion point of the muscle on the globe. P indicates the muscle pulley location.

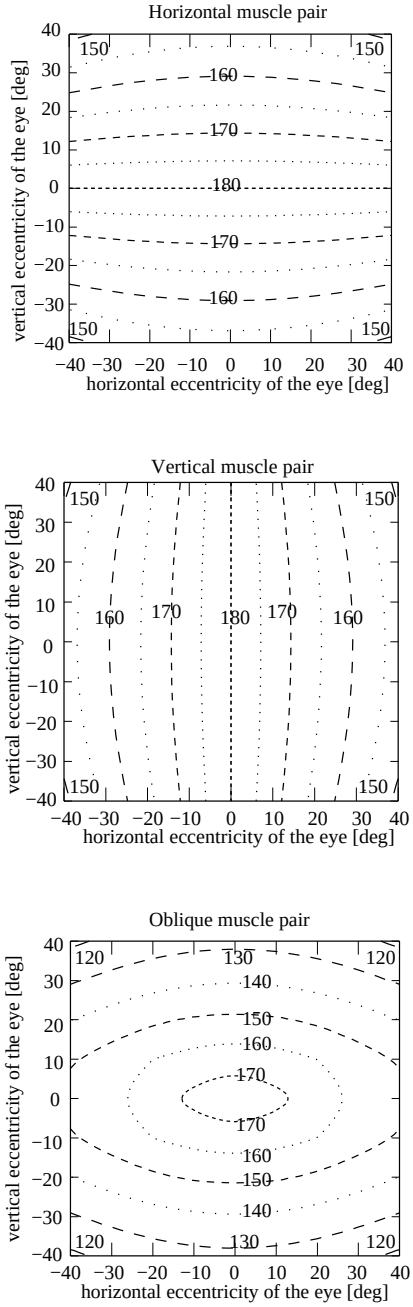

Figure 5.3: Angle ρ between M_{agonist} and $M_{\text{antagonist}}$ of the horizontal, vertical and oblique muscle pairs as a function of eye eccentricity in horizontal and vertical gaze directions.

plane spanned by the insertion point vectors. The orientation of the axes of action of the muscles, that are required in order for the assumption of perfect agonist-antagonist muscle pairing to be valid, are therefore determined by equation 5.6:

$$\hat{M}_{\text{agonist}} = -\hat{M}_{\text{antagonist}} = \frac{\vec{I}_{\text{antagonist}} \times \vec{I}_{\text{agonist}}}{\|\vec{I}_{\text{antagonist}} \times \vec{I}_{\text{agonist}}\|} \tag{5.6}$$

Since the orientation of $\vec{I}_{\text{agonist}}$ and $\vec{I}_{\text{antagonist}}$ is fixed relative to the eye it follows from equation 5.6 that $\hat{M}_{\text{agonist}}$ and $\hat{M}_{\text{antagonist}}$ are also fixed relative to the eye.

Now that we have determined $\hat{M}_i$ we will consider which muscle pulley positions (P_i) would result in these axes of action. From equation 5.5 we know that $\hat{M}_i$ is the cross product of $\vec{I}_i$ and $\vec{P}_i$. Since $\hat{M}_i$ and $\vec{I}_i$ are both fixed relative to the eye one obvious solution would be to have the orientation of the muscle pulley position vector ($\vec{P}_i$) also fixed relative to the eye. This however would require that the muscle pulley positions move along with every rotation of the eye. In order to minimize muscle pulley movement the pulleys would have to be located at positions that are perpendicular to $\hat{M}_i$ for a wide range of eye orientations.

For any given $\hat{M}_i$ the possible muscle pulley positions are restricted to a plane (A_{P_i}) perpendicular to $\hat{M}_i$. In order to find muscle pulley positions that fulfill the requirements for perfect muscle pairing at various eye orientations we therefore need to determine the intersection of the corresponding A_{p_i} planes ($A_{p_i}(\vec{R}_1) \cap A_{p_i}(\vec{R}_2)$ where $\vec{R}_1$ and $\vec{R}_2$ are two eye orientations). Based on the properties of a plane that is rotated in space we find that:

> If the eye moves from $\vec{R}_1$ to $\vec{R}_2$ by rotating θ° about an axis $\hat{R}_{1,2}$ that is neither co-linear with nor perpendicular to $\hat{M}_i(\vec{R}_1)$ then $A_{p_i}(\vec{R}_1) \cap A_{p_i}(\vec{R}_2)$ changes as a function of θ.

We therefore conclude that there are no pulley positions that significantly reduce the frequency of the pulley movement that is required to enable perfect agonist-antagonist muscle pairing.

For all orientations where at least one muscle pair is not aligned (i.e. $\rho \neq 180^\circ$) $\hat{M}_{\text{pair}}$ (the direction of torque of the muscle pair) depends on the relative force generated by the two antagonistic muscles (see equation 5.2). As mentioned at the beginning of section 5.2, most eye plant models (Tweed and Vilis 1987; Schnablok and Raphan 1994; Raphan 1997; Quaia and Optican 1998; Smith and Crawford 1998; Crane and Demer 1999) do not include this dependence of $\hat{M}_{\text{pair}}$ on the force generated by the antagonistic muscles. When the eye is not at the primary orientation, and $\rho \neq 180^\circ$, $\hat{M}_{\text{pair}}$ in these models corresponds to the average direction of the axes of action of the agonist and the antagonist muscles (see figure 5.4).

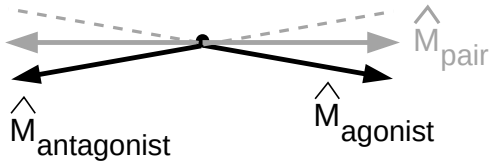

Figure 5.4: M_{pair} as used in most models. Solid lines indicate the actual axes of action of the agonist and antagonist muscles. Dashed lines show the axis of action of the *bi-directional* muscle (i.e. M_{agonist} and $M_{\text{antagonist}}$ as they are realigned to correspond to the muscle-pairing assumption).

5.3 Model comparison

In this section we determine the errors that are made by models that use the muscle-pairing and/or the orthogonality assumption. In order to do this we compare simulated fixation eye orientations for a number of muscle activity sets. In the examples shown here we used variations of the eye plant model used by Raphan (1997) and Quaia and Optican (1998). The relevant characteristics of their models are the elasticity of the eye plant (K), the force-innervation relationship of the muscles and the location of the muscle pulleys. The only one of these parameters that qualitatively influences the outcome of our simulations is the location of the muscle pulleys. As we showed in section 5.2, however, as long as the muscle pulleys are assumed to be stationary, the perfect muscle-pulling assumption is violated for most eye orientations. The general pattern of our results is therefore true for all eye plant models that assume perfect muscle pairing (e.g. Tweed and Vilis 1987; Schnablok and Raphan 1994; Raphan 1997; Smith and Crawford 1998; Quaia and Optican 1998; Crane and Demer 1999).

We first use the model that was developed by Raphan (1997), and also used by Quaia and Optican (1998), to compute the neural activity for a desired eye orientation. With these 'predicted' neural activity sets as input we then simulate the resulting eye orientation using variants of the Raphan/Quaia eye plant model with and without the muscle-pairing and/or orthogonality assumptions. Four variants of the Raphan/Quaia model were compared:

1. Paired Orthogonal: In this version antagonistic muscles are modeled as a single *bi-directional* muscle and the muscle pairs are assumed to act in orthogonal planes (when the eye is at primary position). This version corresponds to the model used by Raphan and by Quaia and Optican.

2. Paired Physiological: In this version antagonistic muscles are modeled as a single *bi-directional* muscle. The insertion points of the muscles on the eye-ball are based on data from physiological studies (Miller 1999). The muscle pairs (especially the Oblique muscles) do not act in orthogonal planes when the eye is at primary position.

LR	MR	SR	IR	SO	IO
-42	42	42	-42	0	0

Table 5.1: Neural activity predicted by the 'Paired Orthogonal' model, at 24° upward and leftward eccentricity, split into separate activity for each muscle, as required by the 'Unpaired' model variants. The activity is given in spikes/second.

3. Unpaired Orthogonal: In this version each muscle is modeled separately ($\hat{M}_{\text{agonist}}$ and $\hat{M}_{\text{antagonist}}$ are determined as described in section 5.2). The insertion points of the muscles on the eye-ball are chosen such that the muscle pairs act in orthogonal planes when the eye is at primary position. (At primary position Paired Orthogonal and Unpaired Orthogonal are identical)

4. Unpaired Physiological: In this version each muscle is modeled separately ($\hat{M}_{\text{agonist}}$ and $\hat{M}_{\text{antagonist}}$ are determined as described in section 5.2). The insertion points of the muscles on the eye-ball are based on data from physiological studies (Miller 1999). The muscle pairs (especially the Oblique muscles) do not act in orthogonal planes when the eye is at primary position.

In accordance with the Raphan/Quaia model the muscle pulleys were assumed to be stationary and were located such that transient torsion during saccades was minimized. The Paired Orthogonal variant faithfully reproduced the results of Raphan (1997) and Quaia and Optican (1998). The Unpaired and Paired variants of the eye plant model have the same muscle pulley locations.

The desired fixation orientations were Listing's law compliant eye orientations with gaze eccentricity ranging from 24° leftward to 24° rightward, and 24° upward to 24° downward, in steps of 8° (see figure 5.5 top left). Figure 5.6 shows the neural activity which, according to the Paired Orthogonal model, would cause the eye to fixate at the desired eye orientations.

For the 'Unpaired' model variants, where the axis of action of each muscle is computed separately, the activity of the muscle pairs (as given in figure 5.6) has to be separated into the activity of each of the six muscles. To split the activity of the muscle pairs into agonist and antagonist activity we assumed that the signal sent to the agonist is reciprocally related to the signal sent to the antagonist. An activity change, relative to the primary position activity, of the muscle pair by X spikes/sec was therefore translated into an activity increase in the agonist by $\frac{X}{2}$spikes/sec and an activity decrease in the antagonist by $\frac{X}{2}$spikes/sec. This assumption has been justified on empirical grounds (Robinson 1975a; Hikosaka and Kawakami 1977; Hikosaka et al. 1978; Igusa et al. 1980; Sasaki and Shimazu 1981; Yoshida et al. 1982; Strassman et al. 1986a,b; Scudder et al. 1988; Cullen and Guitton 1997). As an example, table 5.1 shows the result of separating the muscle pair activity into the neural activity of the six muscles for an eye orientation of 24° upward and leftward eccentricity. It is important to note the negative activity levels that are predicted for the lateral and

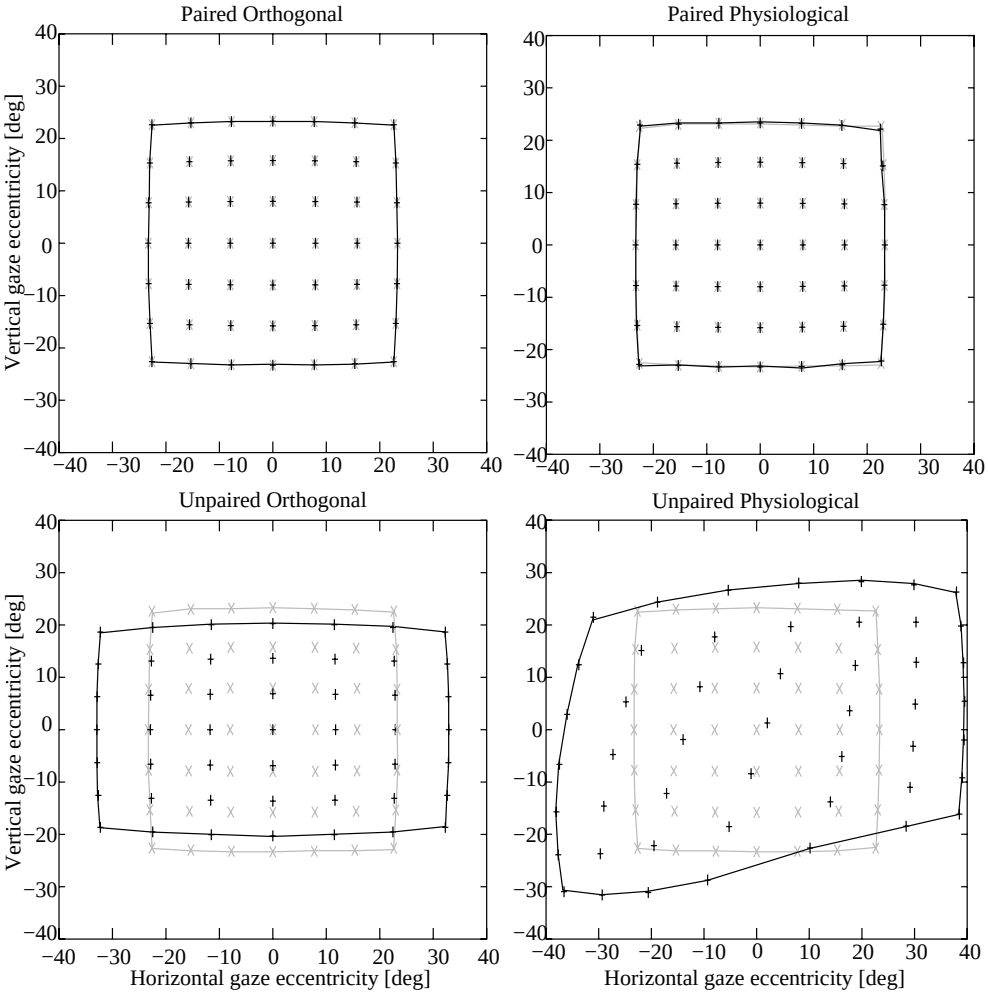

Figure 5.5: Simulated gaze directions resulting from the same neural activity sets applied to eye plant models with and without the muscle-pairing and/or orthogonality assumptions. Top left, the Paired Orthogonal model giving the desired eye orientations. Top right, the Paired Physiological model. Bottom left, the Unpaired Orthogonal model. Bottom right, the Unpaired Physiological model. The gaze directions are given in Euclidean coordinates.

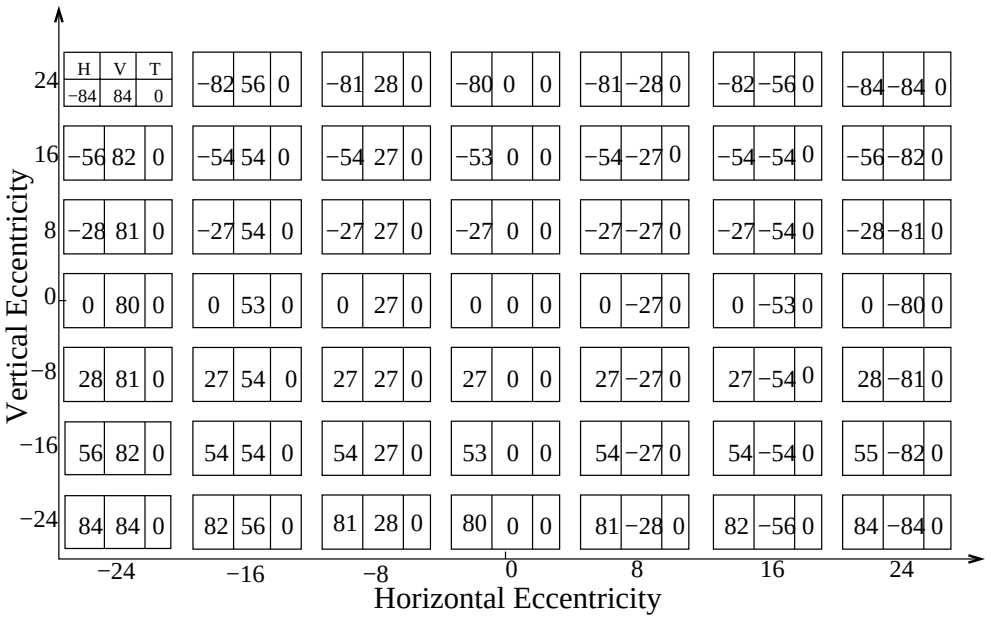

Figure 5.6: Neural activity for desired eye orientation according to Paired Orthogonal model. H, V and T correspond to the predicted activity of the Horizontal, Vertical and Torsional muscle pairs. The activity is given in spikes/second.

LR	MR	SR	IR	SO	IO
3	87	87	3	45	45

Table 5.2: Inclusion of primary position co-contraction activity (45 spikes/sec) in the neural activity predicted by the 'Paired Orthogonal' model, at 24° upward and leftward eccentricity, split into separate activity for each muscle. The activity is given in spikes/second.

the inferior rectus muscles. Negative spike rates are of course impossible. The reason we get negative values is because we have not yet introduced any co-contraction. Co-contraction is required so that the antagonist muscle is able to reduce its activity as the eye moves away from the primary position. If the assumption of reciprocal activity changes in the agonist and antagonist muscles is valid for eye orientations up to, at least, 25° eccentricity then it follows from figure 5.6 that the neural activity of the muscles at primary position must be at least 45 spikes/sec. Table 5.2 shows the result of including the primary position co-contraction in the example previously shown in table 5.1.

Using the muscle activities shown in figure 5.6, split into single muscle activities for the 'Unpaired' model variants, we calculated the orientations at which the eye would fixate. The resulting gaze directions for the four model variants are shown in figure 5.5. The 'x's indicate the desired eye orientation, i.e. the eye orientation as predicted by the Paired Orthogonal model. The '+'s indicate the eye orientations predicted by the various eye plant model variants. The top right panel shows that the Paired Orthogonal and the Paired Physiological model variants result in almost the same gaze directions. The use of physiologically correct, instead of orthogonal muscle insertion points has practically no effect when the muscle-pairing assumption is used. The bottom left panel shows the resulting gaze directions for the Paired Orthogonal and the Unpaired Orthogonal model variants. The main difference between the Paired and the Unpaired Orthogonal models is a scaling factor in both the horizontal and vertical directions. Horizontally, the gaze directions reached by the Unpaired Orthogonal model are scaled up by a factor of ≈ 1.47 relative to the Paired Orthogonal model. Vertically, the gaze directions reached by the Unpaired Orthogonal model are scaled down by a factor of ≈ 0.86 relative to the Paired Orthogonal model. The bottom right panel shows the resulting gaze directions for the Paired Orthogonal (i.e. the Raphan/Quaia model) and the Unpaired Physiological (i.e. the most physiologically correct) model variants. The results for the Unpaired Physiological model are not symmetrical, either in the horizontal or in the vertical directions. The difference between the resulting gaze directions shown in the bottom right panel clearly cannot be described by linear scaling factors. A comparison between the bottom left and the bottom right panels shows that for the 'Unpaired' model variants the use of physiologically correct muscle insertion points (I), rather than orthogonal insertion points, does have a strong effect on the resulting gaze directions. This is in stark contract with the results shown in the top left panel of figure 5.5.

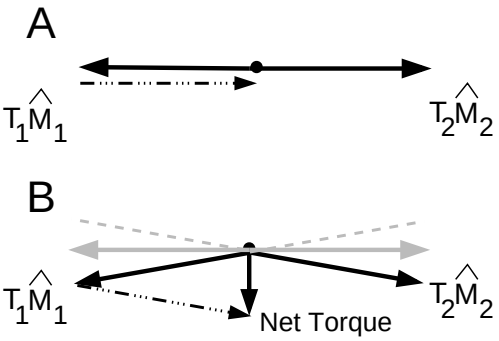

Figure 5.7: Net torque resulting from co-contraction between antagonistic muscles. Panel A: axes of action are aligned. Panel B: axes of action are not aligned. Gray lines indicate the axes of action that are used by the perfect muscle-pairing assumption.

Analysis of results

The differences in the simulated gaze directions (figure 5.5) for the four model variants are the result of two consequences of the muscle-pairing assumption. First, the muscle-pairing assumption ignores the dependence of $\hat{M}_{\text{pair}}$ on the force generated by the antagonistic muscles (see equation 5.3 & section 5.2). Second, the muscle-pairing assumption ignores the net torque that results when co-contracting antagonistic muscles are not perfectly aligned.

As we will now show, the change in the gaze direction patterns when we use model variants that do not assume perfect muscle-pairing (figure 5.5) is caused primarily by the net torques resulting from co-contraction between the non-aligned oblique muscles.

The net torques resulting from co-contraction between non-aligned antagonistic muscles are determined by the vector sum in equation 5.2. As shown in figure 5.7, when the axes of action of the antagonist muscles are not aligned, co-contraction results in a net torque in a direction perpendicular to the assumed axes of action of the muscles in models that use perfect muscle-pairing. From the results in section 5.2 we know that for most eye orientations the antagonistic muscles are not aligned. For most eye orientations co-contraction will therefore result in a net torque perpendicular to the average direction of the axes of action of the agonist and antagonist muscles. Since the average direction of the axes of action of the oblique muscles is in the torsional direction, the net torque generated by the co-contraction of the oblique muscles will cause a horizontal and/or vertical rotation. To show the effect that the net torque resulting from co-contraction between the non-aligned oblique muscles has on the eye orientation we repeated the simulations of section 5.3 with models from which the co-contraction in the oblique muscles has been removed. Figure 5.8 shows the simulated gaze directions resulting from the same neural activity sets applied to a model with the muscle-pairing and orthogonality assumptions and a model without these assumptions.A comparison with figure 5.5, which assumed co-

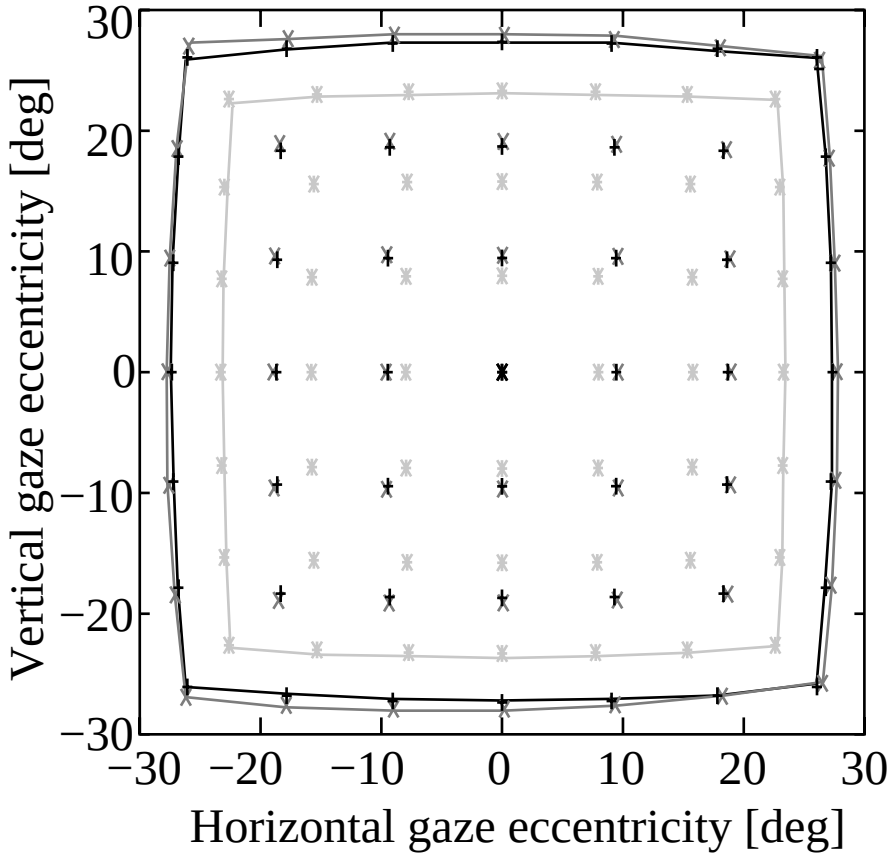

Figure 5.8: Simulated gaze directions resulting from the same neural activity sets applied to variants of the eye plant model. '*' with muscle-pairing and orthogonality assumptions. 'x' without muscle-pairing and orthogonality. '+' without muscle-pairing but with orthogonality assumption. No co-contraction between the oblique muscles. Gaze directions are given in Euclidean coordinates.

contraction activity in the oblique muscles, reveals that the co-contraction of the oblique muscles strongly affects the predicted relation between eye orientation and muscle activity.

5.4 Discussion

The goal of this research was to evaluate the errors that ensue when eye plant models assume that the agonist-antagonist muscle pairs can be treated as a single bi-directional muscle (i.e. a muscle that can both pull and push) and the muscle pairs are assumed to act in orthogonal plaines. These are commonly made simplification (Tweed and Vilis 1987; Schnablok and Raphan 1994; Raphan 1997; Quaia and Optican 1998; etc.) which we will refer to as the muscle-pairing and orthogonality assumptions. In the first part of this study we showed what the implications of muscle-pairing are for the geometrical properties of the eye plant. In the second part we illustrated the impact that the muscle-pairing and orthogonality assumptions (the assumption that the muscle pairs act in orthogonal planes) have on the predicted relation between fixation orientation and the activity in the eye muscles. In our example we compared variants of Raphan's (1997) eye plant model with and without the muscle-pairing and orthogonality assumptions. Using the same muscle activity in all four model variants we found large differences in the predicted eye orientations depending on the use of the muscle-pairing and/or orthogonality assumptions (figure 5.5).

For the model variants that did not use the muscle-pairing assumption it was necessary to separate the activity of the muscle pair into the agonist and antagonist muscle activities. To do this we applied the assumption of reciprocal activity changes in agonist and antagonist muscles (Robinson 1975a; Hikosaka and Kawakami 1977; Hikosaka et al. 1978; Igusa et al. 1980; Sasaki and Shimazu 1981; Yoshida et al. 1982; Strassman et al. 1986a,b; Scudder et al. 1988; Cullen and Guitton 1997). This, in turn, required the introduction of co-contraction between the antagonistic muscles. The co-contraction is required in order to allow the activity of the antagonist to decrease relative to its primary position activity and is a wellknown empirical fact (Robinson 1975b; Collins et al. 1981; Miller et al. 1999). Including this co-contraction raises a problem, since the use of the muscle-pairing assumption in the original model meant that the co-contraction was not defined. For the calculations shown in this paper we chose equal co-contraction in all six eye muscles. The value we chose (45 spikes/sec at primary position) is the lowest co-contraction value that would allow the eye to fixate 25° eccentrically without driving the predicted activity in the antagonist into negative values.

Although the uncertainty about the correct co-contraction values makes it difficult to give a precise measure of the error introduced by the muscle-pairing assumption, it is clear that this error is not negligible. Even when the co-contraction of the oblique muscles is set to zero (figure 5.8) we find that the relation between muscle activity and gaze direction, predicted by the models with and without the muscle-pairing assumption, differs by some 3° when the eye rotates 15° eccentrically. Two conse-

quences of the muscle-pairing assumption are responsible for the differences in the simulated gaze direction. First, the muscle-pairing assumption ignores the dependence of $\hat{M}_{\text{pair}}$ on the force generated by the antagonistic muscles (see equation 5.3 & section 5.2). Second, the muscle-pairing assumption ignores the net torque that results when co-contracting antagonistic muscles are not perfectly aligned.

The effect of the orthogonality assumption is much weaker. For the model variants that assume muscle-pairing the use of the orthogonality assumption has no effect on the relation between gaze direction and muscle activity (see figure 5.5, top right). For the models that do not assume muscle-pairing the impact of the orthogonality assumption depends on the co-contraction between the antagonistic muscles. When we assume high co-contraction between the oblique muscles then there is a noticeable effect (see figure 5.5, bottom) whereas assuming zero co-contraction of the oblique muscles leads to a very weak effect (see figure 5.8, '+' and 'x').

Effect on conclusion based on Raphan's model

The primary conclusion of Raphan's 1997 work (later strengthened by the work by Quaia and Optican 1998) was that due to the characteristics of the oculomotor plant eye movements that obey Listing's law (von Helmholtz 1867) do not require active control of ocular torsion. With properly placed muscle pulleys a 2D control strategy is sufficient to achieve Listing's law with minimal (or no) transient torsion.

To test if this conclusion depends on the use of the muscle-pairing and orthogonality assumptions, we simulated a sequence of three saccades with both the Paired Orthogonal and the Unpaired Physiological models. The saccades we simulated went from the primary position to 15°up, from there to 15° up and 15° right and finally to 15° down and right. The Paired Orthogonal model, which assumes muscle-pairing and orthogonality, is equivalent to the model used by Raphan. The Unpaired Physiological model is the more realistic model that does not use either assumption. Contrary to what we did in section 5.3, this time we did not use the same neural activity patterns for the paired orthogonal and the physiological models. Instead we adjusted the neural activity patterns so that both model variants would achieve the same gaze directions with a 2D control strategy (Oblique muscles are not actively used). The left column of figure 5.9 shows the torsional, vertical and horizontal eccentricity of the eye as a function of time. The right column of figure 5.9 gives the corresponding motoneuron activity in the six eye muscles.

From the top panels in figure 5.9 we see that the Paired Orthogonal model indeed shows no ocular torsion (i.e obeys Listing's law) without requiring any activity changes in the oblique muscles. In the same panels we see that torsional eccentricity produced by the Unpaired Physiological model is within the $\approx 1.5°$ width of Listing's plane that was found experimentally (Tweed and Vilis 1990b; Minken et al 1993; Straumann et al. 1995; Desouza et al. 1997). Further simulations revealed that the torsion generated by the Unpaired Physiological model depends on the strength of the co-contraction in the oblique muscles. The reason the torsion generated by the Unpaired Physiological model does not return to zero at the end of the eye movement is that

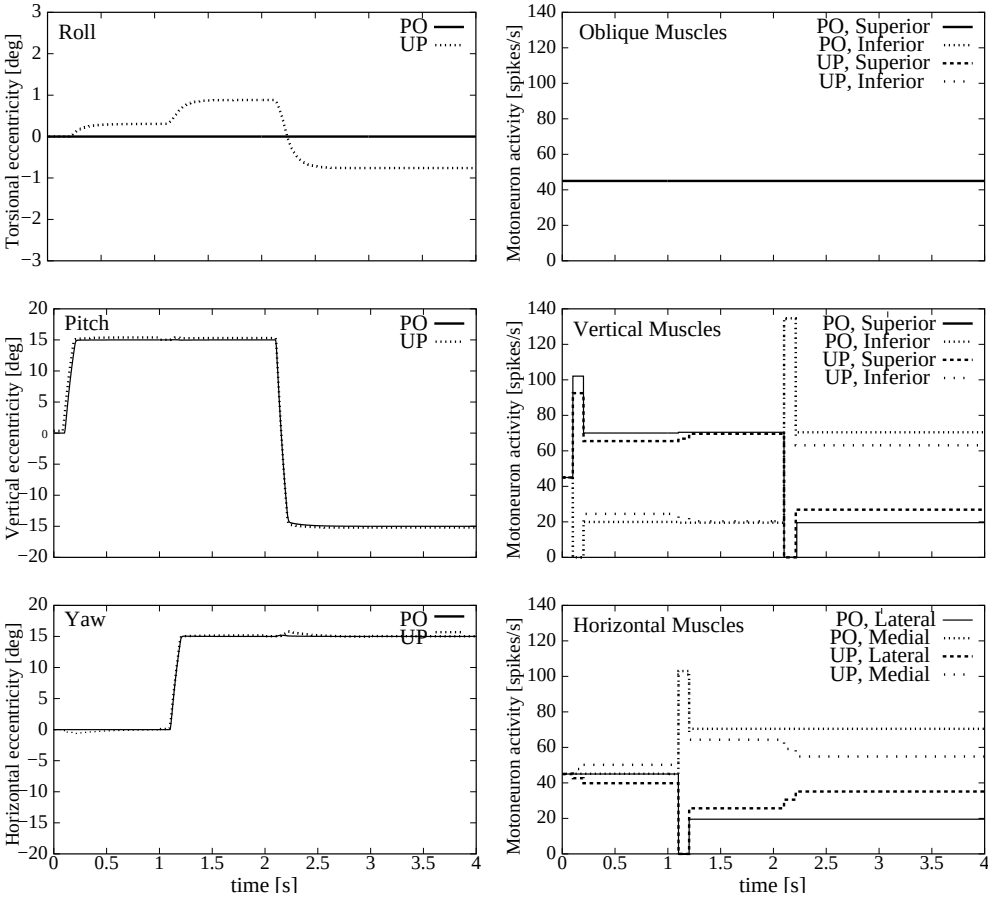

Figure 5.9: Eye orientation and muscle activity during a sequence of three saccades. PO = Paired Orthogonal model, UP= Unpaired Physiological model. Left column gives the eye eccentricity per direction component (Roll, Pitch and Yaw). Right column gives the motoneuron activities of the six eye muscles. Right top shows the activity of the superior and inferior oblique muscles, right middle the superior and inferior rectus muscles and right bottom the medial and lateral rectus muscles.

the net torque is produced by the co-contraction of the oblique muscles.

We conclude from the above that even though the actual neural control signals required for the eye movements are affected by the muscle-pairing and orthogonality assumptions (figure 5.9, right column), the general conclusion drawn from the work by Raphan (and Quaia) is still valid.

Relation to the work by Porrill

The primary conclusion of the work by Porrill et al. (2000) was that the muscle pairs act in orthogonal planes. Horizontal eye movements would require only the horizontal muscle pair to be actively controlled and vertical eye movements would require no active control of the horizontal muscles. In their work, Porrill et al. used a model based on the Orbit$^{\text{tm}}$ model developed by Miller et al. (1999), which does not use the muscle-pairing assumption, and deals only with static situations. The muscle activity which they found would be required for fixation at various eye orientations showed that the activity of the vertical and oblique muscles does not change, or barely changes, as a function of horizontal eye orientation. In our work we showed that the vertical and oblique muscles do contribute to horizontal eye movements. The contribution however is purely a secondary passive effect. Its effect is that it reduces the work that needs to be done by the horizontal muscles. It does not cause any vertical tilting that would need to be compensated by the vertical muscles. As far as the neural activity is concerned there is therefore still only a change in activity in the horizontal muscles during horizontal saccades. The amplitude of the change in muscle activity is altered, not the direction. Our conclusions are in agreement with the findings of Porrill et al. (2000).

Conclusion

Due to the geometrical properties that determine the relation between the axes of action of the eye muscles and eye orientation, the use of eye plant models that treat agonist-antagonist muscle pairs as a single muscle results in incorrect predictions of the oculomotor control signals. The muscle-pairing assumption ignores the dependence of $\hat{M}_{\text{pair}}$ on the force generated by the antagonistic muscles and the net torque that results when co-contracting antagonistic muscles are not aligned.

5.5 Appendix A: Dependence of $\vec{I}$ on eye orientation

Using a rotation vector notation, the eye orientation $\vec{R}$ corresponds to the orientation that the eye would have if it were rotated from the primary position around an axis co-linear with $\vec{R}$ by an angle θ, where $\theta = 2\arctan(\|\vec{R}\|)$. Using this notation the dependence of $\vec{I}$ on $\vec{R}$ can be written as

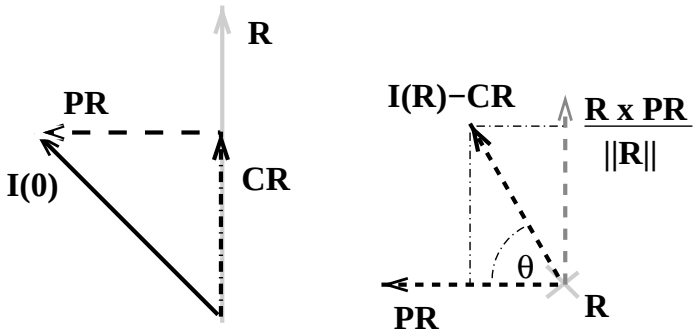

Figure 5.10: Procedure for rotating I(0) around R. The figure on the left shows how I(0) is first decomposed into a component PR perpendicular to R and a component CR co-linear with R. The figure on the right shows how the PR component is rotated around R.

$$\vec{I}(\vec{R}) = \overrightarrow{CR} + \overrightarrow{PR}\cos(\theta) + \frac{\vec{R} \times \overrightarrow{PR}}{\|\vec{R}\|}\sin(\theta), \tag{5.7}$$

with

$$\overrightarrow{CR} = \frac{\vec{R} \cdot \vec{I}}{\|\vec{R}\|\|\vec{I}\|}\frac{\vec{R}}{\|\vec{R}\|}\|\vec{I}\| = \frac{\vec{R} \cdot \vec{I}}{\|\vec{R}\|^2}\vec{R},$$

and

$$\overrightarrow{PR} = \vec{I}(0) - \overrightarrow{CR},$$

where $\vec{I}(0)$ is the muscle insertion point vector during primary orientation gaze and $\vec{I}(\vec{R})$ is the insertion point vector for an eye orientation described by the rotation vector $\vec{R}$. Figure 5.10 gives a graphical illustration.

Chapter 6

Summary and Conclusions

The goal of this thesis was to gain insight into the implications of the mechanics of the eyes for oculomotor control. To this end we employed a computational modeling approach to combine data from anatomy, physiology and psychophysics with basic principles of physics (mechanics) and mathematics (geometry of 3D rotations).

Our study consisted of two parts. In the first part, chapters 2 and 3, we concentrated on the mechanical properties of the muscles during horizontal eye movements, modeling the relationship between eye velocity and muscle innervation. In the second part, chapters 4 and 5, we analyzed the relation between 3D eye orientation and the effective pulling directions of the six eye muscles.

6.1 Chapter 2

The aim of chapter 2 was to determine the cause of the kinematic differences between saccades away from the primary position and saccades towards the primary position. In other words, what causes centrifugal saccades to have a lower maximum velocity and a longer duration than centripetal saccades? For this purpose we systematically analyzed the contribution made by the passive and active eye plant forces to the ocular kinematics.

We measured eye movements during centrifugal and centripetal saccades and used a model of the eye plant to simulate the muscle and orbital tissue forces acting on the eye during these saccades. The resulting force profiles, in combination with data on muscle properties from experiments by Robinson (1975b, 1981), Collins et al. (1975), Miller and Robinson (1984) and Miller et al. (1999), showed that the contribution made by the passive forces (i.e. the muscle elasticity and orbital tissue elasticity and viscosity) to the kinematics of centrifugal and centripetal saccades differs only as a result of the difference in movement profiles. In addition, we showed that the contribution of the passive forces to the ocular kinematics favors the centrifugal saccades. The passive forces, therefore, cannot be the cause of the kinematic differences.

Since the active forces, i.e. the muscle contractile force and the muscle viscosity, both depend directly on the innervation of the muscles we next investigated the muscle innervations. By synthesizing the muscle innervation that would be required to produce the eye movements we showed that the total change in muscle innervation during centrifugal and centripetal saccades is nearly identical and therefore cannot be the cause of the kinematic differences. Based on the length-tension-innervation relationship of the eye muscles that was reported by Robinson (1975b) and Miller (1999) we then showed that the contractile forces resulting from the innervation changes are greater during centrifugal saccades than during centripetal ones. The contractile length-tension-innervation relationship therefore cannot be the cause of the observed kinematic differences either. The muscle viscosity was investigated next. We found that, due to the non-linear characteristics of the muscle viscosity as described by Hill (1938), Cook and Stark (1967), Clark and Stark (1974a,b) and Pfann (1995), the viscous force is much greater during centrifugal movements than during centripetal ones. This means that the muscle viscosity slows down the eye movement more during centrifugal movements, resulting in a lower maximum velocity.

The muscle viscosity was the only force that showed a difference during centrifugal and centripetal saccades that could explain the observed difference in saccade kinematics. We therefore concluded that the cause of the kinematic differences during centrifugal and centripetal saccades is the non-linear force-velocity relationship of the muscles.

6.2 Chapter 3

In chapter 3 we quantified the required cerebellar adjustment of the saccade signal as a function of eye orientation and analyzed the dynamics of the signal changes.

Following the assumption that the cerebellum serves to modify the saccadic command as a function of eye orientation (Dean et al., 1994; Grossberg & Kuperstein, 1989; Optican, 1986; Optican & Miles, 1985) we described the required signal adjustment as a net gain change in the saccadic signal relative to some default signal. If the default signal generated by the superior colliculus depends only on the magnitude of the desired saccadic gaze shift ($\Delta\theta$) (Scudder, 1988; Tweed & Vilis, 1990b), then the dependence of the net saccadic signal $\Delta\mathrm{MN}(\theta_i, \Delta\theta)$ at starting orientation (θ_i) can be expressed by

$$\Delta\mathrm{MN}(\theta_i, \Delta\theta) = \alpha(\theta_i, \Delta\theta)\, \Delta\mathrm{MN}(\theta_d, \Delta\theta) \tag{6.1}$$

where $\alpha(\theta_i, \Delta\theta)$ is the net saccadic signal gain for a saccade of magnitude $\Delta\theta$ and starting orientation θ_i, $\Delta\mathrm{MN}(\theta_d, \Delta\theta)$ is the net saccadic signal for a saccade of size $\Delta\theta$ starting at θ_d, and θ_d is the default starting orientation i.e. the orientation for which the signal from the superior colliculus produces the desired saccades. The required net signal gain changes (α) were thus determined from the measured fixation innervations ($\mathrm{MN}(\theta)$) of the muscles published by Collins et al. (1981), Robinson (1975a) and Miller et al. (1999). An important characteristic of these measured innervations is that $\Delta\mathrm{MN}(\theta_i, \Delta\theta)$ increases when the initial orientation of the eye (θ_i) is more

towards the on-direction of the eye muscle, and decreases when θ_i is more towards the off-direction of the eye muscle. As a result, the agonist and antagonist muscles were found to require different gain factors ($\alpha_{\text{ant}} \neq \alpha_{\text{ag}}$) for the same saccade.

The dynamics of the saccade signal changes were calculated from saccadic eye movement profiles using the same mechanistic model of the horizontal eye plant as in chapter 2. On the basis of comparisons of the maximum burst rate and burst duration of the calculated saccade signals we concluded that the cerebellar adjustment of the saccade signal, as a function of starting orientation, is achieved primarily by changing the burst rate. It can therefore be inferred that the cerebellar adjustment of the saccade signal must take place within, or after, the local feedback loop in the brain stem which controls saccade duration.

6.3 Chapter 4

In chapter 4 we examined the geometrical properties that dictate the relationship between the axes of action (i.e. the unit moment vectors) of the muscles and 3D eye rotations.

First we specified the requirements that the oculomotor system must meet in order for the eye to be able to make the desired gaze changes and fixate at various eye orientations. Then we determined how the axes of action of the muscles are related to the orientation of the eye and the location of the muscle pulleys. We subsequently showed how this relation between eye orientation and the axes of action of the muscles links muscle pulley locations to oculomotor control strategies. This link was illustrated by two examples. The first example dealt with the hypothesis that only the horizontal and vertical muscles are actively used during eye movements that obey Listing's law and the binocular extension of Listing's law. The second example dealt with the assumption of perfect agonist-antagonist muscle pairing.

When comparing the axes of action that are required by these two oculomotor control schemes we found that these control schemes are not compatible. In the Listing's law related scheme the axes of action must be part of a plane that corresponds to Listing's plane rotated relative to the primary direction over half the angle of eccentricity (half-angle rule). In the perfect muscle-pairing scheme the axes of action need to be fixed relative to the eye, i.e. rotate with the eye over the full angle of eccentricity. In order to fulfill the axis of action requirement for one of these control strategies one therefore needs to violate the requirement for the other control strategy. This finding revealed a problem in the work by Raphan (1998) and by Quaia and Optican (1998). In both studies the authors simplified the eye plant by lumping the muscles into three bi-directional muscles, thereby implicitly assuming perfect agonist-antagonist muscle pairing. In the main part of the articles they then go on to show how the muscle pulleys (abstracted into a pulley factor) can allow their model to produce saccades that obey Listing's law, without active use of the oblique (torsion) muscles. The reason why the conflict between these two control strategies did not become apparent in the work by Raphan (1998) and by Quaia and Optican (1998) is

that the lumped muscle pair model which they used does not reveal the requirements for keeping the agonist-antagonist axes of action aligned. Instead of ensuring that the axes of action of the antagonistic muscles remained aligned, so that the co-contraction of the muscles does not produce a net torque on the eye, they simply did not take the co-contraction into account.

Concerning the muscle pulley locations that would allow eye movements corresponding to the binocular extension of Listing's law while using only the horizontal and vertical eye muscles, our calculation revealed that the muscle pulleys would have to rotate about the vertical axis. Recent measurements of muscle pulley movement during vergence (Demer et al. 2002) however have shown that the primary pulley movement is a rotation of the pulley positions about the anterior-posterior axis. The experimentally found muscle pulley movements therefore do not support the hypothesis that vergence-related pulley movement is geared towards the control of Listing's law compliant eye movements while using only the horizontal and vertical muscle pairs.

Chapter 4 focused solely on the direction of the torque (i.e. axis of action) of the muscles. Using first principles that describe the requirements for eye rotation and fixation we showed how the direction of the torques generated by the eye muscles is related to the way the eye rotates. These geometrical properties that dictate the relationship between muscle pulling direction and 3D eye rotations provide further insights into possible oculomotor control strategies and the location and function of the muscle pulleys.

6.4 Chapter 5

In chapter 5 we evaluated the errors that arise when eye plant models assume that the agonist-antagonist muscle pairs can be treated as a single bi-directional muscle (i.e. a muscle that can both pull and push). This is a commonly made simplification (Tweed and Vilis 1987; Schnablok and Raphan 1994; Raphan 1997; Quaia and Optican 1998; etc.) which we refer to as muscle-pairing.

In the first part of this chapter we showed what the implications of muscle-pairing are for the geometrical properties of the eye plant. In the second part we illustrated the impact that the muscle-pairing and orthogonality assumptions (the assumption that the muscle pairs act in orthogonal planes) have on the predicted relation between fixation orientation and the activity in the eye muscles. This was done by comparing variants of an eye plant model (e.g. Raphan 1997) with and without the muscle-pairing and orthogonality assumptions. Using the same muscle activity in all four model variants we found large ($\approx 20\%$) differences in the predicted eye orientations, depending on the use of the muscle-pairing and/or orthogonality assumptions.

For the model variants that did not use the muscle-pairing assumption it was necessary to separate the activity of the muscle pair into the agonist and antagonist muscle activities. To do this we applied the assumption of reciprocal activity changes in agonist and antagonist muscles (Robinson 1975a; Hikosaka and Kawakami 1977;

Hikosaka et al. 1978; Igusa et al. 1980; Sasaki and Shimazu 1981; Yoshida et al. 1982; Strassman et al. 1986a,b; Scudder et al. 1988; Cullen and Guitton 1997). This, in turn, required the introduction of co-contraction between the antagonistic muscles. The co-contraction is required in order to allow the activity of the antagonist to decrease relative to its primary position activity and is a wellknown empirical fact (Robinson 1975b; Collins et al. 1981; Miller et al. 1999). Including this co-contraction in the un-paired variants raised a problem with regard to the comparison of the models since the use of the muscle-pairing assumption in the original model meant that the co-contraction was not defined. Although the uncertainty about the correct co-contraction values made it difficult to give a precise measure of the error introduced by the muscle-pairing assumption, it is clear that this error is non-negligible. Even when the co-contraction of the oblique muscles was set to zero (minimizing the difference between the models) we found that the relation between muscle activity and gaze direction, predicted by the models with and without the muscle-pairing assumption, differed by some 3° when the eye rotates 15° eccentrically.

The effect of the orthogonality assumption was found to be much weaker. In the model variants that assume muscle-pairing the use of the orthogonality assumption had no effect on the relation between gaze direction and muscle activity. In the models that do not assume muscle-pairing the impact of the orthogonality assumption depended on the co-contraction between the antagonistic muscles. When we assumed high co-contraction between the oblique muscles then there was a noticeable effect, whereas assuming zero co-contraction of the oblique muscles led to a very weak effect.

The primary conclusion of Raphan's 1997 work (later strengthened by the work of Quaia and Optican 1998) was that, due to the characteristics of the oculomotor plant, eye movements that obey Listing's law (von Helmholtz 1867) do not require active control of ocular torsion. With properly placed muscle pulleys a 2D control strategy is sufficient to achieve Listing's law with minimal (or no) transient torsion. To test whether this conclusion depends on the use of the muscle-pairing and orthogonality assumptions, we simulated a sequence of three saccades with both the Paired Orthogonal and the Unpaired Physiological models. For the Paired Orthogonal model we found that the simulated eye movements generated no ocular torsion (i.e obeyed Listing's law) without requiring any activity changes in the oblique muscles, thus replicating the results of Raphan (1997) and Quaia and Optican (1998). The torsional eccentricity produced by the Unpaired Physiological model remained within the $\approx 1.5°$ width of Listing's plane that was found experimentally (Tweed and Vilis 1990b; Minken et al 1993; Straumann et al. 1995; Desouza et al. 1997). Further simulations revealed that the torsion generated by the Unpaired Physiological model depended on the strength of the co-contraction in the oblique muscles. We concluded from this that even though the actual neural control signals required for the eye movements are affected by the muscle-pairing and orthogonality assumptions, the general conclusion drawn from the work by Raphan (and Quaia) is still valid.

We concluded that due to the geometrical properties that determine the relation between the axes of action of the eye muscles and eye orientation, the use of eye plant models that treat agonist-antagonist muscle pairs as a single muscle leads to quan-

titative errors in the predicted oculomotor control signals. A potentially important aspect of eye movement control which is absent in models using the perfect muscle-pairing assumption is the way in which the co-contraction between the muscles affects oculomotor control.

6.5 General conclusions

In this thesis we set out to investigate oculomotor control by determining the characteristics of the eye plant mechanics and the demands they make on the neural control of observed eye movement behavior.

In the first part, chapters 2 and 3, we concentrated on the mechanical properties of the muscles during horizontal eye movements, modeling the relationship between eye velocity and muscle innervation. In the second part, chapters 4 and 5, we analyzed the relation between 3D eye orientation and the effective pulling directions of the six eye muscles.

By modeling the mechanical properties of the eye plant we were able to test a number of oculomotor hypotheses which would have been more difficult to do by other means. In chapter 2 we showed that the eye plant mechanics can cause the same control signals to result in eye movements with different kinematics depending on the starting orientation of the saccade. In chapter 4 we developed a simple method for determining the relation between muscle pulling direction and eye orientation, giving more insight into the required coordination between the six eye muscles during 3D eye rotations. The method developed in chapter 4 allowed us to show incompatibilities between two oculomotor control hypotheses (Listing's law without oblique muscles & perfect muscle-pairing). It also revealed a previously overlooked effect of the co-contraction between antagonistic muscles on the control of eye orientation (chapter 5).

The complementary relation between the approach used in this thesis and the study of oculomotor control through the measurement of neural activity was shown most clearly by the results of chapter 3. By using the result of neurophysiological studies and data concerning the length-tension-innervation properties of the eye muscles we were able to make predictions about the signals produced by the cerebellum during saccadic eye movements.

Analyzing the mechanics of the oculomotor plant provides us with a better understanding of the challenges and limitations with which the neural systems controlling eye movements have to deal. We reveal the trade-offs that the oculomotor control system makes in optimizing eye movements and gain insights into the computations that are performed by the controller.

Chapter 7

Samenvatting en Conclusies

Het doel van dit promotie onderzoek was om inzicht te krijgen in de implicaties die de mechanische eigenschappen van het oog hebben voor de aansturing van oogbewegingen. Om dit doel te bereiken hebben wij, middels computer modellen, data afkomstig uit anatomisch, fysiologisch en psychofysisch onderzoek gecombineerd met basis principes uit de natuurkunde (mechanica) en de wiskunde (geometrie van 3D rotaties).

Ons onderzoek bestond uit twee delen. In het eerste deel, hoofdstuk 2 en 3, hebben we ons geconcentreerd op de mechanische eigenschappen van de oogspieren gedurende horizontale oogbewegingen. Hiervoor hebben wij de relatie tussen oogrotatiesnelheid en spier-innervatie gemodelleerd. In het tweede deel, hoofdstuk 4 en 5, hebben we de relatie tussen 3D oog-oriëntatie en de effectieve trek richtingen van de zes oogspieren geanalyseerd.

7.1 Hoofdstuk 2

In hoofdstuk 2 hebben we de oorzaak onderzocht van de kinematische verschillen tussen saccades die naar de primaire positie toe gaan en saccades die van de primaire positie weg gaan. We hebben getracht een antwoord te vinden op de vraag waarom centripetale saccades een hogere maximum snelheid en een kortere duur hebben dan centrifugale saccades. Ten einde hier een antwoord op te vinden hebben wij een systematische analyse gedaan van de bijdrage die de passieve en actieve krachten van de oogbolsysteem leveren aan de kinematica van de oogbeweging.

We hebben de beweging van het oog gemeten gedurende centrifugale en centripetale saccades en een model van de oogmechanica gebruikt om de spier- en weefselkrachten gedurende deze bewegingen te simuleren. De resulterende krachtprofielen, in combinatie met data over spiereigenschappen uit experimenten door Robinson (1975b, 1981), Collins et al. (1975), Miller en Robinson (1984) en Miller et al. (1999), lieten zien dat de passieve krachten niet de oorzaak van de kinematische verschillen

kunnen zijn. We vonden dat de contributie van de passieve krachten (spierelasticiteit en orbitaal weefsel elasticiteit en viscositeit) aan de centrifugale en centripetale saccades alleen verschilt als gevolg van de verschillen in de bewegingsprofielen en dat de contributie van de passieve krachten de centrifugale saccades bevoordelen. Omdat de actieve krachten, zijnde de contractiele spierkracht en de spierviscositeit, direct afhankelijk zijn van de spier-innervatie hebben wij als eerst volgende de spier-innervatie onderzocht. Door de spier-innervaties te synthetiseren die nodig zijn om de oogbewegingen te produceren hebben wij laten zien dat de netto (agonist + antagonist) verandering in spier-innervatie gedurende centrifugale en centripetale saccades bijna identiek is. De spier-innervatie kan daarom niet de oorzaak zijn van de kinematische verschillen. Op basis van de kracht-lengte-innervatie relatie van de oogspieren, welke door Robinson (1975b) en Miller (1999) bepaald is, hebben wij aangetoond dat de contractiele krachten die uit de innervatie veranderingen resulteren groter zijn gedurende centrifugale saccades dan gedurende centripetale saccades. De contractiele kracht-lengte-innervatie relatie kan daarom ook niet de oorzaak van de waargenomen kinematische verschillen zijn. Het volgende wat wij onderzocht hebben was de spierviscositeit. Hiervoor vonden wij dat, door de niet-lineaire karakteristiek van de spierviscositeit, zo als beschreven door Hill (1938), Cook en Stark (1967), Clark en Stark (1974a,b) en Pfann (1995), de viscose kracht gedurende centrifugale bewegingen veel groter is dan gedurende centripetale bewegingen. Dit betekent dat de spierviscositeit de oogbeweging gedurende centrifugale bewegingen sterker vertraagt, het geen resulteert in bewegingen met een lagere maximum snelheid.

De spierviscositeit was de enige kracht die een zodanig verschil tussen centrifugale en centripetale saccades liet zien dat daarmee het waargenomen verschil in saccade kinematica verklaard zou kunnen worden. Wij concluderen daarom dat de kinematische verschillen gedurende centrifugale en centripetale saccades veroorzaakt worden door de niet-lineaire kracht-snelheid relatie (viscositeit) van de spieren.

7.2 Hoofdstuk 3

In hoofdstuk 3 hebben wij kwantitatief onderzocht in welke mate het cerebellum het saccadesignaal moet aanpassen als functie van initiële oog-oriëntatie en hebben we de dynamica van de signaal veranderingen geanalyseerd.

Op basis van de aanname dat het cerebellum de saccade aansturing aanpast als functie van oog-oriëntatie (Dean et al., 1994; Grossberg & Kuperstein, 1989; Optican, 1986; Optican & Miles, 1985) hebben wij de benodigde signaal aanpassing beschreven als netto gain veranderingen in het saccadische signaal ten opzichte van een default signaal. Als het default signaal dat door de superior colliculus gegenereerd word alleen afhangt van de grootte van de gewenste saccade ($\Delta\theta$) (Scudder, 1988; Tweed & Vilis, 1990b), dan kan de afhankelijkheid van het netto saccadesignaal $\Delta\mathrm{MN}(\theta_i, \Delta\theta)$ met begin oriëntatie (θ_i) beschreven worden door

$$\Delta\mathrm{MN}(\theta_i, \Delta\theta) = \alpha(\theta_i, \Delta\theta)\, \Delta\mathrm{MN}(\theta_d, \Delta\theta) \tag{7.1}$$

waarin $\alpha(\theta_i, \Delta\theta)$ de netto saccade-signaal-gain is voor een saccade van grootte $\Delta\theta$ en begin oriëntatie θ_i, $\Delta\mathrm{MN}(\theta_d, \Delta\theta)$ het netto saccadesignaal is voor een saccade met een grootte van $\Delta\theta$ en een beginoriëntatie θ_d en θ_d de default beginoriëntatie is, de oriëntatie waarvoor het signaal van de superior colliculus de gewenste saccade produceert. Op basis van de bovengenoemde vergelijking werden de benodigde netto signaal-gain veranderingen (α) bepaald uit de fixatie innervaties ($\mathrm{MN}(\theta)$) van de spieren die door Collins et al. (1981), Robinson (1975a) en Miller et al. (1999) gemeten zijn. Een belangrijke eigenschap van deze innervaties is dat $\Delta\mathrm{MN}(\theta_i, \Delta\theta)$ toeneemt naarmate de initiële oriëntatie van het oog (θ_i) meer ipsilateraal is tenopzichte van de oogspier , en afneemt naarmate θ_i meer contralateraal is tenopzichte van de oogspier. Als gevolg hiervan vonden wij dat de agonist en antagonist spieren gedurende saccades verschillende gainwaarden ($\alpha_{\mathrm{ant}} \neq \alpha_{\mathrm{ag}}$) moeten hebben.

De dynamica van de veranderingen in het saccadesignaal werden berekend uit saccadische oog-bewegings-profielen door gebruik te maken van het model van de horizontale oogmechanica uit hoofdstuk 2. Op basis van de maximale burst rate en burst duur van de berekende saccadesignalen kwamen wij tot de conclusie dat de aanpassing van het saccadesignaal, als functie van begin oriëntatie, voornamelijk geschied door verandering van de burst rate. Hieruit kan afgeleid worden dat de aanpassing van het saccadesignaal door het cerebellum plaats moet vinden binnen, of na, de locale terugkoppeling in de hersenstam, welke de duur van de saccade regelt.

7.3 Hoofdstuk 4

In hoofdstuk 4 hebben wij de geometrische eigenschappen onderzocht die de relatie bepalen tussen de 'axes of action' (de eenheids momentvectoren) van de oogspieren en 3D oogrotaties.

Als eerste hebben wij bepaald wat de voorwaarden zijn waaraan het oculomotor systeem moet voldoen zo dat het oog gewenste rotaties kan maken en gewenste fixatie oriëntaties kan aannemen. Daarna hebben wij bepaald hoe de 'axes of action' van de spieren afhangen van de oriëntatie van het oog en de locatie van de 'spierpulleys'. Op basis van deze relatie tussen oog-oriëntatie en de 'axes of action' van de spieren hebben wij het verband aangetoond tussen de locaties van de spierpulleys en oculomotor aansturings-strategieën. Ter illustratie hebben wij twee voorbeelden hiervan gepresenteerd. Het eerste voorbeeld betrof de hypothese dat alleen de horizontale en verticale spieren actief gebruikt worden gedurende oogbewegingen die de wet van Listing, en haar binoculaire uitbreiding , volgen. Het tweede voorbeeld betrof de aanname dat agonist-antagonist spieren perfect gepaard zijn (perfect muscle-pairing).

Bij het vergelijken van de 'axes of action' die nodig zijn voor deze twee oculomotor besturingsstrategieën vonden wij dat deze niet met elkaar in overeenstemming zijn. Voor de strategie m.b.t. de wet van Listing moeten de 'axes of action' deel uit maken van een vlak dat overeenkomt met het Listing's vlak geroteerd over de helft van de hoek van excentriciteit ten opzichte van de primaire richting (half-angle regel). Voor de 'perfect muscle-pairing' strategie moeten de 'axes of action' ten opzichte van het

oog vast zijn, en dus met het oog mee roteren met de gehele hoek van excentriciteit. Om aan de 'axis of action' voorwaarden van een van deze aansturings-strategieën te voldoen moet men daarom de voorwaarden voor de andere strategie overschrijden. Dit resultaat toont een probleem in het werk van Raphan (1998) en het werk van Quaia en Optican (1998) aan. In beide studies werd de oogmechanica vereenvoudigd door de zes oogspieren samen te voegen tot drie bi-directionele spieren, waarbij impliciet de 'perfect muscle-pairing' aanname gemaakt werd. Vervolgens werd in deze artikelen getoond hoe de spierpulleys (geabstraheerd tot een pulley-factor) er voor kunnen zorgen dat de, door hun model, gesimuleerde saccades aan de wet van Listing voldoen, zonder gebruik te maken van de oblique (torsie) spieren. De reden waarom het conflict tussen deze twee aansturings-strategieën niet naar voren kwam in het werk van Raphan (1998) en Quaia en Optican (1998) is dat het 'perfect muscle-pairing' model dat zij gebruikten de voorwaarde, dat de agonist-antagonist 'axes of action' opgelijnd moeten blijven, niet expliciet toont. In plaats van zorg te dragen dat de antagonistische spieren opgelijnd bleven, zo dat de co-contractie van de spieren geen netto koppel op het oog uitoefende, werd de co-contractie eenvoudig niet mee berekend.

Voor de hypothese dat alleen de horizontale en verticale spieren actief gebruikt worden gedurende oogbewegingen die de binoculaire uitbreiding van de wet van Listing volgen hebben wij de benodigde spierpulley locaties berekent. Onze berekeningen hebben aangetoont dat, volgens deze hypothese, de spierpulleys bij vergentie bewegingen om de verticale as zouden moeten draaien. Recente metingen van spierpulleybeweging gedurende vergentie (Demer et al. 2002) hebben echter laten zien dat de primaire pulleybeweging een rotatie van de pulleyposities is om de anterior-posterior as. De experimenteel gevonden spierpulleybewegingen geven dus geen ondersteuning aan de hypothese dat vergentie gerelateerde pulley bewegingen als doel hebben om oogbewegingen volgens de wet van Listing te kunnen aansturen.

Hoofdstuk 4 is geheel gewijd aan de richting van het moment (axis of action) dat een spier uitoefent op het oog. Gebruik makend van basis principes, die de voorwaarden voor oogrotaties en fixaties bepalen, hebben wij laten zien dat de 'axes of action' van de oogspieren gerelateerd zijn aan de oriëntatie van het oog. Deze geometrische eigenschappen, die de relatie tussen spierpulleypositie en 3D oog-oriëntaties verzorgen, geven verder inzicht in de mogelijke aansturings strategieën en de locatie en functie van de spierpulleys.

7.4 Hoofdstuk 5

In hoofdstuk 5 hebben wij de fouten geëvalueerd die worden gemaakt als oogmechanica modellen veronderstellen dat de agonist-antagonist spierparen gemodelleerd kunnen worden als een enkele bi-directionele spier (een spier die kan trekken en duwen). Deze aanname is een vaak gemaakte vereenvoudiging (Tweed en Vilis 1987; Schnablok en Raphan 1994; Raphan 1997; Quaia en Optican 1998; etc.) die wij 'muscle-pairing' noemen. We hebben laten zien wat de effecten van de muscle-pairing en orthogonaliteitsaannamen (de aanname dat de spierparen orthogonaal ten opzichte van elkaar

werken) zijn op de voorspelde relatie tussen fixatieoriëntaties en de activiteit van de oogspieren. Dit werd gedaan door een vergelijking te maken tussen varianten van een oogmechanica model (e.g. Raphan 1997) met en zonder de muscle-pairing en orthogonaliteitsaannamen. Gebruikmakend van dezelfde spieractiviteit in alle vier model-varianten hebben we, afhankelijk van het gebruik van de muscle-pairing en/of orthogonaliteits aannamen, grote ($\approx 20\%$) verschillen in de voorspelde oog-oriëntaties gevonden.

Voor de model-varianten die geen gebruik maken van muscle-pairing was het nodig om de activiteit van de spierparen te splitsen in agonist- en antagonist-spieractiviteiten. Hiervoor hebben wij gebruik gemaakt van de aanname van wederkerige activiteitsveranderingen in agonist en antagonist spieren (Robinson 1975a; Hikosaka en Kawakami 1977; Hikosaka et al. 1978; Igusa et al. 1980; Sasaki en Shimazu 1981; Yoshida et al. 1982; Strassman et al. 1986a,b; Scudder et al. 1988; Cullen en Guitton 1997). Dit had tot gevolg dat co-contractie tussen de antagonistische spieren moest worden toegevoegd. De co-contractie maakt het mogelijk dat de activiteit in de antagonistische spier kan afnemen ten opzichte van zijn primaire-positie-activiteit, en is een bekend empirisch feit (Robinson 1975b; Collins et al. 1981; Miller et al. 1999). Toevoegen van deze co-contractie aan de modelvarianten zonder muscle-pairing, zorgde echter voor problemen bij het vergelijken van de modelvarianten. Vanwege het gebruik van de muscle-pairing aanname in het oorspronkelijke model was de co-contractie in dat model namelijk niet gedefinieerd. Ondanks de onzekerheid omtrent de correcte co-contractie waarden, welke het moeilijk maakte om de fout die door de muscle-pairing aanname veroorzaakt werd precies te bepalen, is het duidelijk dat deze fout niet verwaarloosbaar is. Zelfs als de co-contractie van de oblique spieren op nul werd gezet (minimaliseren van het verschil tussen de modellen) vonden wij dat de relatie tussen spieractiviteit en kijkrichting, die door de modelvarianten met en zonder de muscle-pairing aanname voorspeld werd, verschilde met 3° als het oog 15° excentrisch geroteerd was.

Wat de orthogonaliteits-aanname betreft waren de effecten die wij vonden veel zwakker. Bij de modelvarianten met muscle-pairing had de orthogonaliteits-aanname geen effect op de relatie tussen kijkrichting en spieractiviteit. Bij de modelvarianten die geen gebruik maakten van muscle-pairing was het effect van de orthogonoaliteits-aanname afhankelijk van de co-contractie tussen de antagonistische spieren. Wanneer er veel co-contractie tussen de oblique spieren verondersteld werd was er een merkbaar effect. Als we echter er vanuit gingen dat er geen co-contractie tussen de oblique spieren was dan leidde dit tot een heel zwak effect.

De primaire conclusie van het werk van Rapahan (1997) en van Quaia en Optican (1998) was dat de oogmechanica er voor zorgt dat oogbewegingen aan de wet van Listing voldoen (von Helmholtz 1867), zonder dat hiervoor een actieve aansturing van de oogtorsie nodig is. Met goed geplaatste spierpulleys is een 2D besturingsstrategie voldoende om aan de wet van Listing te voldoen, zonder (of met minimale) transiënte torsie. Om te testen of deze conclusie afhankelijk is van de muscle-pairing en orthogonaliteits-aannamen hebben wij een reeks van drie saccades gesimuleerd met zowel het 'Paired Orthogonal' als het 'Unpaired Physiological' model. Bij het 'Paired

Orthogonal' model voldeden de oogbewegingen aan de wet van Listing (geen oogtorsie) zonder dat hiervoor enige activiteits-veranderingen in de oblique spieren nodig was. Hiermee werden dus de resultaten van Raphan (1997) en Quaia en Optican (1998) gereproduceerd. De torsionele excentriciteiten die door het 'Unpaired Physiological' model bij deze oogbewegingen geproduceerd werden bleven binnen de $\approx 1.5^\circ$ breedte van het vlak van Listing (Tweed en Vilis 1990b; Minken et al 1993; Straumann et al. 1995; Desouza et al. 1997). Verder simulaties lieten zien dat de torsie die door het 'Unpaired Physiological' model gegenereerd werd afhankelijk was van de sterkte van de co-contractie tussen de oblique spieren. Wij concludeerden hieruit dat, ook al word het benodigde neurale signaal voor oogbewegingen beïnvloed door de muscle-pairing en orthogonaliteits-aannamen, de algemene conclusie van het werk van Raphan (en Quaia) hierdoor niet ontkracht word.

De geometrische eigenschappen die de relatie tussen de 'axes of action' van de oogspieren en de oog-oriëntatie bepalen leiden er toe dat oogmechanica modellen die agonist-antagonist spierparen als een enkele spier behandelen kwantitatieve fouten maken in hun voorspellingen van de oculomotor besturings-signalen. Een potentieel belangrijk aspect voor de besturing van oogbewegingen, dat afwezig is in de modellen die gebruik maken van muscle-pairing, is de manier waarop de co-contractie tussen de spieren de oculomotor aansturing beïnvloedt.

7.5 Algemene conclusies

In dit proefschrift hebben wij de karakteristieke eigenschappen van de oogmechanica onderzocht en de voorwaarden bepaald die deze stelt aan de neurale aansturing van waargenomen oogbewegingen.

In het eerste deel, hoofdstuk 2 en 3, hebben wij ons geconcentreerd op de mechanische eigenschappen van de spieren m.b.t. horizontale oogbewegingen en het modeleren van de relatie tussen oogrotatiesnelheid en spier-innervatie. In het tweede gedeelte, hoofdstuk 4 en 5, hebben wij de relatie tussen 3D oog-oriëntatie en de effectieve trekrichting van de zes oogspieren geanalyseerd.

Het modeleren van de mechanische eigenschappen van het oog heeft ons in staat gesteld om een aantal oculomotor besturings-hypothesen te testen, die erg moeilijk op een andere manier kunnen worden getest. In hoofdstuk 2 hebben wij laten zien hoe de oogmechanica ervoor kan zorgen dat hetzelfde aansturings-signaal resulteert in oogbewegingen met verschillende kinematische eigenschappen, afhankelijk van de beginoriëntatie van de saccade. In hoofdstuk 4 hebben we een simpele methode ontwikkeld om de relatie tussen spier-trek-richting en oog-oriëntatie te bepalen, wat meer inzicht verschaft heeft in de benodigde coördinatie tussen de zes oogspieren gedurende 3D oogrotaties. De methodiek die in hoofdstuk 4 ontwikkeld werd maakte het mogelijk om ongerijmdheden tussen twee oculomotor aansturings-hypothesen (wet van Listing zonder oblique spieren & perfect muscle-pairing) aan te tonen en het effect van de co-contractie tussen antagonistische spieren op de aansturing van oogbewegingen te laten zien (hoofdstuk 5).

De complementaire relatie tussen ons onderzoek en neurofysiologisch onderzoek naar de aansturing van oogbewegingen werd het meest duidelijk in de resultaten van hoofdstuk 3. Door gebruik te maken van de resultaten van neurofysiologisch onderzoek en data betreffende de kracht-lengte-innervatie eigenschappen van de oogspieren waren wij in staat om voorspellingen te doen over de signalen die door het cerebellum gedurende saccadische oogbewegingen geproduceerd worden.

Het analyseren van de mechanica van het oculomotor systeem heeft ons een beter inzicht gegeven in de neurale aansturing van oogbewegingen. Wij hebben de tradeoffs getoond die het oculomotor aansturings-systeem maakt bij het optimaliseren van oogbewegingen en inzicht verworven in de berekeningen die deze regelaar uitvoert.

References

Abel A., Dell'Osso L.F., Daroff R.B. and Parker L., (1979) Saccades in extremes of lateral gaze, *Invest. Ophthalmol. Visual Sci.*, **18**, 324-327.

Aizawa H. and Wurtz R.H. (1998) Reversible inactivation of monkey superior colliculus. I. Curvature of saccadic trajectory, *J. Neurophysiol.* **79**, 2082-2096.

Arai K., Keller E.L. and Edelman J.A., (1994) Two-dimensional neural network model of the primate saccadic system, *Neural Networks,* **7***,* 1115-1135.

Barmack, N.H., Bell, C.C., and Rence, B.G., (1971) Tension and rate of tension development during isometric responses of extraocular muscles, *J. Neurophysiol.*, **34**, 1072-1079.

Becker W. and Jurgens R., (1979) An analysis of the saccadic system by means of double step stimuli, *Vision Res.*, **19**, 967-983.

Breznen B. and Gnadt J.W., (1997) Analysis of the step response of the saccadic feedback: computational models, *Exp. Brain Res.* **117**, 181-191.

Burr D.C., Morrone M.C. and Ross J., (1997) Selective suppression of the magnocellular visual pathway during saccadic eye movements, *Nature*, **371**, 511-513.

Clark M.R. and Stark L., (1974a) Control of human eye movements: I. Modeling of extraocular muscle, *Math. Biosc.*, **20**, 191-211.

Clark M.R. and Stark L., (1974b) Control of human eye movements: II. A model for the extraocular plant mechanism, *Math. Biosc.*, **20**, 213-238.

Collewijn H., Van der Mark F. and Jansen T.C., (1975) Precise recording of human eye movements, *Vision Res.*, **15**, 447-450.

Collewijn H., Erkelens C.J. and Steinman R.M., (1988) Binocular co-ordination of human horizontal saccadic eye movements, *Journal of Physiology*, **404**, 157-182.

Collins C.C.; Bach-Y-Rita P. and Collins C.C. (Eds), (1971) Orbital mechanics, *The control of Eye Movements*, New-York: Academic Press, 283-325.

Collins C.C.; Lennerstrand G. and Bach-Y-Rita P. (Eds.), (1975) The human oculomotor control system, *Basic Mechanisms of Ocular Motility and their Clinical Implications*: proceedings of the international symposium held in Wenner-Gren Center, Stockholm, June 4-6, 1974. Oxford: Pergamon Press, 145-180.

Collins C.C., O'Meara D. and Scott A.B., (1975) Muscle tension during unrestrained human eye movements, *J.Physiol.*, **245**, 351-369.

Collins C.C., Carlson M.R., Scorr A.B. and Jampolsky A., (1981) Extraocular muscle forces in normal human subjects, *Invest. Opthalmol. Vis. Sci.*, **20**, 652-664.

Cook G. and Stark L., (1967) Derivation of a model for the human eye-positioning mechanism, *Bull. Math. Biophys.*, **29**, 153.

Cook G. and Stark L., (1968) The human eye movement mechanism. Experiments, modeling, and model testing, *Archs Ophthal.*, **79**, 428-436.

Crane B.T. and Demer J.L., (1999) A linear canal-otolith interaction model to describe the human vestibulo-ocular reflex, *Biol. Cybern.* **81**, 109-118.

Crawford J.D. and Guitton D., (1997) Visual-Motor Transformations Required for Accurate and Kinematically Correct Saccades, *J. Neurophysiol.* **78**, 1447-1467.

Cullen C.A. and Guitton D., (1997) Analysis of Primate IBN Spike Trains Using System identification Techniques. I. Relationship to Eye Movement dynamics During Head-Fixed Saccades, *J.Neurophysiol.*, **78**, 3259-3282.

Dean P., Majhew J. and Langdon P., (1994) Learning and maintaining saccadic accuracy: a model of brainstem-cerebellar interaction, *J. Cognit. Neurosci.* **6**, 117-138.

Demer J.L., Miller J.M., Poukens V., Vinters H.V., Glasgow B.J., (1995) Evidence for fibromuscular pulleys of the recti extraocular muscles, *Invest. Ophthalmol. & Vis. Sci.* **36**, 1135-1136

Demer J.L., Oh S.Y. and Poukens V., (2000) Evidence for Active Control of Rectus Extraocular Muscle Pulleys, *Invest. Ophthalmol. Vis. Sci.* **41**, 1280-1290.

Demer J.L., Kono R., Wright W., (2002) Magnetic Resonance Imaging (MRI) of Human Extraocular Muscles (EOMs) During Asymmetrical Convergence, ARVO meeting 2002, Presentation Number 1915 (poster) (http:// www.arvo.org/ abstracts.htm)

Desouza J.F.X., Nicolle D.A. and Vilis T., (1997) Task-dependent Changes in the Shape and Thickness of Listing's Plane, *Vision Res.* **37**, 2271-2282.

Droulez, J. and Berthoz, A., (1988) Spatial and temporal transformations in visuomotor coordination, In: R. Eckmiller, & C. von der Malsburg (Eds.), *Neural computers* Berlin: Springer, 345-357.

Eggert T., Mezger F., Robinson F. and Straube A., (1999) Orbital position dependency is different for the gain of externally and internally triggered saccades, *NeuroReport*, **10**, 2665-2670.

Fuchs A.F. and Lushei E.S., (1970) Firing patterns of abducens neurons of alert monkeys in relationship to horizontal eye movements, *J.Neurophysiol.*, **33**, 382-392.

Fuchs A.F. and Lushei E.S., (1971a) Development of isometric tension in simian extraocular muscle, *J.Physiol.*, **219**, 155-166.

Fuchs A.F. and Luschei E.S., (1971b) The Activity of Single Trochlear Nerve Fibers during Eye Movements in the Alert Monkey, *Exp. Brain Res.* **13**, 78-89.

Fuchs A.F., Kaneko C.R.S. and Scudder C.A., (1985) Brainstem control of saccadic eye movements, *Ann. Rev. Neurosci.*, **8**, 307-337.

Gancarz G. and Grossberg S., (1998) A neural model of the saccade generator in the reticular formation, *Neural Networks*, **11**, 1159-1174.

Grossberg S. and Kuperstein M., (1989) *Neural Dynamics of Adaptive Sensory-Motor Control: Ballistic Eye Movements.* Amsterdam: Elsevier/ North Holland. Expanded ed. New York: Pergamon Press.

Haustein W., (1989) Considerations on Listing's law and the primary position be means of a matrix description of eye position control, *Biol. Cybern.* **60**, 411-420.

Hepp K., (1994) Oculomotor control: Listing's law and all that, *Curr. Opin. Neurobiol.* **4**, 862-868.

Hikosaka O. and Kawakami T., (1977) Inhibitory neurons related to the quick phase of vestibular nystagmus - their location and projection, *Exp. Brain Res.*, **27**, 377-396.

Hikosaka O, Igusa Y, Nakao S and Shimazu H., (1978) Direct inhibitory synaptic linkage of pontomedullary reticular burst neurons with abducens motoneurons in the cat, *Exp. Brain Res.*, **33**, 337-352.

Hilll A.V., (1938) The heat of shortening and the dynamic constants of muscle, *Proc. Roy. Soc.*, **126B**, 136-195.

Igusa Y, Sasaki S and Shimazu H., (1980) Excitatory premotor burst neurons in the cat pontine reticular formation related to the quick phase of vestibular nystagmus, *Brain Res.*, **182**, 451-456.

Jurgens R., Becker W. and Kornhuber H., (1981) Natural and drug-induced variation of velocity and duration of human saccadic eye movements: Evidence for control of the neural pulse generator by local feedback, *Biol. Cyber.*, **39**, 87-96.

Keller E.L., Wurtz R.H. and Goldberg M.E. (eds.), (1989) The cerebellum, *The neurobiology of saccadic eye movements*, North Holland: Elsevier Science Publishers, 391-411.

Lefevre P. and Galiana H.L., (1992) Dynamic feedback to the superior colliculus in a neural network model of the gaze control system, *Neural Networks*, **5**, 871-890.

Lefevre P., Quaia C. and Optican L.M., (1998) Distributed model of control of saccades by superior colliculus and cerebellum, *Neural Networks*, **11**, 1175-1190.

Leigh R.J. and Zee D.S., (1999) *The Neurology of Eye Movements,* Contemporary Neurology Series, Oxford University Press

Miller J.M. and Robinson D.A., (1984) A Model of the Mechanics of Binocular Alignment, *Computers and Biomed. Res.*, **17**, 436-470.

Miller J.M., (1989) Functional Anatomy of Normal Human Rectus Muscles, *Vision Res.*, **29**, 223-240.

Miller J.M. and Robins D., (1992) Extraocular muscle forces in alert monkey, *Vision Res.*, **32**, 1099-1113.

Miller J.M., Demer J.L., Rosenbaum A.L., (1993) Effect of transposition surgery on rectus muscle paths by magnetic resonance imaging, *Ophthalmology*, **100**, 475-487.

Miller J.M., Pavlovski D.S. and Shamaeva I., (1999) Orbit$^{\mathrm{tm}}$1.8 Gaze mechanics simulation, San Francisco: Eidactics.

Minken A.W.H., van Opstal A.J. and van Gisbergen A.J.M., (1993) Three-dimensional analysis of strongly curved saccades elicited by double-step stimuli, *Exp. Brain Res.*, **93**, 521-533.

Misslisch H., Tweed D., (2001) Neural and mechanical factors in eye control, *J. Neurophysiol.*, **86**, 1877-83.

Moschovakis A., (1994) Neural network simulations of the primate oculomotor system, *Biol. Cybern.*, **70**, 291-302.

Optican L. and Robinson D.A., (1980) Cerebellar-dependent adaptive control of the primate saccadic system, *J. Neurophysiol.*, **44**, 1058-76.

Optican L.M., Lennerstrand G., Zee D.S. and Keller E.L. (Eds.), (1982) Saccadic dysmetria, *Functional basis of ocular motility disorders*, Oxford: Pergamon, 441-451.

Optican L.M. and Miles F.A., (1985) Visually induced adaptive changes in primate saccadic oculomotor control signals, *J. Neurophysiol.*, **54**, 940-958.

Optican L.M., Keller E.l. and Zee D.S. (Eds.), (1986) Adaptive control of saccadic and smooth pursuit eye movement, *Adaptive Processes in Visual and Oculomotor Systems*, Oxford: Pergamon Press, 313-320.

Optican L.M., Fuchs A.F., Brandt T., Buettner U. and Zee D.S. (Eds.), (1994) Control of saccade trajectory by the superior colliculus, *, Contemporary ocular motor and vestibular research: A tribute to David A. Robinson*, Stuttgart: Thieme, 98-105.

Pelisson D. and Prablanc C., (1988) Kinematics of centrifugal and centripetal saccadic eye movements in man, *Vision Res.*, **28**, 87-94.

Pfann K.D., Keller E.L. and Miller J.M., (1995) New models of the oculomotor mechanics based on data obtained with chronic muscle force transducers, *Biomed. Eng.*, **23**, 346-358.

Porrill J., Warren P.A. and Dean P., (2000) A simple control law generates Listing's positions in a detailed model of the extraocular muscle system, *Vision Res.*, **40**, 3743-3758.

Quaia C., Aizawa H., Optican L.M. and Wurtz R.H., (1998) Reversible inactivation of monkey superior colliculus. II. Maps of saccadic deficits, *J. Neurophysiol.* **79**, 2097-2110.

Quaia C. and Optican L.M., (1998) Commutative Saccadic Generator is Sufficient to Control a 3-D Ocular Plant With Pulleys, *J. Neurophysiol.*, **79**, 3197-3215.

Quaia C., Lefevre P. and Optican L.M., (1999) Model of the control of Saccades by Superior Colliculus and cerebellum, *J.Neurophysiol.*, **82**, 999-1018.

Raphan T., (1997) Modeling control of eye orientation in three dimensions. In: Three-Dimensional Kinematics of Eye, Head, and Limb Movements, edited by M. Fetter, T. Haslwanter, H. Misslisch, and D. Tweed. The Netherlands: Harwood Academic, 359-374.

Raphan T., (1998) Modeling Control of Eye Orientation in Three Dimensions. I. Role of Muscle Pulleys in Determining Saccadic Trajectory, *J. Neurophysiol.*, **79**, 2653-2667.

Robinson D.A., (1963) A method of measuring eye movements using a search coil in a magnetic field, *IEEE Trans. Biomed. Eng.*, **10**, 137-145.

Robinson D.A., (1964) The mechanisms of human saccadic eye movement, *J.Physiol. Lond.*, **174**, 245-264.

Robinson D.A., O'Meara D.M., Scott A.B. and Collins C.C., (1969) Mechanical components of human eye movements, *J. Appl. Physiol.*, **26**, 548-553.

Robinson D.A., (1970) Oculomotor unit behavior in the monkey, *J. Neurophysiol.*, **33**, 393-404.

Robinson D.A., Bach-y-Rita P. and Lennerstrand G. (Eds), (1975a) Oculomotor control signals, *Basic mechanisms of ocular motility and their clinical implications*, Oxford: Pergamon.

Robinson D.A., (1975b) A quantitative analysis of extraocular muscle cooperation and squint, *Invest. Ophthalmol. & Vis. Sci.*, **14**, 801-25.

Robinson D.A., Zuber B.L. (eds.), (1981) Models of the mechanics of eye movements, *Models of Oculomotor Behavior and Control.* Boca Ratou: CRC Press, 21-42.

Rottach K.G., Das V.E., Wohlgemuth W., Zivotofsky A.Z. and Leigh R.J., (1998) Properties of Horizontal Saccades Accompanied by Blink, *J. Neurophysiol.*, **79**, 2895-2902.

Sasaki S. and Shimazu H., (1981) Reticulovestibular organization participating in the generation of horizontal fast eye movement, *Ann. NY Acad. Sci.*, **374**, 130-143.

Sato H. and Noda H., (1992) Saccadic dysmetria induced by transient functional decortication of the cerebellar vermis, *Exp. Brain Res.*, **88**, 455-458.

Schiller P.H., Treue S.D. and Conway J.L., (1980) Deficits in eye movements following frontal eye field superior colliculus ablation, *J. Neurophysiol.*, **44**, 1175-1189.

Schnablok C. and Raphan T., (1994) Modeling three-dimensional velocity to position transformation in oculomotor control, *J. Neurophysiol.*, **71**, 623-638.

Scudder C.A., (1988) A new local feedback model of the saccadic burst generator, *J. Neurpphysiol.*, **59**, 1455-1475.

Scudder C.A., Fuchs A.F., and Langer T.P., (1988) Characteristics and functional identification of saccadic inhibitory burst neurons in the alert monkey, *J. Neurophysiol.*, **59**, 1430-1454.

Smith M.A. and Crawford J.D., (1998) Neural Control of Rotational Kinematics Within Realistic Vestibuloocular Coordinate Systems, *J. Neurophysiol.*, **80**, 2295-2315.

Somani R.A.B., Desouze J.F.X., Tweed D., Vilis T., (1998) Visual test of Listing's law during vergence, *Vision Res.*, **38**, 911-923.

Stefen H., Walker M.F., Zee D.S., (2000) Rotation of Listing's plane with convergence: Independence from eye position, *Invest. Ophthalmol. & Vis. Sci.*, **41**, 715-721.

Strassman A., Highstein S.M., and McCrea R.A., (1986a) Anatomy and physiology of saccadic burst neurons in the alert squirrel monkey. I. Excitatory burst neurons, *J. Comp. Neurol.*, **249,** 337-357.

Strassman A., Highstein S.M., and McCrea R.A., (1986b) Anatomy and physiology of saccadic burst neurons in the alert squirrel monkey. II. Inhibitory burst neurons, *J. Comp. Neurol.*, **249,** 358-380.

Straube A., Kurzan R. and Buettner U., (1991) Differential effects of bicuculline and muscimol microinjections into the vestibular nuclei on simian eye movements, *Exp. Brain Res.*, **86**, 347-358.

Straumann D., Zee D.S., Solomon D., Lasker A.G. and Roberts D.C., (1995) Transient torsion during and after saccades, *Vision Res.*, **35**, 3321-3334.

Suzuki D.A., Keller E.L., (1984) Visual signals in the dorsolateral pontine nucleus of the alert monkey: their relationship to smooth-pursuit eye movements, *Exp. Brain Res.*, **53**, 473-8.

Thurtell M.J., Kunin M., Raphan T., (2000)Role of Muscle Pulleys in Producing Eye Position-Dependence in the Angular Vestibuloocular Reflex: A Model-Based Study, *J. Neurophysiol.*, **84**, 639-650.

Tweed D. and Vilis T., (1987) Implications of rotational kinematics for the oculomotor system in three dimensions, *J. Neurophysiol.*, **58**, 823-849.

Tweed D.B. and Vilis T., (1990a) The superior colliculus and spatiotemporal translation in the saccadic system, *Neural Networks*, **3**, 75-86.

Tweed D. and Vilis T., (1990b) Geometric relations of eye position and velocity vectors during saccades, *Vision. Res.*, **30**, 111-127.

Tweed D, (1997) Three-dimensional model of the human eye-head saccadic system, *J. Neurophysiol.*, **77**, 654-66.

van Gisbergen J.A., van Opstal A.J. and Schoenmaker J.J., (1985) Experimental test of two models for the generation of oblique saccades, *Exp. Brain Res.*, **57**, 321-36.

van Opstal A.J. and Kappen H., (1993) A two-dimensional ensemble coding model for spatial-temporal transformation of saccades in monkey superior colliculus, *Network*, **4,** 19-38.

van Rijn L.J. and van den Berg A.V., (1993) Binocular eye orientation during fixations: Listing's law extended to include eye vergence, *Vision Res.*, **33**, 691-708.

Vilis T. and Hore J., (1981) Characteristics of saccadic dysmetria in monkeys during reversible lesions of medial cerebellar nuclei, *J. Neurophysiol.*, **46**, 828-838.

von Helmholtz H., (1867) H. Handbuch der physiologischen Optik. Leipzig: Voss (English translation: Treaties on Physiological Optics. New York: Dover, 1962)

Waitzman D.M., Ma T.P., Optican L.M. and Wurtz R.H., (1991) Superior colliculus neurons mediate the dynamic characteristics of saccades, *J. Neurophysiol.,* **66**, 1716-1737.

Westheimer G., (1954) Eye movement responses to a horizontally moving visual stimulus, *Arch. Ophthalmol.*, **52**, 932-41.

Yoshida K., Berthoz A., Vidal P.P. and McCrea R.A., (1982) Morphological and physiological characteristics of inhibitory burst neurons controlling rapid eye movements in the alert cat, *J. Neurophysiol.*, **48**, 761-784.

Young L.R. and Stark L., (1963) Variable feedback experiments testing a sample data model for eye tracking movements, *IEEE Trans. Hum. Factors Electron,* HFE-4:38-51.

Zee D.S., Optican L.M., Robinson D.A. and Engel W.K., (1976) Slow saccades in spinocerebellar degeneration, *Arch. Neurol.*, **33**, 243-251.

Publications

Articles

Ansgar R. Koene and Casper J. Erkelens, "Cause of kinematic differences during centrifugal and centripetal saccades", *Vision Research*, **42**:14, 1797-1808, 2002

Ansgar R. Koene and Casper J. Erkelens, "Quantification of saccadic signal modification as function of eye orientation", *Vision Research*, submitted

Ansgar R. Koene and Casper J. Erkelens, "Properties of 3D rotations and their relation to eye movement control", *Biological Cybernetics*, submitted

Ansgar R. Koene and Casper J. Erkelens, "Error resulting from the use of eye plant models that treat agonist-antagonist muscle pairs as a single muscle", in preperation

M. Setnes, A. Koene, R. Babuska and P. Bruijn, "Data-driven initialization and structure learning in fuzzy neural networks" in *Proceedings Fuzz-IEEE'98*, 1147-1152, 1998.

Refereed abstracts

Ansgar R. Koene, Karel Hol and Raymond van Ee, "Modeling curvature polarity in multi-stable 3D structure-from-motion", *Perception*, **31**:supplement, 151a, 2002.

Ansgar R. Koene and Casper J. Erkelens, "Influence of eye plant mechanics on the control of eye movements" at *Investigative Ophthalmology & Visual Science*, **41**, 2207, 2000.

Acknowledgement

Though we may work in solitude,
tasking our minds to pierce through nature's secrets;
Yet is it only when we are nurtured,
in an environment of loving friendship,
that our thoughts can truly find,
the answers that we seek.

Over the course of the four years during which the research for this thesis was done various people, family, friends and colleagues, made valueable contributions either through moral support or direct scientific input.

Als erstes möchte ich meinen Bruder Randal bedanken den ich immer um Rat fragen konnte. Besonders in den ersten Jahren war seine Hilfe, in sowohl technischen als auch nicht-technischen Sachen, von unschätzbarem Wert.

Mijn promotor Casper Erkelens wil ik graag bedanken voor het feit dat hij mij de vrijheid gaf om mijn eigen onderzoeksinteresse na te streven en aaltijd beschikbaar was voor advies en commentaar, vooral bij het schrijven van de artikelen.

Je voudrais remercier les nombreuses personnes de l'Institut Helmholtz pour leur aide et leur perspicacité, ainsi que les personnes qui m'ont apporté des rétroactions enrichissantes pendant les conférances et séminaires.

Voor de gezellige en motiverende omgeving die ze vormen bedank ik mijn vrienden en collega's bij Fysica van de Mens. Ans, Astrid, Byung-Geun (Bob), Eelco, Elena, Ellen, Els, Gijs, Hans, Harold, Evelijn, Evert-Jan, Jan, Jan-Joris, Jasper, Loes, Lu, Maaike, Martin, Michelle, Mieke, Nicole, Ninke, Paul, Pieter, Raymond, Raymond, Sylvia en Susan, bedankt aan jullie allen.

Meinen Eltern bin ich selbstverständlich auch dankbar. Bei ihnen habe ich mich immer gänzlich ausruhen können damit ich mich mit erneuter Energie wieder in die Wissenschaft stürzen konnte.

Finally I would like to express my gratitude to Joel Miller and Joseph Demer for sharing their data concerning eye muscle forces and muscle pulley locations.

Let never it be said,
we did not truly try,
to find the truth and wisdom,
to answer the age old questions,
of how, wherefore and why.

Curriculum vitae

Ansgar Roald Koene was born on February 19th, 1975 in Braunschweig, Germany. After living in the US and Canada for the first four years of his life, he moved with his parents back to the Netherlands. During the primary and secondary school years he attended the European School in Bergen N.H. where he went to the German language section. In 1993 he graduated from school receiving the European Baccalaureate. From 1993 to 1997 Ansgar studied electrical engineering at the faculty of information and communications technology of the TU Delft. Motivated by the desire to understand how humans and other autonomous system interact and learn he decided to specialize in control engineering with a focus on robotics and artificial intelligence systems. In December 1997 he received his Masters degree. His masters thesis with the title "Data-driven initialization and structure learning in Fuzzy Neural Networks" dealt with the use of a hybrid of artificial neural networks and fuzzy logic for automated systems modeling. Following the example of his father and his brother, Ansgar had long been determined to have a career in scientific research. To this end he set out, in early 1998, to look for a suitable PhD position. By mid april he had found this position at the Utrecht University in the department of Physics of Man which is part of the Helmholtz Institute in Utrecht. It was there that he started his PhD research under the supervision of professor Casper Erkelens. The original title of the research project was "Geometry of Binocular Motor Space". From the beginning however it had been clear that the research would be greatly altered to become a more model/simulation based project with an emphasis on theoretical aspects rather than experiments, as was originally proposed. Thus, molding the research to his own interests, Ansgar spent the first one and a half years getting better acquainted with the neural and physiological properties of the oculomotor system and searching for the best way to apply his engineering background to the problem of understanding the oculomotor control system. The result of this search, and the following two and a half years of research are what lead to this thesis.

Besides the research relating to this thesis Ansgar also supervised the practical course parts of the ALSV (general linear signal processing) and BEEL (Image Processing) courses for 3rd year physics students as well as supervising two students with their research projects. During the last two years he was active in the PhD union, de BAU (Belangenvereniging voor AiOs in Utrecht), as representative for the PhD students of the faculty of Physics and Astronomy and as member of the board of the

BAU (secretary). Starting in December of 2002 Ansgar will begin work as post-doc at the INSERM (Institut national de la senté et de la recherche médicale) in Lyon where he will study the involvement of the cerebellum in the control of eye and head movements.

In his spare time, when he is not occupied by the persuit of science, Ansgar has been known to participate in amateur theater, write poems and short stories or plays violin and piano.

The dragon's choice

Bereft of mortal friends he stood,
upon the Ivory Tower.
Renowned in all the world
for courage, strength and power.

Down upon his lands he looked
as far as the eye could see,
it all was his controlled by he.

Yet for all these earthly goods
his shoulders sagged his breath did sigh.

'See there the youthful couple walking by,
see how she moves to take his hand,
and what I ask, what friends have I?'

'Hand in hand they move along
the caring touch a loving smile,
safe in the knowledge of the trust
that true friendship holds so strong.'

'I look around, what do I see?
whom can I trust implicitly,
but the sharpened steel
and the raging dragon's arm'

'Who am I so to complain,
I had the choice,
I made my choice,
and new full well it held a price'

'For success I am not wanting,
the Jackhals beyond the door
attest to that.'

The Crimson sky grew dark
and beckoned in the night.
Beyond the door the Jackhals vied
for scraps and favors
from the dragon's might

Seated on the basalt throne
the dragon's arm reached out
the hand unfurled,
a shining sphere appeared.

Within the sphere
three handsome forms,
clad as princes
of ancient time.

'Claudio and Benedict,
eternal friendship once we swore,
through happiness
and through war.'

The Sphere of light
Grew dim and fade,
of the three
but one remained,

The Sphere of light
once more showed bright,
no lonely prince
but a dragon of the night.

'To the bitter end
you both I called my friend,
In peace now may you lie
for your vengeance care took I.'

The Sphere again
with forms did play,
to show a youthful couple
on a sunny day

'What is this,
why haunt me so,
dost thou believe
my loss I do not know?'

The dragons hand
forcefully closed,
so was the sphere
swiftly disposed

As darkness settled
heavy on the room,
the dragon sought the refuge
of illusive sleep.

Yet once again it would not be,
with the ease of habit grown by need,
the dragon spread his wings
and laid his hand upon the sharpened steel.

To the sound of heavy feet he called,
'step forward foul demon of the night.'
From the shadows now revealed
came a figure dark and proud.

Relaxing in his seat
his wings refolded,
his sword released
the dragon snarled.

'Be gone you shadow from my past
you hold no threat to me,
I long ago defeated thee.'

The demon mockingly replied,
'My soul from its mortal shell you did release,
but with it you did slay your victory.'

'So much time has passed
and still I find you all alone,
You took my life,
but in exchange I rid you of your prize.'

The silvery light of the rising moon
then basked the Ivory Tower's room,
and so dispatched the demon
from the dragon's past.

Upon the sight
of the moon at night,
the dragon conjured up a vision
of an angel fair.

'My lady dear do not despair
even if it takes ten thousand years,
I will find a way the curse to lift
and your sweet soul to repair.'

'Though grief has taken thee away from me,
thou art and shalt always be,
my immortally beloved.'